Characterizing Intestinal Glucose Absorption in Mammalian Pig and Aquatic Species Tilapia and Trout

A Thesis Submitted to the
College of Graduate and Postdoctoral Studies
In Partial Fulfillment of the Requirements
For the Degree of Doctor of Philosophy
In the Department of Veterinary Biomedical Sciences, pertaining to
Physiology and Biochemistry in the Western College of Veterinary Medicine
At the University of Saskatchewan Saskatoon

By

Marina Subramaniam

PERMISSION TO USE

In presenting this thesis/dissertation in partial fulfillment of the requirements for a Postgraduate degree from the University of Saskatchewan, I agree that the Libraries of this University may make it freely available for inspection. I further agree that permission for copying of this thesis/dissertation in any manner, in whole or in part, for scholarly purposes may be granted by the professor or professors who supervised my thesis/dissertation work or, in their absence, by the Head of the Department or the Dean of the College in which my thesis work was done. It is understood that any copying or publication or use of this thesis/dissertation or parts thereof for financial gain shall not be allowed without my written permission. It is also understood that due recognition shall be given to me and to the University of Saskatchewan in any scholarly use which may be made of any material in my thesis/dissertation.

Requests for permission to copy or to make other uses of materials in this thesis/dissertation in whole or part should be addressed to:

Head of the Department of Veterinary Biomedical Sciences
Western College of Veterinary Medicine
University of Saskatchewan
Saskatoon, Saskatchewan S7N 5B4 Canada

OR

Dean
College of Graduate and Postdoctoral Studies
University of Saskatchewan
116 Thorvaldson Building, 110 Science Place
Saskatoon, Saskatchewan S7N 5C9 Canada

ABSTRACT

Glucose absorption along the intestine primarily occurs through sodium-dependent glucose transporters (SGLTs). Recently, it has been suggested that glucose transport across the brush-border membrane (BBM, or apical side of epithelial cells) can also occur through sodium-independent/facilitative glucose transporters (GLUTs) in mammals. Here, the Ussing chamber was used to characterize sodium-dependent and sodium-independent glucose transport systems across ex-vivo intestinal segments in the mammalian pig, and the aquatic species tilapia and trout.

In our first study, electrogenic sodium-dependent glucose transport in tilapia demonstrated a homogeneous high-affinity, high-capacity (Ha/Hc) transport system across the proximal intestine, mid-intestine, and hindgut segments, associated with transporters from the solute carrier 5A (SLC5A) family. In contrast, trout demonstrated a heterogeneous glucose transport system with a high-affinity, low-capacity (Ha/Lc) in the pyloric caeca, a super-high-affinity, low-capacity (sHa/Lc) in the midgut, and a low-affinity, low-capacity (La/Lc) in the hindgut, associated with different expressions of SLC5A transporters in each segment. Additionally, fish were different from mammals in demonstrating hindgut sodium-dependent glucose absorption.

In our second study, we found that sodium-dependent glucose and galactose transport along the porcine jejunum and ileum followed sigmoidal/Hill kinetics. This strongly suggested that each segment had multiple transporter involvement. The transport systems in the jejunum demonstrated a Ha/super-low-capacity (sLc) for glucose and a La/Lc for galactose. In contrast, the ileum demonstrated a Ha/super-high-capacity (sHc) glucose transport system, and a La/Hc galactose transport system. In support of this, different SLC5A transporters were associated with the kinetics in each segment. Finally, the absence of monosaccharide transport in the colon was supported with pharmacological data and low expression of all SLC5A genes.

Our last study characterized total tissue glucose flux in tilapia, trout, and pig. We demonstrated a Ha/Hc system in tilapia, a Ha/Lc system in trout, and a La/Lc system in the pig. The overall La system in the pig, with differences in pharmacological inhibition and gene expression in comparison to the aquatic species, revealed a different mechanism of glucose transport in the pig. Interestingly, our results revealed the possible involvement of AQPs in tilapia and pig to total tissue glucose absorption.

Overall, our results in each study highlighted the fact that aquatic species have divergently adapted mechanisms for glucose absorption differing from the mammalian pig, which may have evolved to meet their individual needs.

ACKNOWLEDGEMENTS

I would like to thank my supervisor, Dr. Matthew Loewen, for his guidance, supervision, and more importantly, his patience, throughout my Ph.D. program in the Department of Veterinary Biomedical Sciences.

I would also like to thank my advisory committee, Dr. Lynn Weber, Dr. Andrew Van Kessel, Dr. George Forsyth, and my graduate co-chair, Dr. Daniel MacPhee, who have all been very supportive and helpful during the course of this work. I would like to especially thank Dr. Lynn Weber and Dr. George Forsyth, who have helped me tremendously. I really appreciate it!

I want to thank all of my lab members and colleagues, especially Cole Enns, Brandon Keith, and Khanh Luu, for all of their help, support, and encouragement throughout the course of this Ph.D. They all deserve credit for making me a better scientist.

I want to thank all of my friends, the new ones I made in Saskatoon, as well as the ones from BC, who have all supported, guided, and offered me very valuable words of wisdom. Thank you!

Finally, and most importantly, I would like to thank my family, both my parents and my sister and brother, for their endless support and motivational speeches during the course of my Ph.D. degree.

DEDICATION

I would like to dedicate this thesis to my family,
Ratnasingam, Mary Rosalin, Rubika, and Vithuson who always support my career goals and aspirations

TABLE OF CONTENTS

LIST OF TABLES

LIST OF FIGURES

LIST OF EQUATIONS

LIST OF ABBREVIATIONS

BBM = brush-border membrane

SGLTs = sodium-dependent glucose transporters

GLUTs = glucose transporters

SLC5A = solute carrier family 5A

SLC2A = solute carrier family 2A

AQPs = aquaporins

GI = gastrointestinal

TCA = tricarboxylic acid cycle

ATP = adenosine triphosphate

HCl = hydrochloric acid

SCFA = short-chain fatty acid

VFA = volatile fatty acid

COS-7 = **C**V-1 in **O**rigin carrying **S**V40

PKC βII = protein kinase C β II

Ha = high-affinity

sHa = super-high-affinity

La = low-affinity

Hc = high-capacity

sHc = super-high-capacity

Lc = low-capacity

sLc = super-low-capacity

Isc = short-circuit current

CFTR = cystic fibrosis transmembrane conductance regulator

BBMV = brush-border membrane vesicle

CCAC = Canadian council on animal care

RT-qPCR = reverse-transcription quantitative polymerase chain reaction

BLAST+ = basic local alignment search tool +

NCBI = national center for biotechnology information

mRNA = messenger Ribonucleic acid

cDNA = complementary Deoxyribonucleic acid

cRNA = complementary Ribonucleic acid

CT = cycle threshold

3-OMG = 3-O-Methyl D-Glucose

Jms = mucosal to serosal flux

TEA = tetraethylammonium

$NiCl_2$ = nickel (II) chloride

Chapter 1 - Introduction

1.1 Rationale

The digestion and absorption of nutrients in all species are essential to maintaining an animal's homeostasis and development (194). The gastrointestinal (GI) tract is the primary site of digestion and absorption of nutrients (155). Once the food is ingested and digested, the main classes of absorbed nutrients are lipids, amino acids, monosaccharides, as well as other compounds like vitamins, minerals, and electrolytes (155). Specifically, here I focus on monosaccharides, the product of complex oligosaccharide and polysaccharide carbohydrate digestion, providing the major energy source from the diet (20, 21, 118, 160, 199).

A major product of carbohydrate digestion is the monosaccharide glucose (178). Glucose provides energy via its oxidation through glycolysis, the pentose phosphate pathway, and the tri-carboxylic acid (TCA) cycle (178). However, for glucose to be utilized by these pathways, it must first be transported into intestinal epithelial cells (150, 178). The transport of glucose can either be through sodium-dependent or sodium-independent transporters from different solute carrier gene families (53, 75, 95, 179, 191). This transport has been extensively studied in mammals like pigs, cats, humans, and rats, as well as ruminant species like cattle and goats (12, 16, 87, 101, 112, 113, 147, 201). It has also been studied in fish species like the Pacific copper rockfish, as well as avian species like the chicken (4, 68, 130). Interestingly, the transport of glucose along the intestinal length of these species not only revealed the diversity in expression and function of glucose transporters, but it also presented unique patterns of segregation. More specifically, different kinetic sodium-dependent glucose transport systems along the length of the small intestine have been discovered in many species, and the reason for this adaptation is still unknown (4, 21, 22, 75). Nevertheless, these significant differences likely evolved to meet the needs of these individual species.

Here, we investigate the similarities and differences between electrogenic sodium-dependent glucose transport systems present in the omnivorous Nile tilapia (*Oreochromis niloticus*) and the carnivorous rainbow trout (*Oncorhynchus mykiss*). We found that tilapia demonstrated a homogeneous sodium-dependent glucose transport system throughout its gastrointestinal (GI) tract. In contrast, trout demonstrated a heterogeneous sodium-dependent glucose transport

system segregated into each of its intestinal segments. These systems in both fish species were associated with different transporters from the solute carrier 5A family (SLC5A).

Comparatively, the electrogenic sodium-dependent transport of glucose and galactose was studied in the mammalian pig (*Sus scrofa*) revealing differences in transport systems between the jejunum and ileum. More importantly, these transport systems followed sigmoidal/Hill kinetic fits that suggested the involvement of multiple transporters in each intestinal segment. Additionally, different SLC5A transporters were likely associated with the transport systems in each segment.

Finally, the characterization of total tissue glucose flux between tilapia, trout, and pig presented major differences in the glucose transport mechanism between all three species. Overall, this work presents evolutionary adaptations between these three species in terms of differences in glucose transport mechanisms, for the benefit of their individual needs.

1.2 Objectives

1. To characterize electrogenic sodium-dependent glucose transport in the omnivorous Nile tilapia and the carnivorous rainbow trout in Ussing chambers, with pharmacological inhibition, and genomic and gene expression analysis.

2. To characterize electrogenic sodium-dependent glucose transport along the porcine jejunum, ileum, and distal colon in Ussing chambers, with two different substrates, pharmacological inhibition, and genomic and gene expression analysis.

3. To characterize total tissue glucose absorption in the proximal small intestine of tilapia, trout, and pig in Ussing chambers using ^{14}C 3-O-Methyl D-Glucose, pharmacological inhibition, and genomic and gene expression analysis.

1.3 Hypotheses

1. Omnivorous tilapia has a higher capacity of electrogenic sodium-dependent glucose transport than the carnivorous trout, with differences in transport kinetics.

2. The porcine jejunum and ileum have differences in glucose and galactose transport kinetics, involving different transporters.

3. The pig, a representative mammalian model, has a different mechanism of total glucose absorption along the intestinal brush-border membrane in comparison to aquatic species tilapia and trout.

Chapter 2 – Literature Review

2.1 General Overview of Carbohydrate Digestion and Absorption

Carbohydrates are one of the major components present in feed for mammals like pigs, dogs, mice, and rats, and it represents the greatest source of energy from the diet (32, 47, 51, 109, 114). Additionally, the gastrointestinal (GI) tract of these species has adapted to digest and absorb carbohydrates (61). Carbohydrates can be digested and absorbed by the host, beginning in the mouth, and ending in the large intestine (139). Carbohydrate digestion is primarily mediated by enzymes present in the mouth and small intestine (salivary and pancreatic α-amylase, as well as other hydrolytic enzymes) that break down carbohydrates into mono- and di-saccharides (74, 114). In the small intestine, these hydrolytic enzymes are either on the brush-border membrane (BBM, or apical side of the enterocyte) or secreted as a soluble form (114, 152). These monosaccharides that are released from carbohydrate digestion include glucose, galactose, and fructose, which are then absorbed by the enterocytes in the small intestine (114). The absorption of these monosaccharides across the BBM occur via transcellular transporters (114, 152). Once in the enterocytes, these monosaccharides are either oxidized for energy or transported into the blood and used by the animal (139).

Following carbohydrate digestion, absorption occurs specifically in the villi tips, or microvilli (74, 139). These structures are the sites of nutrient absorption, where most of the transporters on the BBM for monosaccharides, amino acids, vitamins, and minerals are located (74, 139). The absorption of carbohydrates across the BBM can be an active process, requiring energy (ATP) or passive transport, not requiring ATP (139). Active absorption occurs using the electrochemical gradient of sodium, which is established by the basolateral sodium/potassium ATPase (202). Sodium is pumped out from the basolateral side, which develops a concentration gradient favoring sodium entry into the enterocyte (97). Along with sodium entry, it can co-transport an amino acid, monosaccharide, or vitamin (114). Therefore, these transporters are called sodium-dependent co-transporters, meaning the transport of the nutrient requires the co-transport of sodium to enter the enterocytes (97, 204). Additionally, monosaccharides can be absorbed passively through facilitative transporters down its concentration gradient, a process that does not require coupling and the use of ATP (106). Such transport is often referred to as sodium-independent glucose transport (44, 106, 203, 213). Thus, glucose, fructose, and

galactose can be absorbed using either type of transport (13, 18, 75, 106, 112, 115, 171, 204). These transporters can also use other ions, like potassium or hydrogen, for co-transport as well (13, 22, 204). After the transport of these monosaccharides into the enterocyte, they can be oxidized for energy, or exit the enterocyte via the basolateral membrane through passive transporters, and into the circulatory system (127). Once in the bloodstream, the resulting average blood glucose levels in the pig is around 6mM, in tilapia it is around 5mM, and in rainbow trout it is around 3mM, all fed on a commercial diet (85, 158, 208).

The digestion and absorption process of carbohydrates can differ between species, depending on many factors including the gastrointestinal tract anatomy. However, I focus on the transport mechanism of glucose specifically, which can vary between species. Understanding the functional GI anatomy in its contribution to glucose absorption is essential, and this is presented below.

2.2 Gastrointestinal Tract Functional Anatomy of Porcine, Nile Tilapia, and Rainbow Trout

Adequate nutrition is essential for all mammals and vertebrates, with the digestive system playing a crucial role in attaining this need (155). The GI tract has the same general function throughout all species, which is to digest and absorb ingested nutrients (74, 98, 139, 194). Its specific functions include the mechanical and chemical breakdown of the food components, followed by absorption mediated by transporters (74, 194). Additionally, specific anatomic functions of the GI tract can depend on many factors including the type of species (omnivore, carnivore, herbivore, etc.), the diet, the amount of food intake, and the natural environment (98, 194). Thus, the anatomy and specific functions of the GI tract can vary among different types of species (98, 194). The description of these species differences in GI tract anatomy allows for a better understanding of glucose absorption. The gastrointestinal tract functional anatomy for porcine, Nile tilapia and rainbow trout are presented below.

2.2.1 Porcine Gastrointestinal Tract Anatomy

Swine are omnivorous species with similar nutrient requirements and GI tract anatomy to humans (74, 98). Digestion of oligosaccharides and polysaccharides to monosaccharides (glucose, galactose, and fructose) and absorption of these components in pigs is essential for providing energy for various bodily functions (3, 114). The entirety of the GI tract is composed of four predominant tissue layers that are similar in humans and other mammals (194). The four layers moving from the innermost layer to the outermost layer consists of the mucosa, submucosa, muscularis, and serosa (139, 194). The mucosa surrounds the lumen of the intestine and is mainly composed of polarized epithelial cells (34). The submucosal layer supports the mucosa and contains the majority of blood vessels and nerves (34). The submucosa is followed by the muscularis layer, which is then covered by the serosal layer (34, 194). These four layers continue throughout the GI tract, being present in the stomach, small intestine, and large intestine (34, 194).

The porcine GI tract starts with the mouth, where absorption is negligible, but the saliva containing water, mucus, and salivary α-amylase begins digestion of the oligo- and polysaccharides (56). Following the mouth and esophagus is the stomach, which is the organ that allows for the mechanical breakdown of food components (Figure 1) (98, 194). Mechanical digestion is defined as the physical contraction and churning of the stomach contents to breakdown the food (194). Little carbohydrate digestion occurs in the stomach, which is primarily involved in protein and lipid digestion (56, 194). However, the stomach does serve to release the carbohydrates from complex food, allowing for carbohydrate digestion in the intestine (194). Once the food components have been digested to smaller particles, they pass through the pyloric sphincter situated at the end of the stomach, and into the small intestine (167).

The porcine small intestine is the longest organ of the GI tract (Figure 1) (98). The small intestine is the major site of digestion and absorption of carbohydrates (especially glucose), in addition to other nutrients (98, 139). This function is present in most mammals, vertebrates, and avian species (98, 139). The small intestine as a whole has a very large surface area that is coated with plicae (circular folds from the mucosal and submucosal layers), villi, and microvilli on the luminal side of the intestine (98, 139). The presence of the villi and microvilli increase the surface area of the small intestine from 30-60 fold (139). The villi are around 300-500 μm in

length and contain blood and lymphatic vessels, which transport the absorbed nutrients to other places in the body (194).

Additionally, the villi are covered by enterocytes/absorptive cells, which represent about 90% of the villi surface (98). The enterocytes have fine extensions called microvilli, which are around 1 μm in length (139). These microvilli are coated with a glycoprotein complex called the glycocalyx, and together, they further increase the absorptive capacity of the small intestine (139). The microvilli and glycocalyx complex are called the brush-border membrane (BBM) (139). The BBM has a variety of digestive enzymes and nutrient transporters that assist in the digestion and absorption of food components present in the chyme (139). This architecture of plicae, villi, and microvilli continues throughout the different sections of the small intestine (98, 139, 194).

The small intestine is further separated into the duodenum, jejunum, and ileum, where the duodenum is the first portion encountered after the stomach (Figure 1) (194). The pancreatic duct and common bile duct both secrete digestive enzymes and bile, respectively, into the duodenum, which makes the duodenum the main hub for degradation of food products (especially carbohydrates) from the stomach (194). The secretory juices from the pancreas and gallbladder contribute to a pH environment of around 6.1-6.7 for the entire pig small intestine (134). The duodenum is composed of four major cell types: the absorptive cells/enterocytes, the goblet cells, the granular cells, and the endocrine cells (194). The absorptive/enterocytic cells are mainly involved in nutrient uptake (194). The goblet cells assist in mucus secretion and protection, thus providing lubrication for the luminal mucosa (139). The granular cells, also called Paneth's cells, protect the lumen by secreting digestive enzymes like lysozymes, to break down invasive bacterial species (194). Finally, the endocrine cells are involved in providing regulatory hormones for various functions in the duodenum (194).

Although absorption occurs in the duodenum, the majority of nutrient absorption occurs in the following segments, the jejunum and ileum (194). The jejunum and ileum both differ from the duodenum by being smaller in diameter and having a reduced number of villi and plicae (194). Additionally, the ileum contains a small number of microbes which assist in initial fermentation of undigested feed (98, 194). Altogether, the duodenum, jejunum, and ileum of the porcine GI small intestine possess the molecular machinery for the digestion and absorption of

nutrients, including oligo- and polysaccharides to monosaccharides such as glucose, galactose, and fructose. (98, 194).

The porcine small intestine is followed by a pouch-like structure called the cecum (Figure 1) (98). The cecum size varies amongst mammals, with the pig's cecum being generally larger than humans (98). Additionally, the cecum pH environment is more acidic than the pH of the small intestine, because of the microbial environment fermenting undigested feed matter into short-chain fatty acids (SCFA) (134).

The cecum is followed by the large intestine/colon, and the small intestine is attached to the large intestine via the ileocecal junction (Figure 1) (194). The large intestine is not as long as the small intestine, and its absorptive properties are different as well (194). The digesta transit time through the large intestine is much longer than the small intestine (compare 2-16 hours for small intestine versus 20-40 hours for large intestine) (139). In contrast to the small intestine, the large intestine does not contain villi, and the microvilli along the colonic enterocytes are less packed together (98). Additionally, the large intestine in the pig contains a unique spiral colon, with digesta moving similarly to the rest of the large intestine (78). Finally, the lumen of the large intestine has a larger diameter than the small intestine (194).

The porcine large intestine is primarily involved in the absorption of water, minerals, electrolytes, and sodium, with little to no absorption of carbohydrate digestive products like glucose (98, 139, 194). By absorbing the majority of the water, it helps concentrate the undigested food particles traveling from the small intestine (194). The sodium/potassium ATPase is the main molecular machinery that creates the gradient for re-absorption of sodium and water into the cells (194). Additionally, the colon houses a diverse population of microbial organisms that ferment indigestible food components passed on from the small intestine (98, 139). Similar to the cecum, the undigestible matter in the colon is broken down by these microbes into volatile fatty acids (VFA), which are passively and actively absorbed across the intestinal epithelium (98, 139). The colon represents the last portion of the digestive tract that can digest and absorb indigestible material, before food and waste components are excreted through the rectum (139, 194).

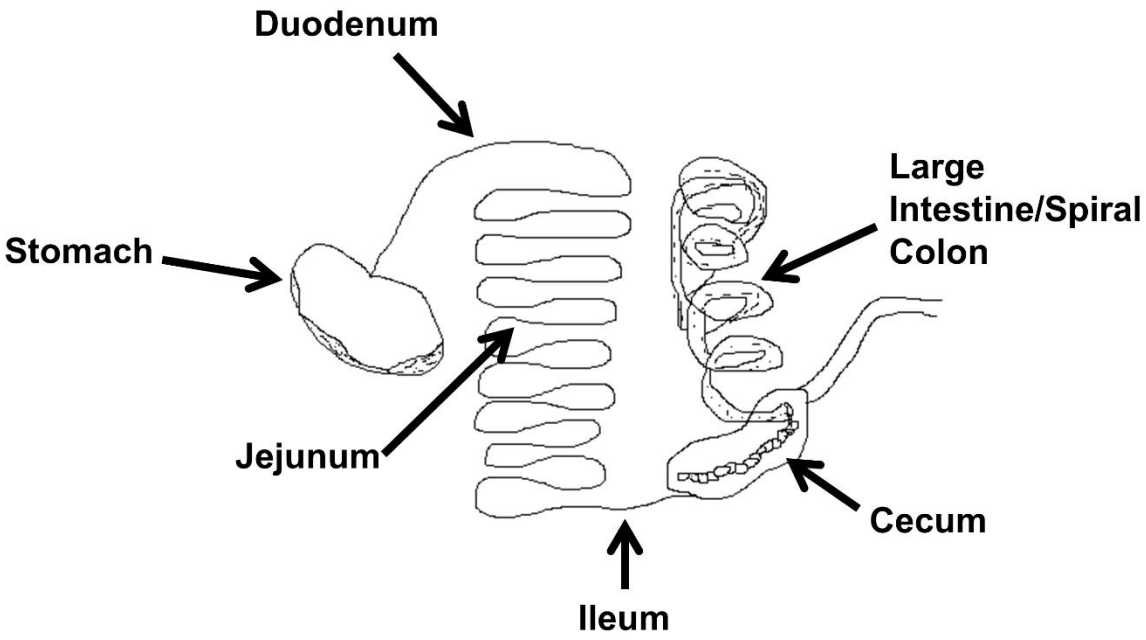

Figure 2.1 Schematic diagram of porcine gastrointestinal tract anatomy.

Schematic diagram representing the stomach, duodenum, jejunum, ileum, cecum, and large intestine and spiral colon.

2.2.2 Overview of Carbohydrate Digestion and Absorption in Fish

Carbohydrate digestion and absorption in fish has become a popular area of study as the inclusion of dietary carbohydrates in fish feed increases (26). Carbohydrates represent the cheapest energy source in fish feed (199). Similar to mammals, carbohydrate digestion and absorption primarily occurs in the small intestine of fish (38). However, the digestion and absorption of carbohydrates can vary between fish species, especially between omnivorous, carnivorous, and herbivorous species (74, 199). Nevertheless, all fish species can use carbohydrates as an essential source of energy, in addition to lipids and protein (199). However, a diet low in carbohydrates would result in more protein and lipids catabolized for energy use (199). Therefore, an appropriate amount of carbohydrates are incorporated into fish feed to reduce the catabolism of expensive protein for energy for farmed fish like rainbow trout and Nile tilapia (9, 59, 199).

The general trend of carbohydrate digestion in fish is that warm water, omnivorous fish tend to consume and digest carbohydrates more efficiently than cold-water, carnivorous fish (199). These differences can be attributed to a greater amount of α-amylase activity in warm water and freshwater fish in comparison to cold water and marine fish species (110, 151, 160). It was shown that in the omnivorous carp, the amylase activity was about 10-30 times greater than rainbow trout (88). Therefore, differences in carbohydrate digestion can exist between fish species.

Similar to mammals, after carbohydrate digestion, the carbohydrate products which are monosaccharides (glucose, galactose, and fructose) are transported through sodium-dependent and sodium-independent transporters (118, 162, 190). These transporters are present on the BBM or apical side of enterocytes along the intestine (4, 79, 130, 161). Depending on the fish species, the amount and locations of these transporters can vary along the intestine (38, 161). This includes some segments of the intestine containing a higher number of monosaccharide transporters than other segments (4, 18, 130). Studies of glucose absorption have been investigated in a limited number of fish species. Of these studies, one investigated the uptake of ^{3}H-D-glucose in brush-border membrane vesicles (BBMVs) of the Pacific copper rockfish (4). This study demonstrated that the kinetics of glucose transport differed between the intestinal segments, pyloric caeca and upper intestine (4). Additionally, another study investigating glucose uptake in herbivorous and carnivorous fish species in the Amazon found glucose

absorption occurred throughout the gastrointestinal tract (156). Nevertheless, the overview of glucose absorption in fish is similar to mammals (presented above). Overall, glucose uptake in the fish GI tract is currently an active area of study, as glucose transport kinetics and identities are discovered and characterized.

2.2.3 Nile Tilapia Gastrointestinal Tract Anatomy

Nile tilapia (*Oreochromis niloticus*) is an omnivorous fish from the Cichlid family of teleosts, and is one of the most popular fish farmed worldwide (38, 67). In the aquaculture industry, the use of carbohydrates in tilapia feed has become more popular since it provides a cheap energy source and tilapia can tolerate the carbohydrates better than their carnivorous counterparts (157).

Little is known about carbohydrate digestion in the mouth of tilapia species. Therefore, we will start with the stomach, which represents a small, sac-like structure that initially received speculation from many researchers on whether it was a functional stomach (Figure 2) (136, 138). However, once its histological characteristics were studied, this structure was confirmed as the stomach (31, 67, 138). Earlier studies of the stomach described it as a single functioning unit containing proteases and a low pH environment (138). Later research, especially by Caceci *et al.* 1997, found that the stomach contained three separate regions, the initial, middle and terminal regions, and they were structurally similar to the cardiac, fundic, and pyloric regions of mammalian stomachs (30, 138). The stomach as a whole has four tissue layers, the tunica mucosa, tunica submucosa, tunica muscularis, and tunica serosa, which is very similar to mammals (30). The tilapia stomach is shaped like a "Y," where the body of the "Y" represents the middle region, and the arms represent the initial and terminal regions of the stomach (30).

The start of the stomach directly after the oesophagus contains gastric glands and columnar epithelial cells (30). It has a smooth mucosal surface with no gastric pits, and merges with the middle region, which is defined by fibers of skeletal muscle and invaginations that contain secretory epithelium (30). The middle region is the largest of the two sections, and its secretory epithelium contains gastric pits and acinar glands (30). These secretory regions provide the distinction between the initial and middle regions of the tilapia stomach (30). This region is primarily responsible for secretion of enzymes and gastric acid (30). The middle region

is lined with simple columnar epithelial cells, and contains large blood capillaries (30). The terminal region continues from the middle region and joins with the small intestine (30). Its epithelial lining is similar to the middle region, containing columnar epithelial cells, but with less secretory function (30). Similar to mammals, the glands present in the terminal region, as well as in the initial region, are thought to secrete mucopolysaccharides that prevent erosion of the stomach epithelium from the gastric acid (31, 138).

The middle region is the most extensively studied by earlier researchers because it is the largest section (30). Therefore, the initial and terminal regions were missed because of their smaller architecture (30). The middle region is thought to represent the site of acid production since low pH values around 3-5 have been reported here (30). A study looking at the pH fluctuation in tilapia stomach fed blue-green algae (a natural part of their diet) found the pH to be the lowest in the middle region (1-4) compared to the initial (2.5) and terminal (2.0) regions (30, 136). Interestingly, the middle stomach is also called a blind diverticulum in tilapia (30). Food components have the ability to bypass the middle region of the stomach, since there is a diverticulum connecting the initial and terminal regions of the stomach (30). Some food components like plant material or resistant starches need a longer time to be digested by the gastric juices, so they reside in the middle region of the stomach, whereas components that are digested easily can bypass the middle region, and enter into the intestine (30). This was discovered when studying the digestibility of blue-green algae in Nile tilapia, where some algae in the stomach were brown due to the acidic conditions, but some of the algae remained green, as it passed along the anterior surface of the stomach, further supporting this bypass mechanism (136, 138). It was hypothesized that this mechanism evolved as tilapia switched from an omnivorous to herbivorous feeding strategy, as plant material incorporated into their diet needed longer time to digest (138).

Once the food components are digested in the stomach, it passes into the intestine where the pancreatic and bile secretions assist with further digestion (141). In Nile tilapia, the pancreas is dispersed along the neighboring blood vessels in the messentery to join the liver and form a hepatopancreas (137). The pancreatic duct, as well as the bile duct extends from the liver and empties into the intestine of tilapia (137).

Information on the intestinal anatomy of tilapia is more limited, with a few studies identifying tilapia intestine as macroscopically indistinguishable from post-stomach to the anus

(Figure 2) (138). However, microscopically, the differences observed distinguish the anterior portion of the intestine (stomach to ¾ length of the intestine) to be in the shape of a U-loop and is more thicker than the posterior portion of the intestine (rest of the intestine to the anus) (138). The posterior portion also has less-folded mucosa and many clear vacuoles in columnar epithelial cells (138). In a related species, *O.mossambicus*, the posterior part of the intestine is considered to be the rectum because it has shallow mucosal folds (153). Additionally, the entire intestine in the tilapia species, *O.mossambicus*, is in the form of a cork screw, and is about eight times longer than the fish itself, similarly in Nile tilapia (153).

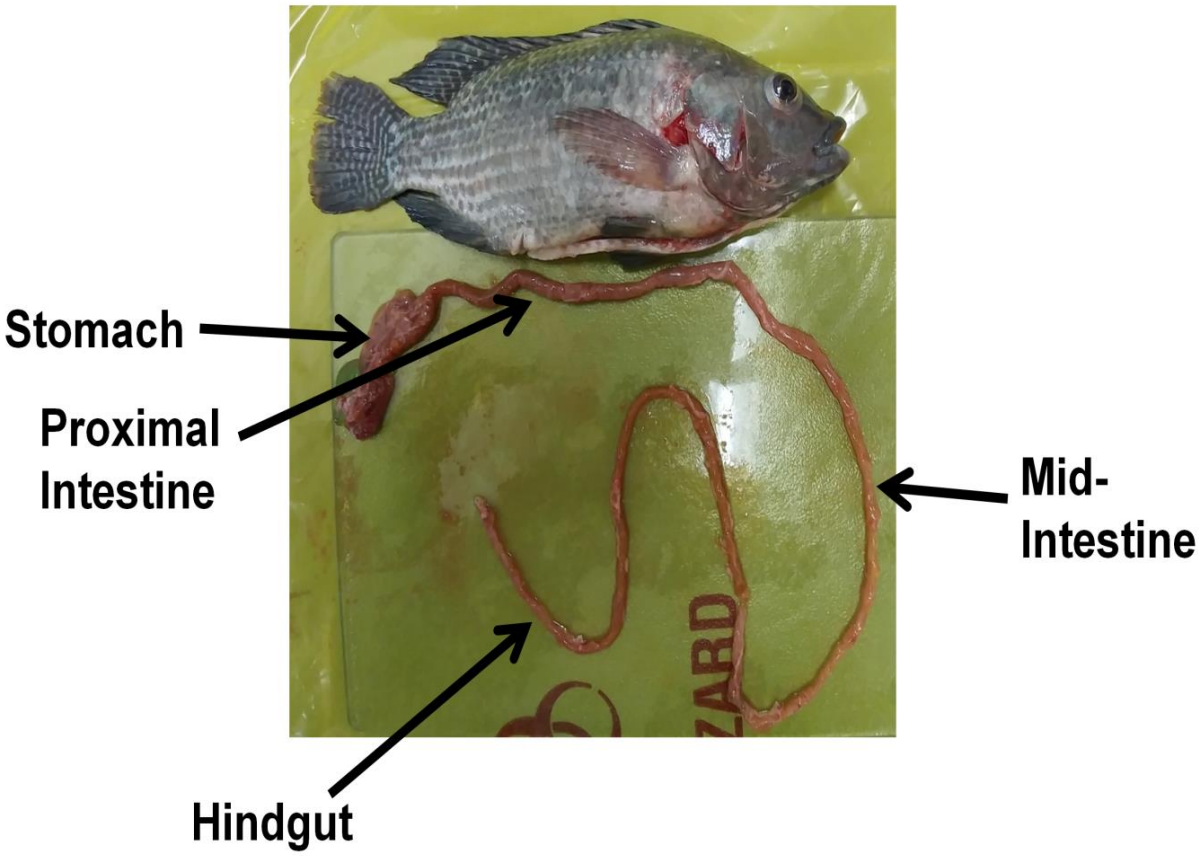

Figure 2.2 Image of Nile tilapia gastrointestinal tract anatomy.

Image of Nile tilapia gastrointestinal tract anatomy, representing the stomach, proximal intestine, mid-intestine, and hindgut.

2.2.4 Rainbow Trout Gastrointestinal Tract Anatomy

Rainbow trout is a strict carnivorous fish with a natural diet that consists of mainly protein and minimal carbohydrates (19, 45, 59, 102, 168). However, with carbohydrates providing a cheaper energy source than protein in fish feed, higher inclusions of carbohydrates are becoming more prominent in trout feed (66, 121, 160, 175). However, trout is a strict carnivore, and this carnivorous nature has influenced the development of its GI tract to present major differences with omnivorous species like the pig and tilapia.

The trout GI tract begins with a short esophagus that opens into a cardiac stomach consisting of inner circular and outer longitudinal smooth muscle (Figure 3) (27). There are valves present at the duct of the oesophagus and the stomach to prevent regurgitation of food material (27). The last portion of the stomach called the pyloric stomach is dominated by circular muscle (27). Finally, the pyloric sphincter at the distal end of the stomach opens up to the intestine (27).

The intestine can be distinguished from the stomach because it is histologically distinct, and contains no submucosa or muscularis mucosa layer (Figure 3) (27). Carnivorous fish, especially trout, have a region in the proximal portion of their intestine called the pyloric caeca (27). The pyloric caeca region occurs directly after the pyloric sphincter of the stomach and extends to the upper regions of the small intestine (214). They are blind projections that come off the upper portions of the small intestine to increase the surface area for absorption, similar to the function of villi in mammalian small intestine (27, 214). In brown trout, it was found that about 45 pyloric caeca come off the intestine, and it is thought that in carnivorous fish species, the number of pyloric caeca can increase as the fish length increases (27, 149, 214).

Pyloric caeca are thought to be the major site for amino acid, monosaccharide, and lipid absorption (168). It has been proposed that the pyloric caeca has the largest amount of monosaccharide uptake in trout and cod fish, compared to the rest of the intestine (52). However, the digesta transit time through the pyloric caeca is similar to the rate of passage in the rest of the intestine (52). These functions of the pyloric caeca continue to be studied, including a study that found trypsin in the pyloric caeca, suggesting this organ as a site for protein degradation (117). The pyloric caeca is not present in omnivorous mammals, like the pig, as well as herbivorous and omnivorous fish, like Nile tilapia (27). It is postulated that the major importance of the pyloric caeca for carnivorous fish is to increase the absorptive capacity to

compensate for the shorter GI tract present in these species (2, 27, 52). Additionally, the luminal epithelium of the pyloric caeca were found to contain large microvilli, where monosaccharide, amino acid, fat, water and sodium absorption occur (214). In contrast, the longer GI tract in herbivores and omnivores increases the transit time for chyme, allowing for a longer absorption period (5). This function of increasing absorptive capacity is supported by the pyloric caeca's contribution to total absorptive surface area of the GI (5). The pyloric caeca's contribution to the total surface area of the intestine is: about 70% in trout, 69% in cod, 42% in largemouth bass, and about 12% in striped bass to the total surface area (52). Finally, the pyloric caeca lacks microflora, thus suggesting no bacterial fermentation occurs in this region (214).

The pancreas in rainbow trout is a diffusive gland, which lies between the pyloric caeca (197). Therefore, the pancreas in trout does not connect with the liver, as it does in tilapia (described above) (197). However, the bile duct that emerges from the liver does penetrate the pancreas and merges with the pancreatic duct, emptying into the proximal portions of the intestine (midgut) (197).

In addition to the pyloric caeca, the small intestine that follows continues the absorptive process already occurring in the pyloric caeca (Figure 3) (27). No histological differences were observed between the small intestinal portion that followed (called midgut, or the duodenal-ileal sections in brown trout) the pyloric caeca (27). However in the northern pike, the small intestine was found to contain columnar and goblet cells, possibly involved in mucous secretions (23). The small intestine joins with the rectum/hindgut of trout, which is visibly and histologically distinct from the rest of the intestine (27). The hindgut/rectum is thicker and larger in diameter, and consists of a darker pigment with circular surrounding blood vessels (Figure 3) (27). The rectum is also known to absorb nutrients in carnivorous fish (2). Comparison between the gut of the carnivorous trout and cats show that they are the only species (as well as a few other carnivorous species) that have the stratum compactum layer throughout their intestine (27). This layer is a dense collagen layer that helps strengthen and preserve the gut from any violent extensions from the eaten prey (27). These carnivorous species have a habit of swallowing large pieces of food that may be whole or active animals, which can violently stretch and damage the intestine (27). Therefore, the stratum compactum layer evolved to adapt to this feeding strategy (27). Similarly to the pig and tilapia, trout's GI tract ends with the rectum, which is involved in the excretion of undigested food material and waste products (27).

This description of the functional anatomy of the gastrointestinal tract of pig, Nile tilapia, and rainbow trout give context and background to the absorptive process described and studied in the following text and chapters.

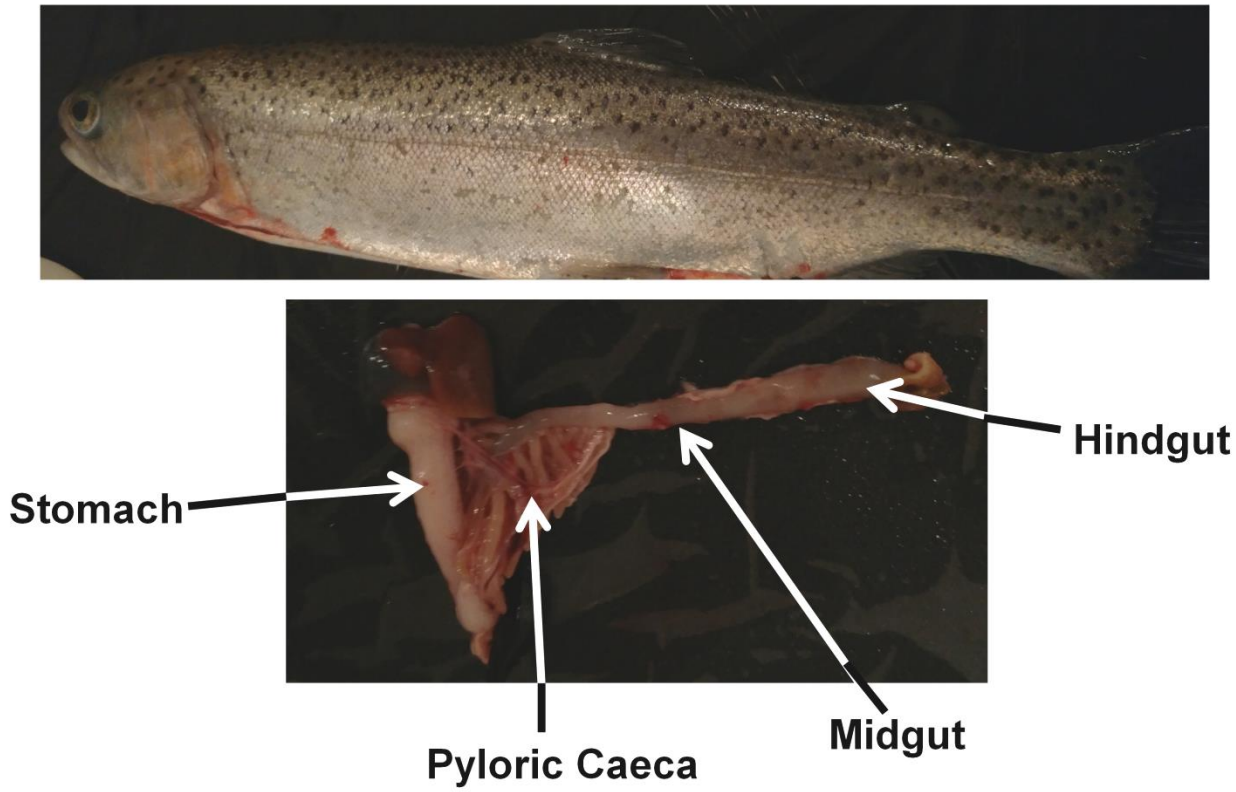

Figure 2.3 Image of Rainbow trout gastrointestinal tract anatomy.

Image of rainbow trout gastrointestinal tract anatomy, representing the stomach, pyloric caeca, midgut, and hindgut.

2.4 Glucose Transporters

2.4.1 Overall Function in Intestinal Epithelium

Glucose is the major constituent derived from carbohydrate digestion and is absorbed across glucose transporters present on the BBM (5, 66, 86, 133, 161). Glucose transporters are present in all mammals, avian, and fish species (4, 5, 7, 68, 75, 130, 170, 196, 202). Sodium-dependent glucose transporters function using the sodium/potassium (Na+/K+) ATPase present on the basal side of these cells to provide a concentration gradient for Na+ to enter into these cells from the luminal side (Figure 4) (4, 55, 75, 170, 202). The presence of sodium-dependent glucose transporters is generally on the BBM/apical side of enterocytes, as well as other cells dispersed throughout the body, and they primarily belong to the solute carrier family member 5A (SLC5A) (75, 84, 112). Comparatively, the sodium-independent glucose transporters are present on both the BBM/apical side and the basal side of enterocytes, as well as other cells throughout the body, and are mainly part of the solute carrier family member 2A (SLC2A) (18, 70, 95, 106, 133, 179). These two families represent the majority of transporters involved in glucose uptake in the entire body of all species. Finally, these families are the most extensively studied and characterized.

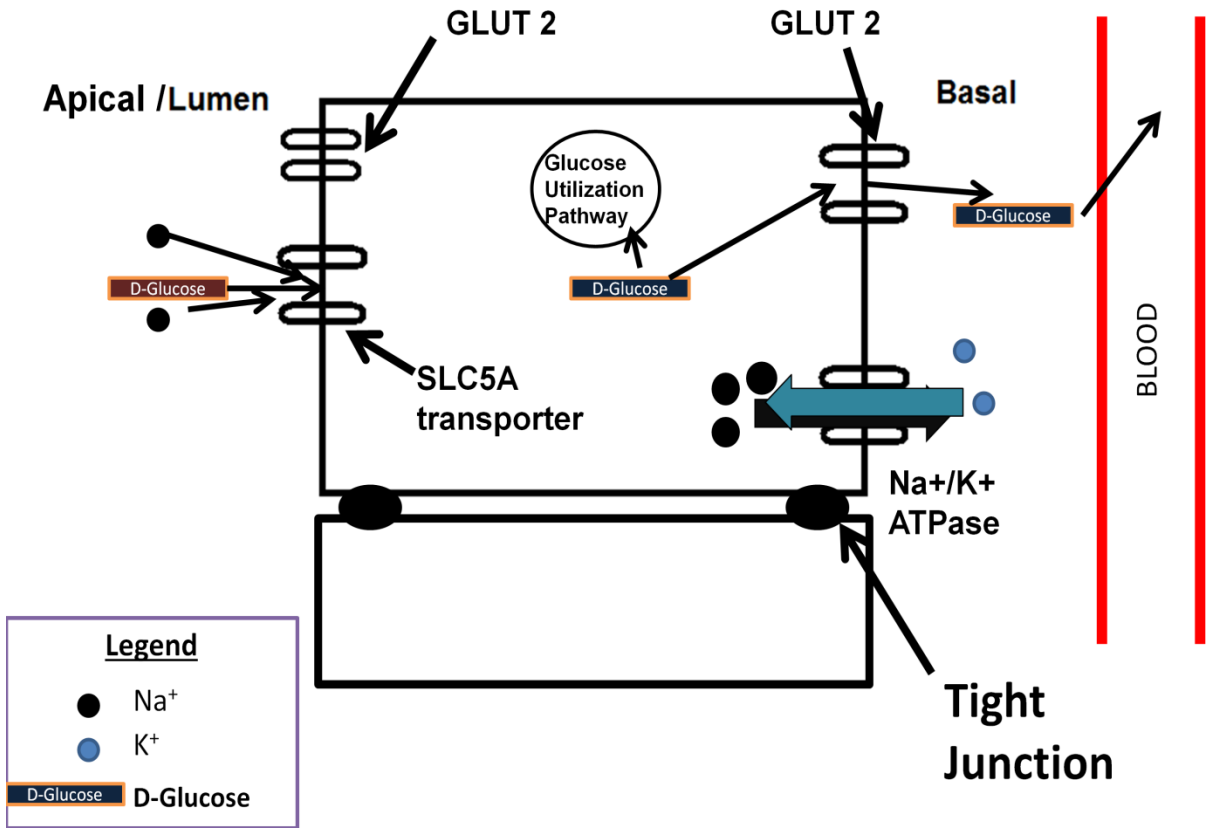

Figure 2.4 Overview of glucose absorption across mammalian enterocyte.

Schematic diagram of sodium-dependent and sodium-independent glucose transport across a mammalian enterocyte.

2.4.2 SLC5A family

The SLC5A family is represented by 12 members of sodium-dependent transporters for glucose (57, 131, 169, 187). Apart from the small intestine, their expression and function exist throughout the mammalian system, including the kidney, thyroid gland, and central nervous system (204). The identities and functions of these 12 members have been characterized using heterologous expression systems like oocytes, or studied using brush-border membrane vesicles and Ussing chambers (51, 64, 191, 204, 212). Most of the genes in this family consist of 14-15 exons, except for SLC5A8 and SLC5A3 (57, 131, 169, 187). Additionally, differences of functions for the same transporter were found between species (13, 53, 204). This includes SLC5A4 in the human characterized as a glucose sensor in neuronal and muscle cells, however in pigs, it was found to function as a sodium-dependent glucose transporter (13, 53, 129). Collectively, all of the SLC5A members have the ability to transport more than one type of substrate, and they all share the common function of transporting substrates using the electrochemical gradient of sodium (204).

Finally, these SLC5A transporters are characterized using Michaelis-Menten fits (4, 22, 55, 75, 132, 147, 148). These fits characterize protein transporters that saturate at certain concentrations of substrate, thus yielding Vmax and Km values (4, 22, 55, 75, 132, 148). A Vmax value characterizes the maximum rate of the transporter, and it is expressed in units based on the technique used (39, 202). In the literature, the Vmax value represents the capacity, where a transporter exhibits either low-capacity (saturation at low concentrations of glucose) or high-capacity (saturation at high concentrations of glucose) transport of glucose (4, 55, 75, 177, 202). A Km value represents the substrate concentration at half of the Vmax value (or half maximum saturation), and it is also used to represent the affinity of the substrate to the transporter's active site (39, 97). The affinity can be represented as either low-affinity (sensitivity to transport at high glucose concentrations) or high-affinity (sensitivity to transport at low glucose concentrations) (4, 55, 75, 177, 202). A summary of the major characteristics for each of these transporters are presented in Table 2.1. Additionally, the identities and functions of these transporters present in mammals and fish are explained in more detail below.

Table 2.1 SLC5A Family members.

SLC5A member	Tissue Expression	Major Substrate Transported	Co-Transporter Ion
SLC5A1/SGLT1	Small Intestine, kidney, brain, prostate, trachea	Glucose, Galactose	Na^+
SLC5A2/SGLT2	Kidney, brain, liver, heart muscle	Glucose	Na^+
SLC5A3/SMIT1	Brain, heart, kidney, lung	Myo-inositol, glucose	Na^+
SLC5A4/SGLT3	Cholinergic neurons, skeletal muscle, kidney, uterus, testis	Glucose (some species)	Na^+ (some species)
SLC5A5/NIS	Thyroid, lactating breast, stomach	Iodide	Na^+
SLC5A6/SMVT	Brain, heart, kidney, placenta	Biotin, lipoate, panthothenate	Na^+
SLC5A7/CHT	Spinal cord, medulla	Choline	Na^+/Cl^-
SLC5A8/SMCT1	Small intestine, kidney, brain, retina, muscle	Monocarboxylates	Na^+
SLC5A9/SGLT4	Kidney, small intestine, brain, liver, heart	Mannose, fructose, glucose	Na^+
SLC5A10/SGLT5	Kidney cortex	Mannose, fructose, glucose	Na^+
SLC5A11/SMIT2	Thyroid, brain, heart, muscle, spleen, liver	Myoinositol, D-chiro-inositol	Na^+
SLC5A12/SMCT2	Intestine, brain, retina, muscle	Monocarboxylates	Na^+

Summary of the characteristics of the SLC5A members. Adapted from Wright 2013.

2.4.2.1 SLC5A1/SGLT1

SLC5A1 represents the founding member of this family because it was the first transporter cloned and characterized (24, 97, 191, 204). The common name for SLC5A1 is SGLT1 or sodium-glucose co-transporter type 1 (53, 75, 187, 191, 204). The identity of this transporter was first proposed in 1956 as one of the apical/brush-border components of glucose absorption in the intestine (105). It was also found in the brush-border kidney of mammals, where it was involved in glucose reabsorption (13, 204). Following this discovery, the rabbit SGLT1 was cloned in 1987 (105). It revealed a high-affinity, low-capacity transporter for glucose, meaning it had high sensitivity to glucose, and saturated at low concentrations (55, 203). Additionally, SGLT1 was found to transport glucose and sodium at a ratio of 1:2, respectively (204).

The versatility of SGLT1/SLC5A1 in transporting other substrates along with sodium includes the monosaccharide galactose, which is another major monosaccharide generated from carbohydrate digestion (43, 165, 204). However, SGLT1/SLC5A1 transports galactose at a much lower affinity than glucose, and mutations in the SLC5A1 gene lead to glucose-galactose malabsorption in humans (43, 165, 204). Finally, inhibitors against SGLT1/SLC5A1 were used to further its characterization, and it includes the SGLT1 inhibitor, phloridzin dihydrate (4, 130, 177, 184, 200). Phloridzin dihydrate is a phenyl-β-glucoside, and was first isolated in the 1800s where it was used in diabetes and renal physiology research to inhibit against the high-affinity, low-capacity (Ha/Lc) SGLT1 transporter (64, 96, 116, 128). This inhibitor has been used in many studies ranging from mammals to fish, to inhibit SGLT1 (75, 77, 84, 86, 96, 116, 206).

The SGLT1/SLC5A1 transporter has been studied in many different species. In humans, SGLT1/SLC5A1 was identified as the major sodium-dependent glucose transporter on the brush-border membrane of the small intestine and proximal tubules of the kidney (97). Additionally, it was confirmed as a high-affinity, low-capacity transporter for glucose that was inhibited by phloridzin dihydrate (97). Similarly, in a human colon epithelial cell line called HT-29-D4 cell line, the expression of SGLT1/SLC5A1 confirmed a high-affinity, low-capacity transporter, reporting a Km value of 1.2 ± 0.12mM and a Vmax value of 3.24 ± 0.25 nmol/mg protein/min (147). Additionally, identification of the protein in this study confirmed the presence of SGLT1/SLC5A1 transporters on the apical membrane, using rabbit SGLT1/SLC5A1 antibodies (147). In another mammalian species the rat, glucose transport in perfused rat jejunal

membranes demonstrated sodium-dependent glucose transport mediated by SGLT1/SLC5A1, as the replacement of sodium with choline eliminated transport of glucose through SGLT1/SLC5A1 (107). Finally, in the pig, SGLT1/SLC5A1 expression was greater in the jejunal segment of the small intestine, in comparison to the duodenum and ileal sections, suggesting most of the high-affinity, low-capacity sodium-dependent transport of glucose occurred in the jejunum (84, 112).

In fish, the mRNA expression of SGLT1/SLC5A1 has been shown including in salmon and rainbow trout (163). Additionally, SGLT1/SLC5A1 was found to be upregulated when a high glucose load is administered in fish, and these effects were seen in the carnivorous rainbow trout, and the omnivorous black bullhead fish (121, 163, 177). Finally, studies on sodium-dependent glucose transport along the intestine of carnivorous fish found higher SGLT1/SLC5A1 expression along the pyloric caeca and upper intestine, especially in the gilthead sea bream (172). It was found that the SGLT1/SLC5A1 transporter was inhibited with phloridzin dihydrate, with kinetic parameters that were similar to mammalian SGLT1/SLC5A1 characteristics (172). Overall, SGLT1/SLC5A1 seems to be involved in sodium-coupled Ha/Lc transport in the intestine and kidney of many species.

2.4.2.2 SLC5A2/SGLT2

SLC5A2, also known as sodium-glucose cotransporter 2 (SGLT2) was the second transporter identified in this family (203, 204). This transporter was identified in earlier studies using BBMVs from rodent proximal tubule sections of the kidney cortex (204). It was first found to be responsible for the majority of glucose reabsorption in the kidney, and represented a low-affinity, high-capacity (La/Hc) system for glucose in comparison to SGLT1/SLC5A1 (128, 203, 204). Specifically, the Km and Vmax values for SGLT2/SLC5A2 was found to be higher for glucose than SGLT1/SLC5A1 (128). SGLT2/SLC5A2 transport stoichiometry also differed from SGLT1/SLC5A1 in that it co-transported glucose at a 1:1 ratio with sodium (128). Additionally, it was found to be a poor transporter of galactose (128). Nonetheless, the transporter seems to play a significant role in glucose absorption, particularly in the kidney (128).

Since its discovery, SGLT2/SLC5A2 has been identified in the mammalian kidney and intestine of multiple species, including pigs, humans, and rabbits (97, 128). Its identification and importance in kidney glucose reabsorption made it a potential target for novel therapeutic drugs

against diabetes mellitus (93, 97, 116, 143, 154). Therefore, specific glycosides were created to specifically target SGLT2/SLC5A2 (93, 116, 143, 154). These inhibitors included dapagliflozin and canagliflozin, which had more sensitivity towards SGLT2/SLC5A2 than SGLT1/SLC5A1 (93, 116, 143, 154).

However, in contrast to mammals, its identity and importance in fish species is minimal. Specifically, SGLT2-like transporters were identified in the shark (*Squalus acanthias*) kidney (7). However, a SGLT transporter identified in rainbow trout kidney shared similar amino acid identity with both mammalian SGLT1/SLC5A1 and SGLT2/SLC5A2 transporters, suggesting fish have an SGLT2-like transporter with similar function to those in mammals (7).

2.4.2.3 SLC5A3/SMIT1

SLC5A3, or sodium-myoinositol cotransporter 1 (SMIT1) differs from the other members of the SLC5A family because it primarily transports myo-inositol (11). Myo-inositol is important in the signal transduction pathways, and it is a precursor for compounds like phosphoinositides and inositol phosphates (11). SMIT1/SLC5A3 was the first myo-inositol transporter identified, and it is primarily present in the brain and renal medulla (11, 42, 111). Apart from myo-inositol being a preferred substrate, it does transport glucose but at a lower affinity than inositols (11, 204). Physiologic concentrations for myo-inositols in the plasma are around 30 μM, which is lower than plasma glucose concentrations (around 3-5mM in mammals), thus suggesting SMIT1/SLC5A3 is very sensitive for myo-inositols (11, 158). Overall, the primary function of SMIT1/SLC5A3, apart from being a low-affinity glucose transporter, was its involvement with osmoregulation, by maintaining osmotic balances for neural and renal cells in hypertonic environments (111, 185).

2.4.2.4 SLC5A4/SGLT3

SLC5A4, or sodium-glucose cotransporter 3 (SGLT3) was found to have different functions depending on the type of species (53). Specifically, in humans it was found to function as a glucose sensor in neuronal and muscle cells, whereas in the pig, it was characterized as a low-affinity, sodium-dependent glucose transporter (53, 129, 171, 204). Additionally, the pig SGLT3/SLC5A4 was initially called a neutral amino acid transporter (SAAT1), and then later

identified as pig SGLT2, and finally confirmed to be pig SGLT3/SLC5A4 (53). In pigs, SGLT3/SLC5A4 demonstrated intermediate functions between SGLT1/SLC5A1 and SGLT2/SLC5A2, where it exhibited similarities to SGLT1/SLC5A1 by transporting sodium and glucose at a ratio of 2:1 respectively, and it showed similarities to SGLT2/SLC5A2 for its low affinity for both glucose and sodium (53). Finally, SGLT3/SLC5A4 was found to be sensitive to phloridzin dihydrate, but not as sensitive as SGLT1/SLC5A1 (204).

As mentioned above, one of the more interesting finds for SGLT3/SLC5A4 was the difference in its function between humans and pigs (53, 171). These differences in function were found to be due to a single amino acid (17, 53, 171). In human SGLT1/SLC5A1, the amino acid at position 457 (glutamate) was found to play a critical role in glucose binding and transport (17). In fact, a mutation of this amino acid to another residue causes glucose-galactose malabsorption in humans, thus emphasizing the important role of this residue (17). In human SGLT3/SLC5A4, the residue at position 457 is a glutamine, and substituting this glutamine with a glutamate found an increase in glucose uptake by about 100 fold compared to native human SGLT3/SLC5A3 expressed in ooctyes (17). Thus, SGLT3/SLC5A4 illustrates the diversity in function of specific SLC5A members between different species.

2.4.2.5 SLC5A5/NIS

SLC5A5, or sodium-iodide cotransporter (NIS) is a sodium/iodide symporter that transports iodide using the downhill gradient of sodium (48, 62). It is dominantly expressed in the thyroid gland of mammalian species, and transports iodide necessary for the production of thyroid hormones, T3 and T4 (48, 62). NIS/SLC5A5 was first cloned in 1996 from rats, and later found to transport sodium and iodide at a ratio of 2:1 respectively, similar to the ratio of sodium to glucose in SGLT1/SLC5A1 (62). Even though NIS/SLC5A5 does not transport glucose, its function of transport by coupling iodide transport to the downhill gradient of sodium, justifies its inclusion with the SLC5A family members (62).

2.4.2.6 SLC5A6/SMVT

SLC5A6, or sodium-multivitamin transporter (SMVT) was identified as a sodium-dependent vitamin transporter, for substrates like panthothenic acid, biotin, and alpha-lipoic acid

(195). Similarly to SMIT1, it is widely distributed throughout the mammalian body, and it shares a high sequence similarity with NIS (204). Additionally, it transports sodium and vitamins at a 2:1 ratio respectively, similar to SGLT1/SLC5A1 and NIS/SLC5A5 (195). The SMVT/SLC5A6 transporter has been studied in human placental BBMVs, as well as BBMVs from rat, rabbit, and human kidney and intestine (195). Similarly to NIS/SLC5A5, SMVT/SLC5A6 is not a transporter of glucose, but it does utilize the electrochemical gradient of sodium to cotransport vitamin molecules, which allows it to be a part of the SLC5A family members (195).

2.4.2.7 SLC5A7/CHT1

SLC5A7, or chloride-dependent sodium-choline transporter (CHT1) was characterized as a member of this family due to its co-transport with sodium (146). However, it differs from the other members of the SLC5A family because it is dependent on the chloride electrochemical gradient, in addition to the sodium electrochemical gradient (204). Similarly to NIS/SLC5A5 and SMVT/SLC5A6, its main substrate is choline and not glucose (146). It is mainly expressed in the central nervous system, and its absorption of choline contributes to the acetylcholine (type of neurotransmitter) synthesis pathway (146). Despite its dependence on the chloride gradient and transporting choline as its preferred substrate, its function is more homologous to the SLC5A members than the neurotransmitter transporters (146). Finally, this transporter is sensitive to changes in pH, which can affect the concentration gradient of chloride, thus impeding choline uptake by CHT1/SLC5A7 (204).

2.4.2.8 SLC5A8/SMCT1

SLC5A8, or sodium-coupled monocarboxylate transporter 1 (SMCT1) primarily transports monocarboxylate substrates that include lactate, pyruvate, and nicotinate (72). The stoichiometry of transport for sodium to substrate was found to be 2:1, similar to the ratio of sodium to glucose in SGLT1/SLC5A1 (41). SMCT1/SLC5A8 was characterized as a high-affinity transporter for lactate in the mouse kidney cortex (72). Its function in the kidney of mice was found to be similar to the function of SGLT1/SLC5A1 in mammalian kidneys, where both

functions were to re-absorb any left over substrate (glucose or lactate) in the distal proximal tubules (72).

2.4.2.9 SLC5A9/SGLT4

SLC5A9, or sodium-glucose co-transporter 4 (SGLT4) is primarily known as a mannose transporter (73, 183). This transporter is mainly expressed in the liver, intestine, and kidneys of mammals (204). Studies in COS-7 cells found that it was able to transport α-methyl-D-glycopyranoside along with sodium, resulting in a Km of 2.6mM, which defined it a very low-affinity transporter (183). However, the transport of mannose was at a much higher affinity, and was found to exhibit transport into COS-7 cells (183). In fact, the uptake of α-methyl-D-glycopyranoside was impeded more by D-mannose than D-glucose, further confirming mannose as a preferred substrate for this transporter (183). Finally, in comparison to SGLT1/SLC5A1, its sensitivity to phloridzin was found to be much less (204).

2.4.2.10 SLC5A10/SGLT5

SLC5A10, or sodium-glucose cotransporter 5 (SGLT5) is similar in function to SGLT4/SLC5A9, where it has a much higher affinity for mannose than glucose (73). It is mainly expressed in the kidney cortex of humans (73). Apart from its high-capacity transport for mannose, it was also found to transport fructose at a high-capacity (73). However, its transport of glucose, galactose, and α-methyl-D-glycopyranoside were at a much lower capacity in comparison (73). Finally, the inhibition of α-methyl-D-glycopyranoside transport in SGLT5/SLC5A10 with SGLT2/SLC5A2 inhibitors canagliflozin, dapagliflozin, empagliflozin, phlorizin, remogliflozin, and T-1095A had a low potency, revealing poor inhibition of SGLT5/SLC5A10 with SGLT2/SLC5A2 inhibitors (73).

2.4.2.11 SLC5A11/SMIT2

SLC5A11 was formally identified as sodium-glucose cotransporter 6 (SGLT6), but is currently identified as a sodium-myoinositol co-transporter 2 (SMIT2), because of its higher affinity to transport inositols than glucose (124). It is the second isoform of SMIT, exhibiting

similar functions to SMIT1 (124). In contrast to SMIT1, it is a low-affinity myo-inositol transporter and a very-low affinity glucose transporter (124). SMIT2/SLC5A11 transports both myo-inositol and D-chiro-inositol, which is mostly involved in the bioactivity of insulin (124). Similar to the function of SGLT2/SLC5A2 in kidneys, SMIT2/SLC5A11 is involved in the bulk reabsorption of myoinositol, demonstrating a low-affinity and high-capacity for myo-inositol (124). Finally, this transporter has the lowest amino acid sequence similarity with SGLT1/SLC5A1 (204).

2.4.2.12 SLC5A12/SMCT2

SLC5A12, or sodium-coupled monocarboxylate transporter 2 (SMCT2) is similar in function to SMCT1/SLC5A8, in primarily transporting monocarboxylates like lactate and pyruvate (72). It is widely expressed throughout the mammalian body, but is predominant in the kidney cortex (72, 204). Both SMCT1/SLC5A8 and SMCT2/SLC5A12 share about 75% amino acid sequence similarity (72). However, in comparison to SMCT1/SLC5A8, SMCT2/SLC5A12 is a low affinity monocarboxylate transporter with a Km for lactate around 35mM (compare Km around 0.25mM for lactate by SMCT1/SLC5A8) (72). Finally, both transporters exhibit sodium-dependency of substrate transport, but SMCT1/SLC5A8 demonstrates stronger electrogenic signals than SMCT2/SLC5A12 (72).

2.4.3 SLC2A Family

SLC2A is the second dominant family of glucose transporters that do not require energy, nor the co-transport of glucose with sodium (97, 203). They are facilitative glucose transporters, transporting glucose down its concentration gradient (108). These transporters either passively diffuse glucose across the BBM or via the basolateral membrane to exit the cell (80). The first member of this family, GLUT1 (SLC2A1) was first identified in 1985, and since then, 13 members of this family have been identified and most have been functionally characterized (91, 108, 203). The major characteristics of these transporters are presented in Table 2. Their general structure represents a 12-membrane spanning domain, with the N- and C- termini buried intracellularly (203). The GLUTs range between 28-65% identity in nucleotides with each other, but they all carry two common amino acids, glycine and tryptophan (203). Similar to the SLC5A

members, GLUT members vary in the type of substrates they transport (108, 203). The GLUTs are further classified into three families, which are explained in more detail below.

Table 2.2 SLC2A Family members.

SLC2A member	Tissue Expression	Major Substrate Transported
GLUT1	**Erythrocytes, brain, kidneys, muscle, liver, adipose tissues**	**Glucose**
GLUT2	**Liver, pancreatic beta cells, small intestine, kidneys**	**Glucose, fructose**
GLUT3	**Brain, adipose tissue, liver, adult skeletal muscle**	**Glucose**
GLUT4	**Heart, skeletal muscle, white and brown adipose tissue, brain**	**Glucose**
GLUT5	**Small intestine, testes, kidneys**	**Fructose, glucose**
GLUT6	**Brain, spleen, leucocytes**	**Glucose**
GLUT7	**Small intestine, colon, testis, prostate**	**Glucose, fructose**
GLUT8	**Liver, heart, testes, adipose tissue, brain**	**Glucose**
GLUT9	**Liver, kidneys**	**Glucose, fructose, urate**
GLUT10	**Skeletal, heart, pancreas, liver, brain, placenta, kidney**	**Glucose**
GLUT11	**Short variant – heart, skeletal muscle** **Long variant – lungs, trachea, brain**	**Short variant – glucose** **Long variant – fructose**
GLUT12	**Heart, skeletal muscles**	**Glucose**
HMIT	**Brain**	**Glucose, inositols**

Summary of the major characteristics of the SLC2A family members.

2.4.3.1 Class 1: GLUTs 1- 4

Class 1 represents the GLUT1-4 transporters, all involved in the facilitative transport of glucose (108). GLUT1 (SLC2A1) is mostly expressed in the brain and erythrocytes, with some expression in the muscle, liver, and adipose tissues (140). GLUT2/SLC2A2 demonstrates low-affinity for glucose, with its expression dominating in the liver, pancreatic beta cells, the small intestine, and kidney (80, 108). GLUT2/SLC2A2 has been extensively studied in the literature, and its characterization is described in more detail below (see section 2.4.3.1.1 GLUT2). GLUT3 (SLC2A3) is a high-affinity glucose transporter primarily expressed in the brain (103). GLUT3/SLC2A3 is mostly found in tissues where there are high levels of glucose (103). GLUT4, coded by the gene SLC2A4 is another glucose transporter that has been extensively studied because it is the only one sensitive to insulin (181). It is present in the heart, skeletal muscle, adipose, and brain tissues, and it transports glucose from the blood plasma into the tissue (181). When blood glucose levels rise, insulin binds to insulin receptors on skeletal muscle tissues, which initiates a cascade resulting in GLUT4/SLC2A4 translocation to the membrane, thus increasing glucose uptake into cells (181, 203).

The identification and characterization of GLUTs 1-4 in fish species is more limited (18). One study attempting to identify GLUT1 and GLUT4 in the white muscle of eel, rainbow trout and catfish, using northern blots of mammalian GLUT1 and GLUT4 probes, and found no hybridization in any of the tissues (121). However, this does not conclude the lack of GLUT1 or GLUT4 in these fish species, but it provides evidence that GLUT1 and GLUT4 transporters in the eel, rainbow trout, and catfish may be drastically different in sequence similarities to their mammalian counterparts (121). Apart from the intestine, GLUTs have been identified in other tissues in fish, specifically in the Atlantic cod where GLUT3 was found expressed in the kidney (76). Comparatively, GLUT2 was expressed in the liver, intestine, and kidney of rainbow trout, and it shared 58% and 52% nucleotide sequence similarity with chicken and mammalian GLUT2 sequences, respectively (6). Additionally, this GLUT2 called OmnyGLUT2 in rainbow trout had an extracellular loop that connected the first and 12^{th} transmembrane segments of this transporter (6). This was associated with an additional 14 amino acids in trout compared to humans (6). In contrast in Nile tilapia, GLUT1 was cloned from the cDNA library and exhibited 74% homology with mammalian GLUT1 (91). It was called tGLUT1 and present in the white muscle, where it was further characterized to increase its expression in the white muscle after a high glucose load

or carbohydrate-rich meal (91). Finally, tGLUT1 was similar to mammalian GLUT1 based on amino acid and mRNA levels, as well as its function as a constitutive glucose transporter at basal conditions (91). Comparisons and differences between fish and mammalian GLUTs exist and become more prominent as more GLUTs are identified and characterized in fish species.

2.4.3.1.1 GLUT2

It would appear that GLUT2 is the major or only GLUT involved in glucose absorption in the small intestine (80). In 1960, two components of glucose absorption in the small intestine were identified (80). The first was SGLT/SLC5A1, which represented active uptake of glucose into intestinal epithelial cells (80). The second transporter was a diffusive component that did not appear to saturate, even when glucose concentrations were higher than 100mM (80).

It has been proposed with supporting studies that GLUT2/SLC2A2 traffics to the apical membrane of enterocytes when luminal glucose concentrations reached levels higher than 30-50mM (80). However, the trafficking of GLUT2 to the apical membrane was highly reliant on SGLT1/SLC5A1 activation (80). When glucose is present in the lumen of the small intestine, SGLT1 is first activated in transporting glucose into the enterocytes (80, 97). Its active transport initiates the function of another enzyme called protein kinase C βII (PKC βII) (80). PKC βII initiates downstream processes to activate GLUT2's translocation to the brush-border membrane, which then assists in the absorption of higher amounts of glucose (80). GLUT2/SLC2A2 trafficking to the apical side is very rapid, usually within a couple of minutes, to start transporting the glucose at the high concentrations (80). Further confirming this mechanistic link between PKC βII and GLUT2/SLC2A2, it was found when PKC βII levels were high, GLUT2 levels were high as well, indicating a correlation between the two (80). To understand the commensal behaviour between SGLT1/SLC5A1 and GLUT2/SLC2A2, it was demonstrated that when sodium was replaced with choline or potassium, GLUT2/SLC2A2 levels on the apical side would decrease as SGLT1/SLC5A1 would not function (80). Comparatively, phloridzin dihydrate inhibition of SGLT1/SLC5A1 also decreased levels of GLUT2/SLC2A2 on the apical membrane of enterocytes (80).

However, other studies found GLUT2/SLC2A2 to have more of a permanent position on the BBM of diabetic and insulin-resistant rats (106). This study demonstrated that in diabetic

rats, GLUT2/SLC2A2 traffics to the apical side, where its apical membrane presence was further confirmed using western blots and biotinylation (106). The western blots performed on apical membrane vesicles perfused with 0-20mM glucose found GLUT2/SLC2A2 levels remained constant on the basal membrane (106). However, around 30mM glucose, GLUT2/SLC2A2 was detected on the apical side, and around 100mM glucose, GLUT2/SLC2A2 levels on the apical side were double that on the basal side (106). This suggested that GLUT2/SLC2A2 was a high-capacity transporter for glucose when SGLT1/SLC5A1 transport reached saturation (106). Therefore, the proposal of GLUT2/SLC2A2 as the diffusive component responsible for absorbing glucose when luminal glucose concentrations are high is a possibility, and a current area of active study (80). Other endocrine hormones, like insulin, growth factors, and cytokines, have shown to be involved in GLUT2/SLC2A2 trafficking as well, but further investigation in this area is needed (80) .

2.4.3.2 Class 2: GLUTs 5, 7, 9, and 11

Class 2 of GLUT transporters are represented by GLUT 5, 7, 9, and 11 members (203). Class 2 of GLUTs was created because of the sequence similarity between these GLUT members (70). GLUT5 (SLC2A5) mainly transports fructose, and is present in the small intestine, testes, and kidneys of mammals (13, 70). GLUT7 (SLC2A7) has shown to be expressed in the small intestine and colon, as well as exhibited expression in the testis and prostate (37). It represents a high-affinity transporter for glucose and fructose, with a Km less than 0.5mM (37). GLUT9 (SLC2A9) is mostly expressed in the liver and kidneys, and known to transport glucose, fructose, and urate (166). GLUT9/SLC2A9 has two splice variants, with the longer variant predominantly present on the basal membrane of epithelial cells, and the shorter variant present on the apical side (166). Finally, GLUT11 (SLC2A11) is mainly expressed in the heart and skeletal muscle, with high amino acid identity to GLUT5 (41.7%) (54). Similarly to GLUT9/SLC2A9, GLUT11/SLC2A11 has two splice variants, each with different functions (203). The shorter variant is characterized as a low-affinity glucose transporter and is expressed in the heart and skeletal muscle tissues (203). In contrast, the longer splice variant is expressed in the liver, lungs, trachea, and brain, and involved in the transport of fructose (203).

2.4.3.3 Class 3: GLUTs 6, 8, 10, 12, and HMIT

The main difference between members of class 3 with classes 1 and 2 is the presence of a glycosylation site on loop 9 of the 12 membrane-spanning transporter, whereas this glycosylation site is present in loop 1 on members in classes 1 and 2 (203). Additionally, all of the members in this class have a targeting motif, but the importance of this motif in their function is still not known (203). GLUT6 (SLC2A6) has been shown to transport glucose, but its affinity for glucose, as well as its ability to transport other substrates is unknown (28). It is mainly expressed in the brain, spleen, and leucocytes of humans (28). Additionally, it shares high amino acid sequence similarity to GLUT8/SLC2A8 (44.8%) (28). GLUT8 (SLC2A8) is dominantly expressed in the liver, heart, testes, adipose, and brain tissues, and it mainly functions in the transport of glucose and fructose (49). It was found that in female mice lacking the GLUT8/SLC2A8 transporter impeded fructose uptake in the liver, demonstrating its essential function as a fructose transporter in the liver (49). GLUT10, encoded by the gene SLC2A10, is present in the skeletal muscles, heart, pancreas, liver, brain, placenta, and kidney (46). It has the longest amino acid sequence than other GLUT members, and it is present on the chromosome containing the Type 2 diabetes-linked region, suggesting its possible involvement with Type 2 diabetes (46). Additionally, in a *Xenopus laevis* oocyte expression system, GLUT10/SLC2A10 was found to transport 2-deoxy-D-glucose, with a resulting Km of about 0.3mM (46). GLUT12 (SLC2A12) is a glucose transporter suggested to be insulin-sensitive, similarly to GLUT4/SLC2A4 because of its abundancy in the skeletal muscle and heart (193). Finally, HMIT (myo-inositol glucose transporter) is a glucose transporter that primarily transports inositols and is mostly present in the brain (203).

2.4.4 Alternative Pathways of Glucose Absorption

Many pathways have been suggested to contribute to the diffusive component of glucose absorption along the BBM of the small intestine, including the involvement of aquaporins. Aquaporins are a large family currently consisting of 13 members, all primarily involved in water absorption and secretion contributing to the maintenance of osmotic balances (50). Each porin differs in its tissue specificity as well as its sensitivity to transport certain substrates (50). The possibility of aquaporins transporting other substrates apart from water has been suggested

(50). A study carried out by Tsukaguchi *et al.* 1999, re-evaluated the function of human AQP9, after discovering that rat AQP9 could transport both water and other small, neutral solutes (186). They expressed hAQP9 in *Xenopus oocytes* and found it to transport neutral solutes like carbamides, purines, and even mannitol (186). If AQP9 was found to transport solutes other than water, then other isoforms of aquaporins have the possibility of transporting substrates like glucose. However, more study is needed in this area.

Additionally, paracellular transport of glucose has been proposed when luminal glucose concentrations are very high, and it was termed the "solvent drag theory" (213). This theory follows as SGLT1 reaches its maximum capacity, downstream processes lead to the tightening of the cytoskeleton, which in turn increase the paracellular space (213). Tight junctions also open up, creating space that drags large amounts of solvent and solutes (like glucose) across the intestinal epithelium (213). This theory represents a possible alternative pathway for glucose absorption, only when luminal glucose concentrations are very high.

2.5 Heterogeneous and Homogeneous Intestinal Segregation of Sodium-Dependent Glucose Transport

The heterogeneous system defined below for some species represents the kinetic transport systems of glucose, segregated according to the intestinal segment. One example follows in the pig that found two kinetic glucose transport systems high-affinity, low-capacity (Ha/Lc) and high-affinity, high-capacity (Ha/Hc) in the jejunum and ileum respectively, representing a heterogeneous system (112). A homogeneous system means one kinetic glucose transport system that dominates throughout the intestine. One example follows in tilapia (presented below), where a Ha/Hc system exists in all three segments of the intestine, representing a homogeneous system (180). Finally, these heterogeneous and homogeneous systems can contain one or multiple transporters that contribute to each transport system. For example: the homogeneous system in tilapia (Ha/Hc throughout the intestine) is likely associated with two transporters in all three intestinal segments (180). Overall, these definitions for homogeneous and heterogeneous sodium-dependent glucose transport systems are used to characterize the transport systems in the species presented below.

Generally, sodium-dependent glucose transport along the small intestine of mammals is defined as a heterogeneous system. The need for this heterogeneous system is not understood, but it dominates sodium-dependent glucose transport across the apical membrane of the small intestine of many species (4, 68, 75, 101, 202).

In mammals, a heterogeneous system of glucose transport exists in the kidneys, where a La/Hc SGLT2/SLC5A2 transporter dominates the proximal tubules, and a Ha/Lc SGLT1/SLC5A1 transporter is present in the distal tubules (148, 171, 188, 191). The purpose of the segregation of this transport activity in the mammalian kidney is better understood than the segregation present in the small intestine. The SGLT2/SLC5A2 present in the kidney proximal tubules is responsible for the majority of glucose re-absorption, thus exhibiting high-capacity transport, whereas the high-affinity characteristic of SGLT1/SLC5A1 is beneficial in the distal tubule where glucose concentrations are low (148, 171, 188, 191). However, in contrast to the kidney, the segregation of sodium-dependent glucose transport along the mammalian small intestine is often found to be opposite, where a Ha/Lc sodium-dependent glucose transporter is present in the proximal sections of the intestine, and the distal sections are dominated by a La/Hc sodium-dependent glucose transporter (21, 22, 75, 101, 112, 202).

Comparatively, this does not hold true for all mammalian and avian species, where some present a homogeneous system of sodium-dependent glucose transport along the small intestine (68, 94, 99). This system of sodium-dependent glucose transport that exists in these different species is presented in more detail below.

2.5.1 Porcine Heterogeneous System

The heterogeneous system of sodium-dependent glucose transport has been extensively studied in the mammalian model, the pig (75). In the pig, a Ha/Lc and La/Hc sodium-dependent glucose transport system was found using jejunal and ileal BBMVs (75). Both transport systems demonstrated Michaelis-Menten kinetics, where the first component (Ha/Lc) was confirmed to be SGLT1/SLC5A1 in the jejunum (75). SGLT1/SLC5A1 exhibited sodium-dependent glucose absorption at lower concentrations of glucose (75). In contrast, the identity of the second system in the ileum has not been confirmed yet, but its function demonstrates a La/Hc sodium-dependent transport for glucose, transporting glucose at the higher concentrations (75).

Additionally, the second La/Hc system had no preference for sodium or potassium in transporting glucose, and D-mannose was also transported by this system (75). It was concluded from this study that more work needed to be done to identify this second system (75).

Following this study, Herrmann *et al.* 2012 further confirmed the first system to be carried out by SGLT1/SLC5A1 using quantitative polymerase chain reaction (qPCR) and western blots (84). They also discovered that the segregation of sodium-dependent glucose absorption was only present in mature pigs, and not in suckling pigs (84). It was suggested that in suckling pigs, the intestine was not completely developed, therefore intestinal glucose segregation would not be present (84). Thus, their research focused on mature pigs, and found SGLT1/SLC5A1 was more abundant in the jejunum than the ileum (84). Using Ussing chambers to measure basal short-circuit current (Isc), they found that the ileum produced higher electrogenic current in response to glucose transport compared to the jejunum (84). Additionally, using jejunal and ileal BBMVs, they found that both the jejunum and ileum followed Michaelis-Menten kinetics, and resulted in a 2-fold higher Vmax value in the ileum compared to the jejunum (84). However, both segments resulted in similar Km values (84). The influence of different breeds of pigs and different diets were also conducted to see changes in Vmax and Km values between both segments, and again it was found that the ileum had higher sodium-dependent glucose transport than the jejunum and it was unaffected by pig breed or diet (84). Finally, the use of phloridzin dihydrate resulted in a greater decrease in the Isc in the ileum in comparison to the jejunum (84).

Herrmann *et al.* 2012 discovered that SGLT1/SLC5A1 was glycosylated in the jejunum of pigs, and its protein expression was higher in the jejunum than ileum, but with no significant difference between the two (84). Therefore, they suggested that glycosylated SGLT1/SLC5A1 was responsible for the lower electrogenic Isc in the jejunum, and responsible for the Ha/Lc sodium-dependent glucose transport (84). Additionally, they proposed that the glycosylated SGLT1/SLC5A1 may be responsible for the segregation of glucose transport between the jejunum and ileum (84). However, the importance of this glycosylated SGLT1/SLC5A1 was not confirmed (84). Additionally, they suggested two more reasons for this heterogeneous system along the pig GI tract (84). One involves the higher expression of CFTR (cystic fibrosis transmembrane conductance regulator) in the jejunum than the ileum, which contributes to the higher secretion of chloride into the lumen (84). They suggested that the higher concentration of

luminal chloride impedes with sodium binding to SGLT1/SLC5A1, thus resulting in lower electrogenic currents for the jejunum (84). Comparatively, the porcine ileum expresses more apical potassium channels than the jejunum, which increases the driving force of sodium into enterocytes, thus resulting in higher electrogenic currents in this segment (84).

Recently, in response to the study by Herrmann *et al.* 2012, the possibility of a glycosylated SGLT1/SLC5A1 contributing to the heterogeneity of sodium-dependent glucose transport along porcine small intestine was rejected (112). This study found that even though SGLT1/SLC5A1 expression was similar in both the jejunum and ileum, and a modified SGLT1/SLC5A1 (phosphorylated SGLT1/SLC5A1, or glycosylated SGLT1/SLC5A1) may compensate for the decreased glucose transport in the jejunum, these observations were not responsible for the heterogeneous differences between both segments (112). Additionally, they confirmed through western blots that SGLT1/SLC5A1 protein was similar between the jejunum and ileum, even though the ileum demonstrated higher Isc for sodium-dependent glucose transport (112). From this study, it was concluded that regardless of glycosylated or phosphorylated SGLT1/SLC5A1 in the jejunum, it did not determine the heterogeneity present along the porcine GI tract (112). In fact, the identification of this second La/Hc system in the ileum of the porcine GI has yet to be identified, along with no answers to understand the purpose of the intestinal segregation of glucose transport.

2.5.2 Feline Heterogeneous System

Using intestinal BBMV of the cat, D-glucose transport was measured to find two glucose systems that exhibited Michaelis-Menten kinetics (202). The two systems demonstrated different Vmax and Km values, representing a Ha/Lc system in the jejunum and a La/Hc system in the ileum for sodium-dependent glucose transport (202). These findings were shown to be similar to those found in the pig, rabbit, and bovine species (202). Interestingly, sodium-dependent glucose uptake in the cat BBMV exhibited higher transport capacity in comparison to the cattle and rabbit, suggesting an adaptation to compensate for the shorter GI tract and low levels of carbohydrates present in its natural, carnivorous diet (202). However, the identities of these two transport systems were not found, due to the technical limitations present at the time.

2.5.3 Guinea Pig Heterogeneous System

Similar heterogeneity was found along the intestinal segment of guinea pigs, which were designated systems 1 and 2 (21). Using BBMVs of guinea pig, they identified that system 1 was a Ha/Lc sodium-dependent glucose transporter identical to the functions of SGLT1/SLC5A1 in the jejunum (21). However, the identity of the transporter of system 2, a La/Hc system in the ileum, was not determined (21). Their study of system 1 and 2 in response to control, fasted, and semistarved guinea pigs revealed that semistarved animals demonstrated an increase in glucose uptake via system 2 (increases in both Vmax and Km values), whereas no changes were present in system 1 (21). Additionally, guinea pigs exposed to lactation or cold-temperature were found to increase their system 2 transport, whereas system 1 did not change (21). They suggested that system 2 may be an adaptable system of glucose uptake, whereas system 1 may represent a constitutive system of glucose uptake, mediated by SGLT1/SLC5A1 (21). Overall, this study demonstrated the existence of two sodium-dependent glucose uptake systems in guinea pig small intestine, but the identity of the second system remains to be elucidated (21).

2.5.4 Rabbit Heterogeneous System

In contrast to the above mammals, a study using rabbit jejunal BBMVs found the presence of two sodium-dependent glucose transport systems in the jejunum itself (55). These two systems revealed a Ha/Lc system and a La/Hc system (55, 101). The first system was confirmed to be SGLT1/SLC5A1, similar to other mammals (55, 86, 209). Both systems were found to be inhibited by phloridzin dihydrate (55). Overall, it was concluded that two glucose transport systems exist along the rabbit intestine (55). However, the identification of the second system (La/Hc) has not been confirmed.

2.5.5 Bovine Heterogeneous System

Similar to the monogastric species mentioned above, heterogenous sodium-dependent glucose absorption has also been observed in ruminant species, specifically bovine (101). Using BBMV of steers, it was demonstrated that at glucose concentrations over 20mM, a high-capacity sodium-dependent transporter was present (101). This transporter exhibited a sodium to glucose

coupling ratio of 1:1 (101). Comparatively, at glucose concentrations lower than 0.05mM, a minor, high-affinity sodium-dependent glucose transporter dominated (101). Altogether, the presence of two sodium-dependent glucose transport systems, a Ha/Lc and a La/Hc , was discovered in steer small intestine (101). However, intestinal segments were not specified.

2.5.6 Equine Heterogeneous System

Horses represent a nonruminant, herbivorous species that generally consume pasture forage (grass) (58). However, to increase their energy and work performance, they are fed diets containing hydrolyzable carbohydrates, usually in the form of grain (58, 94). Very few studies exist studying glucose uptake in equine species. One of the preliminary studies that investigated D-glucose uptake along the BBM of the equine small intestine discovered the presence of a Ha/Lc SGLT1 transporter (94). It was demonstrated that the highest transport of glucose (in pmol/s/mg protein) in BBMVs was in the duodenum, followed by the jejunum, and then the ileum (94). Additionally, it was concluded that D-glucose uptake along the BBM of equine small intestine was mediated by only SGLT1/SLC5A1 (94).

The pattern of glucose uptake along the equine small intestine is different in comparison to most of the mammalian models studied (presented above) (94). However, all three intestinal segments in the horse followed Michaelis-Menten saturation kinetics, and the Km values between jejunal and ileal BBMVs were not significantly different from each other, similarly to the results found in pigs (94). In contrast to the pigs and other mammals, the Vmax values were reported to be higher in the jejunum BBMV than the ileum BBMV, which were 918 ± 73.3 pmol/s/mg protein and 698 ±61 pmol/s/mg protein, respectively (94). It was suggested that the higher Vmax value in the jejunum was due to an increase in protein expression of SGLT1/SLC5A1, rather than a different sodium-dependent glucose transporter (94). Therefore, the characterization of sodium-dependent glucose transport along the equine small intestine does represent a heterogeneous system of glucose absorption, dominated by one transporter, SGLT1/SLC5A1 (94).

2.5.7 Aquatic Heterogeneous and Homogeneous Systems

Many studies in aquatic species revealed the presence of an SGLT1/SLC5A transporter present on the BBM of the intestine, but very few studies identified a heterogeneous system of sodium-dependent glucose transport along the GI tract (110). One of the few studies that discovered a heterogeneous system of glucose uptake was in the carnivorous seawater fish, the pacific copper rockfish (4). The BBMVs from the pyloric caeca and upper intestine were prepared and the transport of ^{3}H-D-glucose was found to exhibit sodium-dependent Michaelis-Menten kinetics in both intestinal segments (4). The pyloric caeca demonstrated a lower affinity binding of ^{3}H-D-glucose compared to the upper intestine, revealing a higher affinity of glucose uptake in the upper intestine (4). Interestingly, the mucosal to serosal flux, or the Vmax values, between the two segments were similar, revealing no differences in glucose transport capacities (4). It was concluded that in the pacific copper rockfish, the upper intestine adapted to transport glucose at a higher affinity than the pyloric caeca possibly because of the lower nutrient content that reaches the upper intestine, after passing through the pyloric caeca (4). Additionally, it represented a heterogeneous system where the upper intestine represented a Ha/Lc and the pyloric caeca represented a La/Lc glucose transport system (4).

A homogeneous system has been defined in tilapia, which is presented in Chapter 1. This homogeneous system is represented as a Ha/Hc glucose transport system that is present throughout the proximal, mid-intestine, and hindgut segments of the tilapia GI tract (180). This is the only reported homogeneous sodium-dependent glucose transport system reported in any fish species. As more glucose transport studies are conducted in fish species, more heterogeneous and homogeneous glucose transport systems will be characterized.

2.5.8 Invertebrate Sodium-Dependent Glucose Transport System

The few studies that have investigated glucose uptake along the intestine include the American lobster (144). This study demonstrated that mucosal-to-serosal glucose uptake along the BBM of lobster intestine exhibited hyperbolic saturation with a Km around 15.2 µM (144). Additionally, it was suggested that an SGLT1-like transporter was responsible because of its inhibition with phloridzin dihydrate (144). Similarly in another invertebrate, the parasitic wasp, a detailed study of glucose and fructose uptake was performed on intestinal epithelial cells, and found a sodium-dependent glucose transporter on the BBM (29). Immunohistochemical studies

that were performed further confirmed the presence of a SGLT1-like transporter present on the apical membrane of the intestine, that was sensitive to inhibition by phloridzin dihydrate (29). Nevertheless, sodium-dependent glucose transport similar to mammals is present along the intestine of invertebrates studied, but the presence of glucose transporter segregation has not been confirmed or studied as of yet.

2.5.9 Avian Homogeneous and Heterogeneous Transport Systems

D-glucose transport has been measured along the small intestine of different avian species. One study investigated D-glucose transporter expression in jejunal, ileal, and rectum BBMVs of the chicken (68). It has been characterized previously that enterocytes in the small and large intestine of chickens express a BBM sodium-dependent glucose transporter that is electrogenic and sensitive to inhibition by phloridzin dihydrate (68). In fact, this transporter exists along the length of the intestine, including the proximal cecum and rectum of chickens (68). It was demonstrated in this study that SGLT1/SLC5A1 was responsible for the sodium-dependent glucose absorption along the small intestine and large intestine of chickens, with no heterogeneous transport of glucose present (68). Therefore, chicken sodium-dependent glucose transport represents a homogeneous system along the entire GI tract (68).

In another avian species, the Rufous hummingbird, active glucose transport decreased moving distally along the intestine, which is different from mammals (99). Additionally, it was concluded that all intestinal glucose absorption was mediated by an active process, thus suggesting sodium-dependent transport for all glucose absorption in the hummingbird (99). Finally, this study demonstrated a single, Michaelis-Menten saturation kinetics of glucose transport along the intestine of hummingbirds (99). With decreasing glucose uptake moving distally along the intestine possibly defines glucose transport kinetics as a heterogeneous system in the hummingbird.

2.5.10 Conclusion

Most of the mammalian small intestine, as well as the avian species, presents a heterogeneous system of sodium-dependent glucose transport (55, 75, 101, 202). The few fish and avian studies that were studied, demonstrate heterogeneous and homogeneous systems of

glucose transport along their intestine (4). Overall, this intestinal glucose transport segregation that has been discovered in many species presents itself with a confusing paradigm: why the need for this heterogeneous system in the intestine? Some studies speculate heterogeneous systems have evolved to meet the needs of individual species, but no assumptions have been confirmed (21). As more studies are conducted and newer techniques are developed, possible answers may arise to this question. Additionally, it will help us to understand the importance of this segregation.

Chapter 3 - Intestinal Electrogenic Sodium-Dependent Glucose Absorption In Tilapia And Trout Reveal Species Differences In SLC5A-associated Kinetic Segmental Segregation

Marina Subramaniam[1]; Lynn P. Weber[1]; Matthew E. Loewen[1b]

1. Department of Veterinary Biomedical Sciences, Western College of Veterinary Medicine, University of Saskatchewan. 52 Campus Drive. Saskatoon, Saskatchewan, Canada S7N 5B4

AUTHOR CONTRIBUTIONS

M.L. conceived and designed research; M.L. & M.S. performed experiments; M.L., M.S. analyzed data; and M.L., L.W., M.S. interpreted results of experiments; M.S. prepared figures; M.L. and M.S. drafted manuscript; M.S., L.W. and M.L. edited and revised manuscript; M.S., L.W. and M.L. approved final version of manuscript.

* In Press, doi: 10.1152/ajpregu.00304.2018

3.1 Abstract

Electrogenic sodium dependent glucose transport along the length of the intestine was compared between the omnivorous Nile tilapia (*Oreochromis niloticus*) and the carnivorous rainbow trout (*Oncorhynchus mykiss*) in Ussing chambers. In tilapia, a high-affinity, high-capacity (Ha/Hc) kinetic system accounted for the transport throughout the proximal intestine, mid-intestine, and hindgut segments. Similar dapagliflozin and phloridzin dihydrate inhibition across all segments support this homogenous Ha/Hc system throughout the tilapia intestine. Genomic and gene expression analysis supported findings by identifying 10 of the known 12 SLC5A family members, with homogeneous expression throughout the segments with dominant expression of SGLT1 (SLC5A1) and SMIT2 (SLC5A11). In contrast, trout's electrogenic sodium-dependent glucose absorption was 20-35 times lower and segregated into three significantly different kinetic systems found in different anatomical segments. A high-affinity, low-capacity (Ha/Lc) system in the pyloric caeca, a super-high-affinity, low-capacity (sHa/Lc) system in the midgut, and a low-affinity, low-capacity (La/Lc) system in the hindgut. Genomic and gene expression analysis found 5 of the known 12 SLC5A family members with dominant expression of SGLT1 (SLC5A1), SGLT2 (SLC5A2), and SMIT2 (SLC5A11) in the pyloric caeca, and only SGLT1 (SLC5A1) in the midgut, accounting for differences in kinetics between the two. The hindgut presented a La/Lc system partially attributed to a decrease in SGLT1 (SLC5A1). Overall, the omnivorous tilapia had a higher electrogenic glucose absorption than the carnivorous trout, represented with different kinetic systems and a greater expression and number of SLC5A orthologs. Fish differ from mammals having hindgut electrogenic glucose absorption and segment specific transport kinetics.

3.2 Introduction

Glucose is the major molecular constituent of carbohydrate digestion entering the intestinal enterocytes via the apically located sodium-dependent glucose transporters (SGLTs) (4, 12, 18, 20, 75). These transporters are members of the SLC5A (solute carrier family member 5A) family, simultaneously transporting glucose and sodium, creating a measurable current during absorption (13, 16). The transporters exist in both omnivorous and carnivorous species and represent the first ports of entry for glucose into the enterocytes (53, 105, 115, 161).

Since their initial discovery, a total of 12 SLC5A isoforms have been identified in the omnivorous human genome and are expressed in various tissues (60, 191). Ten of these genes are sodium-coupled substrate transporters for solutes like glucose, myoinositol, and anions, while the other two genes have different coupling ions and functions (124, 191). The stoichiometry of this transport is dependent on the family member (124, 132). Generally, the SGLTs are characterized kinetically in two categories. First is a high-affinity (Ha) transporter, with sensitivity to low concentrations of glucose and low-capacity (Lc), saturating at low concentrations of glucose (35, 75, 86, 124, 132, 147). Second is a low-affinity (La) transporter with sensitivity to glucose at higher concentrations and high-capacity (Hc), saturating at high concentrations of glucose (35, 75, 86, 124, 132, 147). This classification developed due to the initial difference in kinetics between the first SGLTs discovered (4, 35, 75, 84, 101, 188, 201). The SGLT isoform 1 (SLC5A1) transporter demonstrated a Ha/Lc transport and SGLT2 (SLC5A2) exhibited La/Hc transport (4, 13, 75, 97, 116). Physiological studies identifying two transport systems supported the existence of both a Ha/Lc and La/Hc for glucose in the intestine of both omnivorous and carnivorous mammals including: cat, rat, pig, human, and cattle (12, 16, 87, 101, 112, 147, 201). Only a few of these studies have segregated the Ha/Lc to the proximal small intestine in omnivores and carnivores, but gene association is minimal or lacking (75, 84, 132). However, defining specific physiological attributes to members of the SLC5A family has been challenging due to a previous lack of genomic information, substrate promiscuity, species differences, and tissue specific regulation (84, 129). In fish, this is particularly true, with the identification of SGLTs being minimal and their functions mostly presumed from sequence identity with mammalian SGLTs despite sequence differences (4, 95, 130).

Studies comparing intestinal glucose absorption kinetics and association with SLC5A gene family between omnivores and carnivores are lacking in mammalian literature and unknown in fish, despite the generally accepted notion that omnivores can absorb larger amounts of glucose than carnivores (15, 25, 32, 36, 47, 86, 157). This gap in the literature is particularly salient in fish, which have a lower importance for carbohydrates in their natural diet, but have known differences between omnivorous and carnivorous utilization of glucose (162). Here, using ex-vivo intestinal segments mounted in Ussing chambers, we measured the sodium-coupled electrogenic absorption of glucose along the gastrointestinal tract of omnivorous Nile tilapia (*Oreochromis niloticus)* and carnivorous rainbow trout (*Oncorhynchus mykiss*).

Differences and absences of intestinal segmental kinetic segregation and pharmacological inhibition were successfully compared to expression of specific SLC5A family members with previously described functions, some supporting known glucose absorption. Tilapia demonstrated similar kinetics throughout all of its intestinal segments, which was defined as a one-kinetic homogeneous system. Specifically, tilapia has a single Ha/Hc sodium-dependent glucose transport system along the entirety of its intestinal tract. In contrast, trout demonstrated different transport kinetics in the pyloric caeca, midgut, and hindgut intestinal segments. This was defined as a three-kinetic heterogeneous system, with a Ha/Lc, sHa/Lc, and La/Lc transport occurring in the pyloric caeca, midgut, and hindgut, respectively. Overall the data presented here define a high-capacity, one-kinetic homogenous system in tilapia and a low-capacity, three-kinetic heterogeneous system of sodium-dependent glucose transport in trout, supported by SLC5A gene expression.

3.3 Materials and Methods

3.3.1 Maintenance of Animals

All fish were maintained in accordance with the guidelines of the Canadian Council on Animal Care (CCAC, 2005) (33). All animal protocols were approved by the Animal Care Committee at the University of Saskatchewan (AUP#: 19980142).

3.3.1.1 Nile Tilapia. Nile tilapia were obtained from AmeriCulture Inc. (New Mexico, USA) as fingerlings. They were housed in 360L tanks filtered via a biological filtration system. Photoperiod was kept constant at 14h light/10h dark, and the water temperature maintained at 27 ± 2^{o}C. Fish were fed a standard ration of commercial feed by hand twice per day to visual satiety. The contents of the feed contained: crude protein (54%), crude fat (16%), crude fibre (1%), vitamin A (15000 IU/kg), vitamin D_3 (5000 IU/kg), vitamin E (400 IU/kg), calcium (2.3%), phosphorous (1.5%), and sodium (0.2%) (EWOS). The average weight of fish at the time of study was 500 grams.

3.3.1.2 Rainbow Trout. Female rainbow trout were obtained as wild-type, fertilized eggs from Trout Lodge Inc (Sumner, Washington State, USA). After hatching, the fish were reared in standard 1000-4000L density tanks, provided with biologically-filtered recirculation systems until two years of age when used for this study. They were housed in municipal, dechlorinated water at temperatures between 11 ± 2^{o}C, with a photoperiod at 12h light/12h dark. They were fed a standard ration of commercial feed at 2-5% of their body weight. The contents of the feed contained: crude protein (53%), crude fat (20%), crude fibre (1%), vitamin A (15000 IU/kg), vitamin D_3 (5000 IU/kg), vitamin E (300 IU/kg), calcium (2.3%), phosphorous (1.6%), and sodium (0.2%) (EWOS). At the time of study, the average weight of fish used was 400 grams.

3.3.2 Ex-vivo Tissue Collection

Fish were euthanized by blunt trauma and the entire intestinal section was dissected out of both fish. In Nile tilapia, the intestine was much longer than the trout, and it contained no pyloric caeca. Its intestinal section was separated as proximal intestine (2 inches distal from the stomach), mid-intestine (5 inches distal from the stomach) and hindgut (5 to 6 inches distal from the stomach). In rainbow trout, the intestine was separated according to the pyloric caeca region (located directly distal to the stomach), midgut (located right after the pyloric caeca, 2 inches from the stomach), and hindgut (5 to 6 inches from the stomach). The pyloric caeca is visually distinct from the midgut section. Similarly, the hindgut is visually distinct from the midgut and it was represented as a thicker, larger diameter tissue, darker in pigment, along with visual differences in musculature (27).

3.3.3 Electrophysiology

3.3.3.1 Ussing Chamber technique. The fish intestinal sections were examined in Ussing chambers using techniques adapted from this group (125, 126, 164, 182). The Ussing chamber system used in this study was an EasyMount Ussing Chamber System (Physiologic Instruments Inc., San Diego, CA). Sections were washed in teleost saline: 118mM NaCl, 2.9mM KCl, 2.0mM $CaCl_2 \cdot 2H_2O$, 1.0mM $MgSO_4 \cdot 7H_2O$, 0.1mM $NaH_2PO_4 \cdot H_2O$, 2.5mM Na_2HPO_4 and 1.9mM $NaHCO_3$ at pH 7.9 (63). This physiological buffer was used for both tilapia and trout.

No glucose was added to the buffer. The lumen of the intestine for both fish was also washed with buffer using an 18gage needle, to clean the luminal membrane of any residual chyme.

The dissected tissue sections were exposed as a flat sheet between two sliders of inserts (Slider Number: P2304, Physiologic Instruments Inc., San Diego, CA). The available tissue area for tilapia and trout was constant and equal to 0.3 cm^2. The teleost saline buffer solutions bathing the apical and basal sides of the intestine had a buffer volume of 5ml, and were continuously gassed throughout the experiment with 1% CO_2 and 99% O_2 for the fish (40).

The transepithelial voltage and passing current set across the tissue was measured via agar bridges and Ag/AgCl reference electrodes. These electrodes were connected to leads that are connected to the voltage/current clamp. The short-circuit current (Isc) was measured by the computer (in µA), and this was a result of the tissue current opposing the current induced by the electrodes. The pulse was kept constant at 0.001V. A recirculating bath capable of chilling and heating controlled the temperature of the jacketed chambers, with tissues examined at fish housing temperatures. The temperature used for tilapia was between 25°C-26°C and for trout was between 11°C-12°C. Needle valves were also present for the adjustment of gas flow into the chambers.

Once mounted, the tissue was allowed to reach a steady baseline current for 30-40 minutes prior to adding 1mM increments of glucose to the apical side and measuring the short-circuit current in µA. An equivalent amount of D-mannitol was added to the basal side in order to prevent the development of osmotic gradients from the addition of glucose. Also, mannitol would not be transported across the epithelium, which presents no interference with the movement of glucose transport. Before each addition of glucose and mannitol, a wait period of 3-4 minutes was allowed for equilibration of the current.

3.3.4 Chemicals. Dapagliflozin is a competitive inhibitor of glucose for mammalian SGLT2 (La/Hc) transporters, with EC_{50} values around 1.12nM for human SGLT2 (35, 93, 116). Phloridzin dihydrate is a competitive inhibitor against mammalian SGLT1 (Ha/Lc) transporters, with a Ki around 1 µM for renal and intestinal sodium-glucose cotransporters (4, 177, 198). For pharmacological characterization, 0.001µM, 0.01µM, 0.1µM, 1µM, 10µM, 100µM, 200µM, and 300µM of dapagliflozin, and 1µM, 10µM, and 100µM of phloridzin dihydrate (AdooQ® Bioscience, Irvine, CA) were used in sequential order in the Ussing Chamber as final

concentrations. The inhibitors were added after each tissue segment reached a final glucose and mannitol concentration of 50mM. For tilapia, dose responses of dapagliflozin followed by phloridzin dihydrate addition were performed. Additionally, a dose response of phloridzin dihydrate by itself was conducted in tilapia after final glucose and mannitol concentrations of 50mM was reached. In trout, dose responses of dapagliflozin followed by phloridzin dihydrate were used.

3.3.5 RNA extraction and cDNA synthesis using RT-PCR. Approximately 1mg samples of tissue were obtained from the dissection of the intestinal tract, and stored in RNA*later*® RNA Stabilization Solution at -80^{o}C. RNA was isolated using the TRIzol reagent, and cDNA was synthesized through reverse transcription PCR using the qScript™ cDNA SuperMix (Quanta Biosciences, Maryland, USA). The reaction was run as: incubation for 5 minutes at 25^{o}C, then 30 minutes at 42^{o}C, and the final 5 minutes at 85^{o}C. The cDNA samples were stored at -80^{o}C for subsequent use in quantitative PCR.

3.3.6 Genomic Identification of SLC5A Genes. A detailed BLAST+ (Basic Local Alignment Search Tool) application was used to identify all of the annotated SLC5A transporters in both tilapia and trout. The twelve human SLC5A transporter sequences retrieved from the National Center for Biotechnology Information (NCBI) website (http://www.ncbi.nlm.nih.gov/) were used in a "blastn" command to search for similar mRNA sequences in the tilapia and trout genome (204). The expect value (e-value) was used to assess the significance of the match, where an e-value close to zero was considered significant and an e-value higher than 10^-15 was considered as a non-significant match. Once SLC5A transporters were identified from tilapia and trout, phylogenetic trees were generated using the alignment program CLUSTAL W and MEGA7 (www.megasoftware.net) software.

3.3.7 Gene transcript expression levels by quantitative polymerase chain reaction. Quantitative PCR was performed on the RT-PCR reaction using the GoTaq®qPCR Master Mix containing SYBR®Green1 (Promega, Madison USA). The BioRad QPCR system was used to perform these reactions. The total volume of the PCR reaction was 12.5µL. A total of 40 cycles

of qPCR was performed, with each cycle consisting of GoTaq® Hot Start Polymerase activation at 95ºC for 2 minutes, and then denaturation at 95ºC for 15 seconds, followed by annealing/extension at the primer's hybridization temperature (59ºC) for 1 minute. The dissociation step was at 60-95ºC. Serial dilutions of cDNA were also used to generate a standard curve for each target gene, where the efficiency of each primer was calculated. The efficiencies for the tilapia primers ranged from 1.9-2.1, and similar range of efficiencies were determined for trout primers as well. EFα1 (α-elongation factor 1) was the housekeeping gene and it was used to normalize the relative expression levels in tilapia and trout. The method of analysis used to represent the relative expression levels was calculated using delta CT, where the amount of the gene of interest was normalized to the amount of EFα1 in that sample (173).

The primers for tilapia and trout SLC5A genes and EFα1 were designed using the Integrated DNA Technologies website (https://www.idtdna.com/site), where the sequences and their accession numbers are presented in Tables 3.1 and 3.2, respectively.

Table 3.1 Tilapia Primer Sequences used for quantitative PCR

Gene	Forward Primer (5`-3`)	Reverse Primer (5`-3`)	Accession Number
SGLT1	CCCGAGTACTTGAAGAAGAG	GCAATAACAGCGAGGTAGA	XM_019361130.1
SGLT2	AGGAGGATGAGGGAGAATAA	ACACTGGGTCCTCACTAA	XM_013273846.2
SMIT1	CAACGCCAAGTACAGAAAC	CTCTGCGATTCTCCCTTATAG	XM_019353114.1
SGLT4	ATGGTGGTTGGAATCTGG	GTCCCTGCTAGACCAATAAA	XM_005475685.3
NIS	TCCATGTCCTACCTCTACTT	GACCCTCCACTTTCTTCTT	XM_005453978.3
SMCT1	TCAGTGTTGAGTGAGAAGG	AGAGCGAACACCACATAG	XM_013271289.2
SGLT5	CACCGTGGACTCTGATTT	TACATCTGCGTGTGAAGAG	XM_003455975.4
SMIT2	GAGACGGAAGAAGGAAGATG	GCCCAGTAACCAATGATAAAG	XM_005461087.3
SMIT	GCTGTCTGTGGATCTCTATT	GAACTGTGTCCGTGTAGAT	XM_019352280.1
SMVT	CAGGAGGAATAGCAGAAGTC	CTTGGTTCACACCGTACA	XM_005460242.3
EFα1	CTCTTCTACCGTCGGATTAC	ATTGACTCCCTCGTAGAAAC	XM_005476483.3

Table 3.2 Trout Primer Sequences used for quantitative PCR

Gene	Forward Primer (5`-3`)	Reverse Primer (5`-3`)	Accession Number
SGLT1	CTAAGTGTCACGGCTCTATAC	GCGTCTGGAAGTTCTCATAA	XM_021591066.1
SGLT2	ATTGGTAGTGGTCACTTTGT	AAACAGCCAGCCCAATAG	NM_001124432
SGLT4	GTGCTGGTGTTTGTGTATG	AGATGGTGCTCTGGAATG	XM_021604024.1
NIS	GGCTTGTGTCTCGTTGTA	TGTCCAGCACCAAGTATG	XM_021573060.1
SMIT2	CAAGATCCTGCCCTTCTT	GTAGCTTCATGACCAGTTTG	XM_021592865.1
SMVT	ATCTTACCAGCGCTTACC	CCCATAGATCAAAGCCAGTA	XM_021573745.1
EFα1	AGCGAGCTCAAGAAGAAG	GACCAAGAGGAGGGTATTC	NM_001124339.1

3.3.8 Statistical Analyses. Vmax (represented in $\mu A/cm^2$) and Km (represented in mM) values were determined for each intestinal section in each species using GraphPad Prism 8 (GraphPad Software, Inc.) (100, 119, 142, 145). Here, the Km values for both fish species represents the concentration at 50% maximum rate of the transporter, and the assumption is made that the rate of transport (catalysis) and rate of binding are similar. Tilapia intestinal segments followed Sigmoidal kinetics, whereas trout pyloric caeca and midgut followed Michaelis-Menten kinetics and the kinetics in trout hindgut fit Sigmoidal Hill kinetics (F-test, $P < 0.05$). The equation used for the Sigmoidal Hill kinetics and Michaelis-Menten fits were:

Equation 3.1

Sigmoidal Hill fit: $Y=Vmax*X^h/(Kd^h + X^h)$

Equation 3.2

Michaelis-Menten fit: $Y = Vmax*X/(Km + X)$

A 1-way ANOVA was performed on the three intestinal sections of each species to determine whether the Vmax and Km values for each gut section was significantly different (210). All data met parametric assumptions, being normally distributed and exhibited homogeneity of variance so ANOVA analyses were used (210). After ANOVA, pairwise comparisons were made using Tukey's posteriori tests, as appropriate. A $P < 0.05$ was considered significantly different. To compare the Vmax values between tilapia and trout, a student's t-test was performed to confirm significance. For the inhibitor dapagliflozin, the percent activity remaining was calculated from the division of the 50mM increment short-circuit current (the concentration where the transporter is 100% saturated and it is 100% un-inhibited) and the resultant drop in current from the addition of each drug concentration. For phloridzin dihydrate, the percent activity remaining was calculated from the division of the 300uM concentration of dapagliflozin (concentration where Ha/Lc transporter is un-inhibited) and the resultant drop in current from the addition of the drug. Parametric 2-way ANOVAs (two factors: intestinal sections and dosage of the drug) were performed on the three intestinal sections of each species and the dosages of each inhibitor to determine significance (210). The Ki values for the dapagliflozin response and the phloridzin dihydrate only responses were calculated for tilapia using the "One-Site Fit logIC50" from GraphPad Prism 8 (GraphPad Software, Inc.). This fit follows the equation: $Y = Bottom + (Top-Bottom)/(1+10^{(X-LogIC50)})$. Parametric 1-way ANOVA was performed on the three intestinal

sections to determine significance. For the qPCR analyses, fold differences were determined by the BioRad system, where the threshold cycle was established using the housekeeping gene, EFα1. A 2-way ANOVA (two factors: intestinal location and gene) was conducted on the gene expressions followed by Tukey's posteriori test for pairwise comparisons. All statistical analyses were performed on SigmaPlot (Systat).

3.4 Results

3.4.1 Nile Tilapia

3.4.1.1 Ha/Hc Electrogenic Glucose Absorption kinetics

In tilapia, glucose gradients performed in an Ussing chamber measured short-circuit current and demonstrated electrogenic sodium-dependent glucose absorption that followed Sigmoidal Hill kinetics in all intestinal segments, with Hill coefficients greater than 1 (proximal intestine, mid-intestine, and hindgut). All three intestinal sections saturated around 30mM glucose in tilapia (Figure 3.1). Additionally, the calculated Vmax and Km values were consistent with that of a Ha/Hc system in all segments (Figure 3.1 and Table 3.3). No statistically significant differences in Vmax and Km values were found among the different intestinal segments in tilapia (Table 3.3; Vmax: $P = 0.5$, Km: $P = 0.4$), demonstrating a single Ha/Hc system throughout the tilapia gastrointestinal tract. Generally, low Km values around 4-6mM and high Vmax values around 47μA/cm^2 - 60μA/cm^2 were found throughout tilapia gut. Sodium-dependency of glucose transport was confirmed by replacement of sodium with potassium creating a sodium-free teleost saline Ussing chamber buffer, which eliminated the glucose stimulated current (Figure 3.1). Similarly, a sodium-free teleost saline using N-Methyl-D-glucamine as a substitute for sodium was performed, which eliminated the glucose stimulated current as well (data not shown).

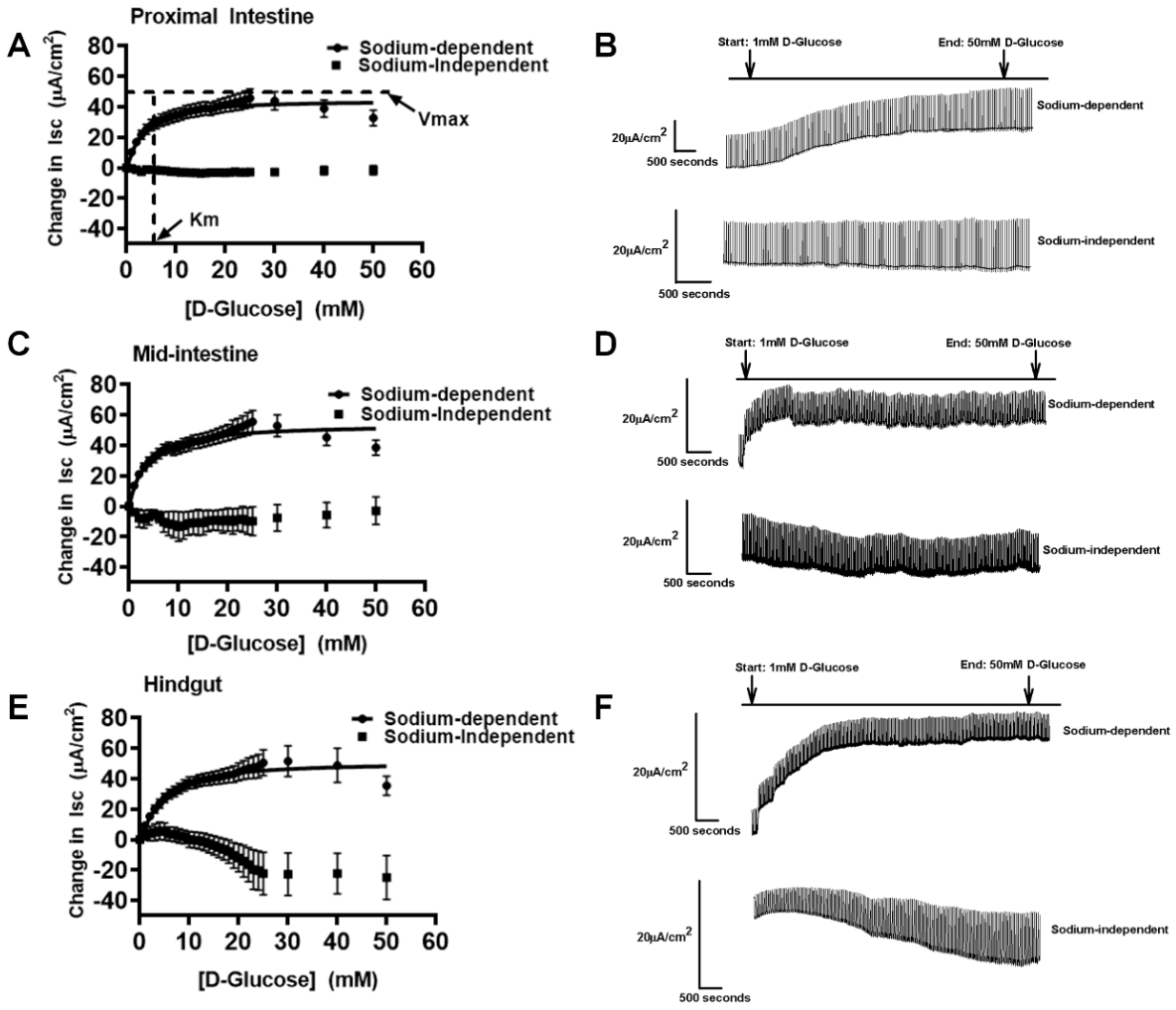

Figure 3.1 Kinetics of sodium-dependent glucose transport in tilapia.

Sigmoidal Hill kinetics for sodium-dependent and sodium-independent electrogenic glucose transport for tilapia in **A)** proximal intestine, illustrated with representative trace on the right side **(B)** (Sodium-dependent: Fish N = 26; Sodium-independent: Fish N = 7), **C)** mid-intestine, illustrated with representative trace on the right side **(D)** (Sodium-dependent: Fish N = 30; Sodium-independent: Fish N = 6), and **E)** hindgut, illustrated with representative trace on the right side **(F)** (Sodium-dependent: Fish N = 31; Sodium-independent: Fish N = 6). The maximal velocity (Vmax) and Michaelis-Menten constant (Km) is represented in **A)** proximal intestine for illustration. Data are represented as means ± SEM. *Isc*, short-circuit current.

Table 3.3 Vmax and Km Values for Nile Tilapia and Rainbow Trout

Nile Tilapia			Rainbow Trout			
Tissue	**Vmax ± SEM ($\mu A/cm^2$)**	**Km ± SEM (mM)**	**Tissue**	**Vmax ± SEM ($\mu A/cm^2$)**	**Km ± SEM (mM)**	**$\frac{Tilapia_{(Vnax)}}{Trout_{(Vmax)}}$**
Proximal	47.0 ± 6.7^{A}	4.2 ± 0.7^{A}	Pyloric Caeca	$2.3 \pm 0.4^{A,B}$	4.2 ± 1.0^{A}	2043%*
Mid-intestine	59.6 ± 7.0^{A}	6.0 ± 1.0^{A}	Midgut	1.7 ± 0.3^{A}	1.8 ± 0.3^{B}	3506%*
Hindgut	56.2 ± 9.3^{A}	5.7 ± 1.1^{A}	Hindgut	2.4 ± 0.2^{B}	12.3 ± 1.6^{C}	2342%*

Vmax (µA) and Km (mM) represented for each tissue type in Nile Tilapia and rainbow trout. Area of intestinal segment was $0.3cm^2$. Data are presented as means ± SEM. Different letter superscripts indicate significances (Tukey's test after 1-way ANOVA, $P < 0.05$). Asterisks represent significances for Vmax values between tilapia and trout (Student's t-test, $P < 0.05$).

3.4.1.2 Inhibition of Ha/Hc Kinetics

Dapagliflozin, a selective inhibitor for SGLT2 (SLC5A2) or La/Hc sodium-dependent glucose transport, and phloridzin dihydrate, an SGLT1 (SLC5A1) or Ha/Lc system inhibitor were used to help decipher some of the kinetics (116, 143, 170). Figure 3.2 illustrates the percent activity remaining in each intestinal tissue after the cumulative addition of increasing dosages of inhibitors dapagliflozin and then phloridzin, as well as phloridzin addition alone.

The three intestinal sections in tilapia were similarly inhibited by dapagliflozin in a dose-dependent manner (Figure 3.2Ai, $P > 0.5$ for tissue differences), with ~50-60 % activity remaining at a final 300µM dose in all intestinal segments (Figure 3.2Ai, $P < 0.05$ for inhibitor effect). The Ki (inhibition at 50%) values for the proximal intestine was 7.7 ± 1.5 µM, mid-intestine was 7.4 ± 1.7 µM, and the hindgut was 5.7 ± 1.6 µM. These values were not significantly different from each other ($P = 0.6$). No significant inhibition was found upon addition of phloridzin dihydrate added sequentially after dapagliflozin (Figure 3.2Aii, $P > 0.5$). However, addition of phloridzin by itself resulted in significant inhibition (Figure 3.2Aiii, $P < 0.05$ for inhibitor effect) at a final concentration of 100 µM, with ~60-80% activity remaining, again with no significant differences found between intestinal segments (Figure 3.2Aiii, $P > 0.5$ for tissue differences). Additionally, the Ki values for the proximal intestine was 11.1 ± 0.002 µM, the mid-intestine was 11.6 ± 0.002 µM, and the hindgut was 7.6 ± 0.002 µM. The Ki values between the intestinal segments were not significantly different from each other ($P = 0.4$).

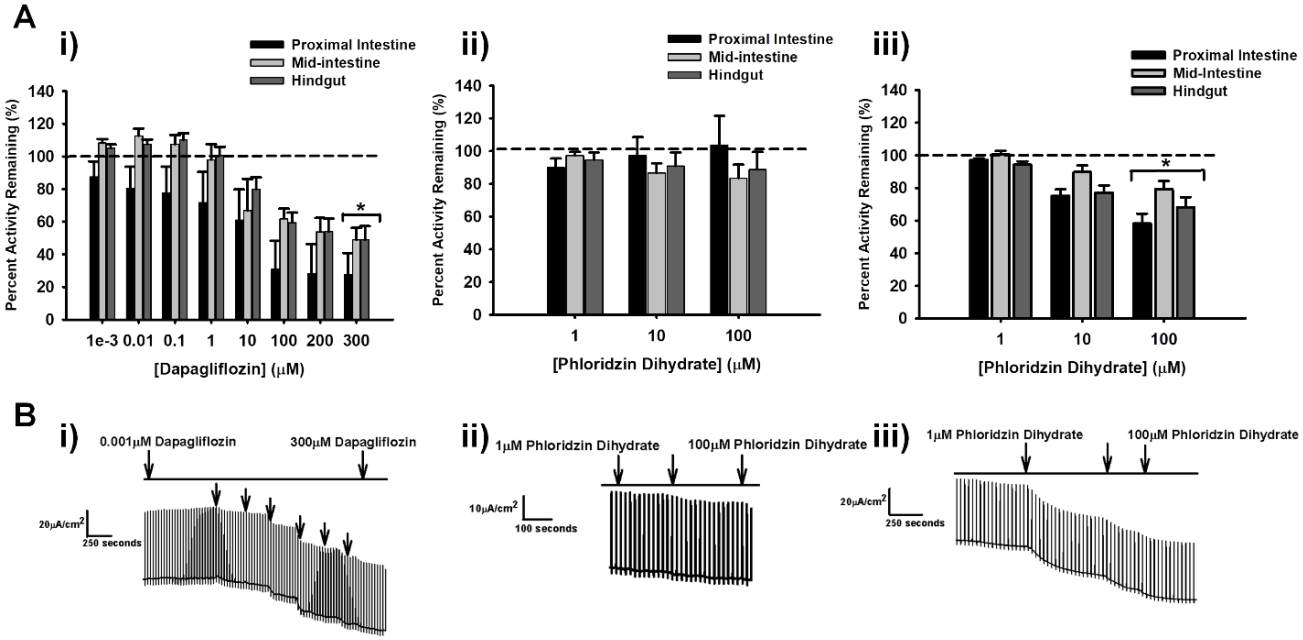

Figure 3.2 Pharmacological inhibition in tilapia.

Percent activity remaining of short-circuit current (Isc) in Nile tilapia of **A) i)** dapagliflozin (0.001, 0.01, 0.1,10, 100, 200, and 300μM) (all tissues: N = 25), following addition of **ii)** phloridzin dihydrate (1, 10,100 μM) (all tissues: N = 25) and **iii)** phloridzin dihydrate (1, 10,100 μM) without previous addition of dapagliflozin (proximal: N = 22, mid-intestine: N = 18, and hindgut: N = 20) on intestinal tissues. **B)** Representative traces for proximal tissue of **i)** dapagliflozin addition, **ii)** phloridzin dihydrate addition following dapagliflozin, and **iii)** phloridzin dihydrate only addition. Asterisks represent significance from 100% transporter activity before inhibition, which is presented as the dotted line (2-way ANOVA, $P < 0.05$).

3.4.1.3 SLC5A Gene Profiling Affirms Kinetics

To identify the genes responsible for the observed current, tilapia genomic analysis was performed which found 10 of 12 known SLC5A family members. The SLC5A transporters identified were SGLT1 (SLC5A1, sodium/glucose cotransporter 1), SGLT2 (SLC5A2, sodium/glucose cotransporter 2), SMIT1 (SLC5A3, sodium/myoinositol cotransporter 1), SGLT4 (SLC5A9, sodium/glucose cotransporter 4), NIS (SLC5A5, sodium/iodide cotransporter), SMCT1 (SLC5A8, sodium/monocarboxylate cotransporter), SGLT5 (SLC5A10, sodium/glucose cotransporter 5), SMIT2 (SLC5A11, sodium/myoinositol cotransporter 2), SMIT (SLC5A3, sodium/myoinositol cotransporter), and SMVT (SLC5A6, sodium/multivitamin cotransporter) in the genome using the BLAST+ application (Table 3.1). The expression levels of each gene were then compared among the different tissues using quantitative real-time PCR.

All intestinal tissues in tilapia had similar gene profiling with no significant differences in expression from each other, supporting the similarity in physiological responses of the three segments (Figure 3.3A, $P > 0.5$ for tissue differences). Overall, SGLT1 (SLC5A1) and SMIT2 (SLC5A11) expression were significantly higher than the expression of the other genes in all tissues (Figure 3.3A, $P < 0.001$). The proximal intestine and hindgut had significantly higher SMIT2 (SLC5A11) expression than SGLT1 (SLC5A1) (Figure 3.3A, $P < 0.05$ for transporter type within each tissue location), whereas the mid-intestine had statistically similar SGLT1 (SLC5A1) and SMIT2 (SLC5A11) expression (Figure 3.3A, $P > 0.5$ for transporter type in mid-intestine). Sequence similarities in identified tilapia SLC5A transporters were compared in a phylogenetic tree (Figure 3.3B). In a CLUSTAL W analysis, the nucleotide identities of SLC5A family members found in the genome relative to tilapia SGLT1 (SLC5A1) were 60.6% SGLT2 (SLC5A2), 47.9% SMIT1 (SLC5A3), 57.5% SGLT4 (SLC5A9), 35.5% NIS (SLC5A5), 33% SMCT1 (SLC5A8), 53.8% SGLT5 (SLC5A10), 55.3% SMIT2 (SLC5A11), 48.3% SMIT (SLC5A3), and 37.4% SMVT (SLC5A6).

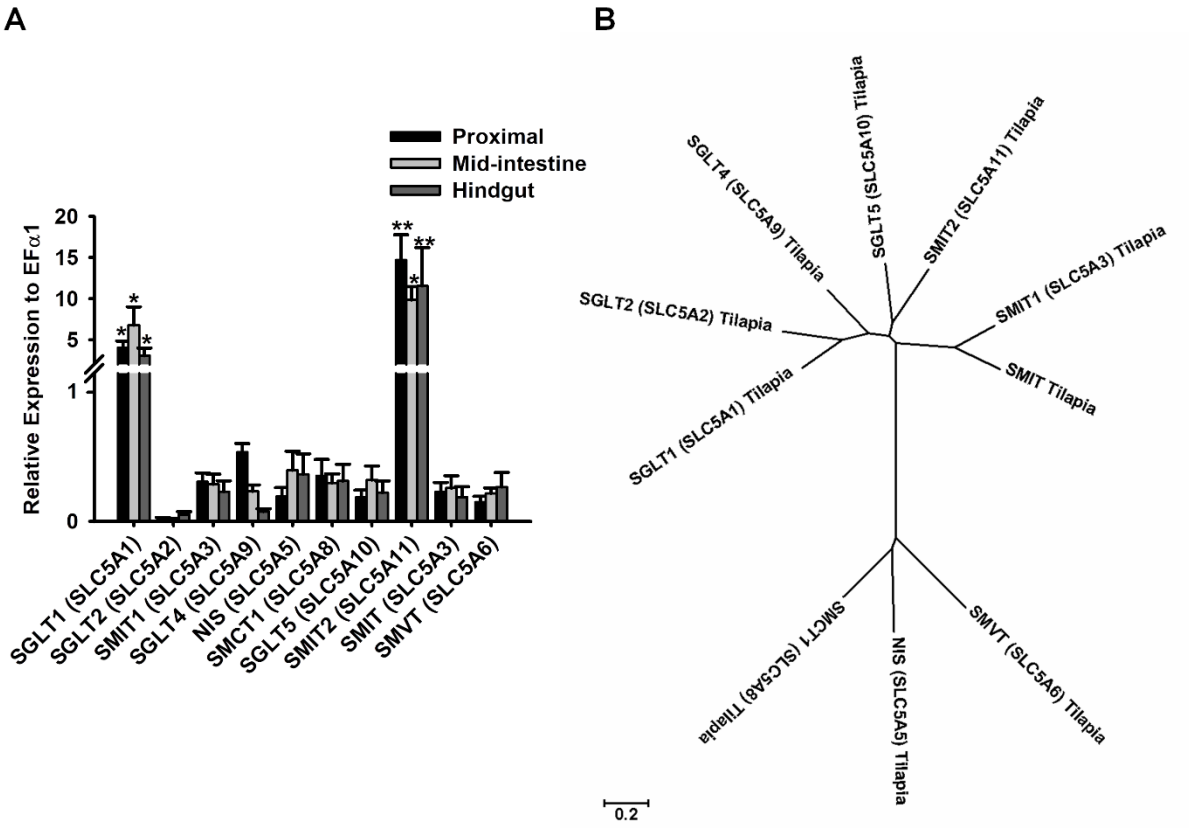

Figure 3.3 Genomic and gene expression analyses in tilapia.

A) Relative expression levels of SLC5A transporters in Nile tilapia (Proximal intestine: N = 8-10, Mid-intestine: N = 6-10, Hindgut: N = 6-10) using quantitative PCR. Expression levels were normalized against EFα1 housekeeping gene. Asterisks represent significance between genes and tissues (2-way ANOVA, $P < 0.05$). **B)** Phylogenetic tree of the ten members of the SLC5A family of cotransporters. The alignment program CLUSTAL W and the phylogenetic display program MEGA7 were used to generate the tree.

3.4.2 Rainbow Trout

3.4.2.1 Electrogenic Glucose Absorption reveals a Three-Kinetic System

A glucose gradient performed in the Ussing chamber using the pyloric caeca, midgut, and hindgut intestinal segments of trout resulted in short-circuit current. The pyloric caeca and midgut both followed Michaelis-Menten kinetics whereas the hindgut followed Sigmoidal Hill kinetics (Figure 3.4). The pyloric caeca and midgut both saturated around 5mM glucose, with a significantly higher Km value in the pyloric caeca (4.2 mM) compared to the midgut (1.8 mM) (Table 3.3, $P < 0.05$), but not significantly different Vmax values between the two trout tissues (2.3 $\mu A/cm^2$ versus 1.7 $\mu A/cm^2$) (Table 3.3, $P > 0.5$). These values characterize a Ha/Lc system in the pyloric caeca and a super-high-affinity (sHa)/Lc system in the midgut of trout (Figure 3.4 and Table 3.3). The trout hindgut saturated around 50mM glucose, but with a significantly higher Km value than the midgut and pyloric caeca (Figure 3.4 and Table 3.3, $P < 0.05$). The hill coefficient was greater than 1 for the hindgut. The Vmax value in the trout hindgut was slightly higher than midgut, but was similar to the pyloric caeca and not significantly different from each other (Figure 3.4 and Table 3.3, $P > 0.5$). The observed Vmax (2.4 $\mu A/cm^2$) and higher Km (12.3 mM) values in the hindgut in comparison to the proximal sections of the trout intestine support a low-affinity, low-capacity (La/Lc) system. Thus, trout presents with three different kinetic systems along their gastrointestinal tract, with large differences in affinity for glucose and an overall low-capacity for glucose transport compared to tilapia. Specifically, tilapia Vmax values were significantly (2043-3506% or approximately 20 -35 times, $P < 0.05$ in Student's t-test) higher compared to trout (Table 3.3). Finally, sodium dependency of glucose transport was demonstrated in a sodium free buffer (Figure 3.4). Additionally, a sodium-free teleost saline using N-Methyl-D-glucamine as a substitute for sodium was performed, which eliminated the glucose stimulated current as well (data not shown). Interestingly, in trout, there was no significant inhibition in any of the kinetic systems in response to both dapagliflozin and phloridzin dihydrate (Figure 3.5Ai and ii, $P > 0.5$ for inhibitor effect in 2-way ANOVA).

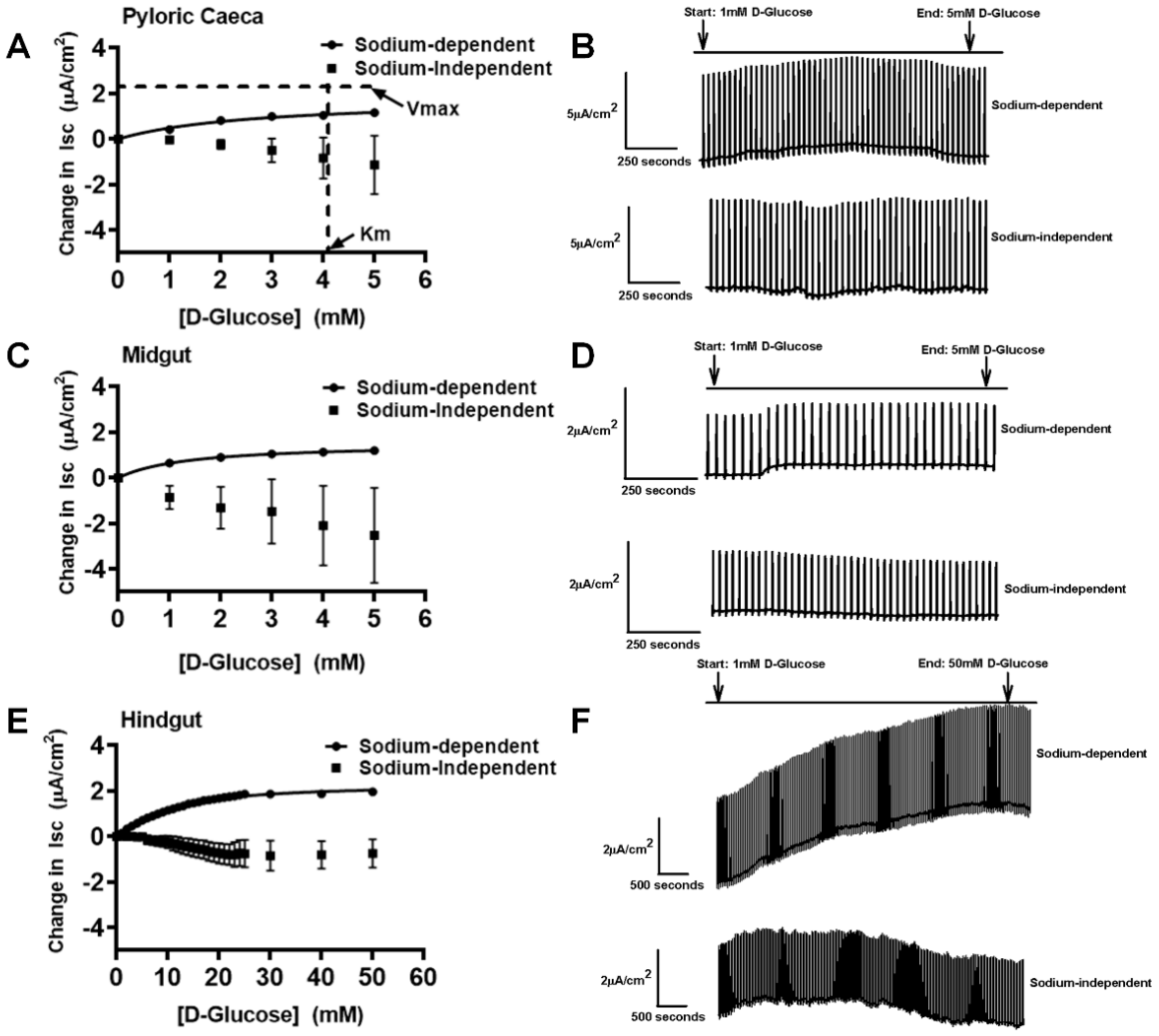

Figure 3.4 Kinetics of sodium-dependent glucose transport in trout.

Michaelis-Menten and Sigmoidal Hill kinetics for sodium-dependent and sodium-independent electrogenic glucose transport for trout in **A)** pyloric caeca, illustrated with representative trace on the right side **(B)** (Sodium-dependent: Fish N = 12; Sodium-independent: Fish N = 5), **C)** midgut, illustrated with representative trace on the right side **(D)** (Sodium-dependent: Fish N = 18; Sodium-independent: Fish N = 4), and **E)** hindgut, illustrated with representative trace on the right side **(F)** (Sodium-dependent: Fish N = 24; Sodium-independent: Fish N = 4). The Vmax and Km is represented in **A)** pyloric caeca for illustration. Data are represented as means ± SEM.

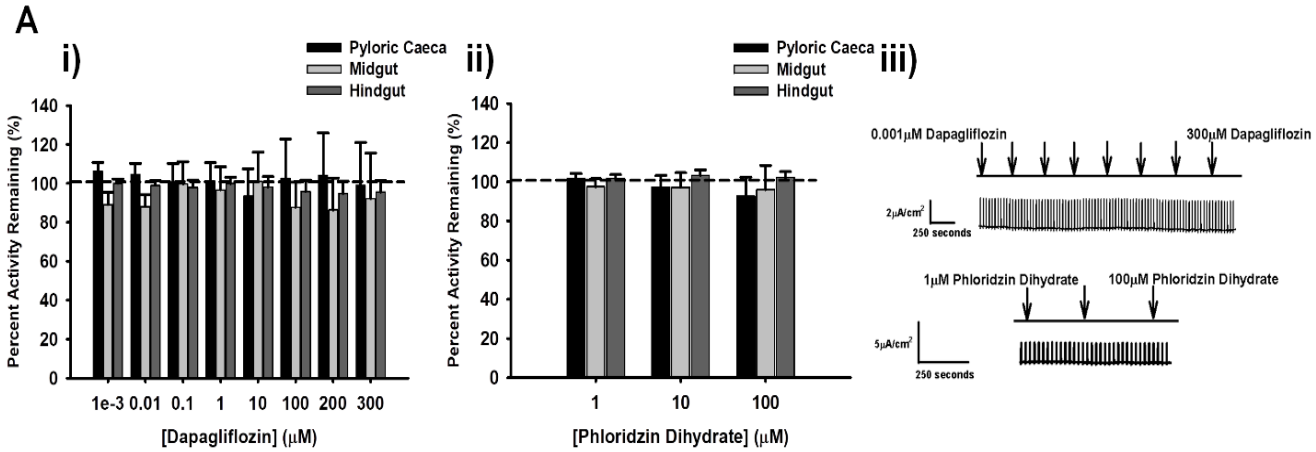

Figure 3.5 Lack of pharmacological inhibition in trout.

A) Percent activity remaining in rainbow trout of **i)** dapagliflozin (0.001, 0.01, 0.1,10, 100, 200, and 300μM) (all tissues: N = 12), following addition of **ii)** phloridzin dihydrate (1, 10,100 μM) (all tissues: N = 12) and **iii)** representative trace for pyloric caeca of dapagliflozin and phloridzin dihydrate additions. Data are represented as means ± SEM. Dashed line represents 100% transporter activity before inhibition.

3.4.2.2 SLC5A Gene Profiling Affirms Kinetics

To identify the genes responsible for the observed kinetics, trout genomic analysis was performed and identified 5 of 12 known SLC5A family members. Trout SGLT1 (SLC5A1, sodium/glucose cotransporter 1), SGLT2 (SLC5A2, sodium/glucose cotransporter 2), SGLT4 (SLC5A9, sodium/glucose cotransporter 4), NIS (SLC5A5, sodium/iodide cotransporter), SMIT2 (SLC5A11, sodium/myoinositol cotransporter 2), and SMVT (SLC5A6, sodium/multivitamin cotransporter) were identified in the trout genome after using the BLAST+ application (Table 3.2). The expression levels of each gene were compared among the different tissues using quantitative real-time PCR.

In trout, SGLT1 (SLC5A1) expression in the pyloric caeca and midgut were significantly higher than the expression levels of the other genes, supporting the higher affinity and low-capacity kinetics in both tissue segments (Figure 3.6A, $P < 0.001$). In addition, SGLT2 (SLC5A2) and SMIT2 (SLC5A11), two low-affinity transporters had significantly higher expression in the trout pyloric caeca than the midgut, supporting the high-affinity (Ha) to super-high-affinity (sHa) paradigm between pyloric caeca and midgut (Figure 3.6A, $P < 0.05$). A significant drop in SGLT1 (SLC5A1) was found in the trout hindgut, potentially explaining the reduced affinity in this segment (Figure 3.6A, $P < 0.05$). However, significant drops in SGLT2 (SLC5A2) and SMIT2 (SLC5A11) were also noted, leaving the observed glucose absorbing capacity unexplained (Figure 3.6A, $P < 0.05$). The phylogenetic tree identifying sequence similarities between trout SLC5A transporters are illustrated in figure 3.6B. In a CLUSTAL W analysis, the nucleotide identities relative to trout SGLT1 (SLC5A1) were 62.3% SGLT2 (SLC5A2), 56.5% SGLT4 (SLC5A9), 38.3% NIS (SLC5A5), 59.4% SMIT2 (SLC5A11), and 40.5% SMVT (SLC5A6).

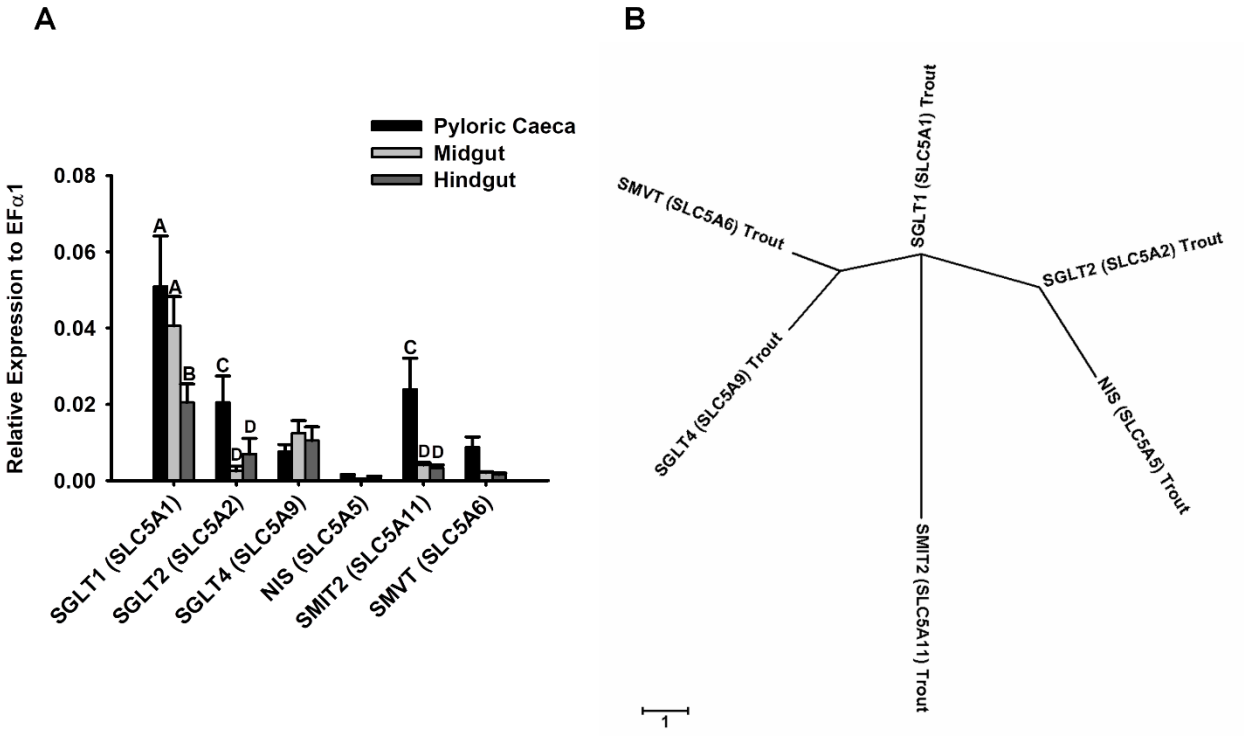

Figure 3.6 Genomic and gene expression analyses in trout.

A) Relative expression levels of SLC5A transporters in rainbow trout (Pyloric Caeca: N = 6-10, Midgut: N = 10, Hindgut: N = 8-10) using quantitative PCR. Expression levels were normalized against EFα1 housekeeping gene. Letters represent significance between genes and tissues (2-way ANOVA, $P < 0.05$). **B)** Phylogenetic tree of the six members of the SLC5A family of cotransporters. The alignment program CLUSTAL W and the phylogenetic display program MEGA7 were used to generate the tree.

3.5 Discussion

This study demonstrated that tilapia intestine possesses higher electrogenic glucose absorption and greater expression of glucose transporter orthologs than trout intestine. Differences between the two fish species portray tilapia as a homogeneous, one-kinetic glucose absorption system (Ha/Hc) throughout the gastrointestinal tract. In contrast, trout have heterogeneous, three-kinetic glucose absorption systems (Ha/Lc, sHa/Lc, and La/Lc) corresponding to the three different intestinal segments. Comparative studies between omnivore and carnivore sodium-dependent glucose absorption has been minimally explored in mammals and birds, with studies lacking in fish (5, 51, 99). Additionally, the existence of two different segment-specific sodium-dependent glucose transport systems along the small intestine associated with SLC5A transporters have been shown in mammals, but has not been described in fish (112, 130, 201). In the current study, we present fundamental differences that exist between the omnivorous tilapia and carnivorous trout in terms of sodium-dependent glucose transport along the gastrointestinal tract. Additionally, both fish species have hindgut sodium-dependent glucose absorption suggesting a divergent adaptation from mammals, where colonic glucose absorption is lacking.

3.5.1 One-Kinetic SLC5A-associated Homogeneous Glucose Absorption in Tilapia

Tilapia, an omnivorous fish, would generally consume a higher carbohydrate diet in their natural environment, and has been shown to better tolerate a higher glucose load than trout in terms of its clearance from the plasma (176). In captivity, tilapia are generally fed a higher carbohydrate-inclusion diet (up to 50% dietary carbohydrate), which is correlated with good growth (118, 142, 159, 176, 199). In contrast, trout can tolerate up to 20% carbohydrate in their diet, before exhibiting poor growth (60, 199). Both dietary carbohydrate levels in fish are generally lower than mammalian diets, which are up to 60% inclusion (32). Our study adds to these known nutritional physiological differences by demonstrating that tilapia have approximately 20 – 35 times (around 2000-3500%, Table 3.3) higher capacity for sodium dependent glucose transport than corresponding segments in trout. The higher absorption in tilapia is driven by a single unique Ha/Hc kinetic system, which is demonstrated by low Km and high Vmax values along the entirety of the intestinal tract, which would enhance their ability to

absorb more glucose, a characteristic of omnivores (Table 3.3) (199). Similarly, a study carried out in the omnivorous freshwater fish black bullhead (*Ictalurus melas*) using isolated enterocytes found brush-border transport of 3-O-methylD-glucose (3-OMG, non-metabolizable form of D-glucose) to saturate around 40mM (177).

Further characterization with pharmacological inhibitors supported the homogenous Ha/Hc kinetic system in tilapia. In mammals, these inhibitors have been used to differentiate the kinetic systems (Ha/Lc and La/Hc) of SGLTs (64, 84, 89, 116, 198). Specifically, the recently developed dapagliflozin and the traditionally used phloridzin dihydrate, have been used to inhibit SGLT2 (SLC5A2), a La/Hc transporter and SGLT1 (SLC5A1), a Ha/Lc transporter, respectively, in the kidney of rats, pigs, and humans (64, 96, 116, 191). Additionally, phloridzin dihydrate has been used with studies in fish using techniques like brush-border membrane vesicles (BBMVs) exhibiting inhibition of sodium-dependent glucose transport (4, 130, 177, 184, 200). Here, dapagliflozin was first applied, to selectively inhibit La/Hc transporter kinetics, followed by phloridzin dihydrate to inhibit any further Ha/Lc kinetics.

Dapagliflozin resulted in inhibition with all intestinal segments responding similarly, with sequential addition of phloridzin dihydrate not resulting in any further inhibition. In contrast, phloridzin addition by itself resulted in similar significant inhibition in all segments. All segments reacting the same to all inhibitors with similar Ki values exhibited throughout the intestine support a one-kinetic, homogeneous system throughout tilapia gut. The lack of sequential inhibition of phloridzin after dapagliflozin suggest that a) dapagliflozin can inhibit Ha/Lc transporters (SGLT1-like) in tilapia or b) the unique Ha/Hc system is created by a single SGLT which is sensitive to both drugs. Arguing against the latter possibility is the fact that genomic and gene expression analysis suggested the former.

Bioinformatic analysis identifying 10 SLC5A transporters exhibited similar gene expressions across all three intestinal segments in tilapia. Such similar expression would explain homogenous segmental sodium-dependent glucose kinetics and inhibition. More specifically, the similar, but significantly higher levels of SGLT1 (SLC5A1) and SMIT2 (SLC5A11) expression in all three segments compared to all the other SLC5A genes, support two different transporters contributing to the Ha/Hc system. The elevated expression of SGLT1 (SLC5A1), a well characterized Ha/Lc transporter supports the high affinity kinetics and phloridzin inhibition (16). Interestingly, although SMIT2 (SLC5A11) had the highest expression compared to all the

other genes, it is known to primarily transport inositols (204). However, it is previously known as SGLT6, and was characterized as a very low-affinity glucose transporter in mammals (11, 14, 42). The high capacity of glucose transport was demonstrated with rabbit SMIT2 (SLC5A11) cRNA injected into *Xenopus* oocytes, and detected glucose transport around 50mM (124). In the phylogenetic tree (Figure 3.3B), SMIT2 (SLC5A11) is divergent from SGLT1 (SLC5A1) with only 55.3% homology, suggesting differences in function. Nonetheless, the putative high capacity glucose transporter could explain Hc kinetics found in each of the tilapia intestinal segments. Altogether, the combined dominant expression and function of these two transporters are further supported by a Sigmoidal Hill fit. Together, this suggests that the heterogeneous expression in tilapia of ten different SLC5A transporters along all areas of gastrointestinal tract, with a dominance of SGLT1 (SLC5A1) and SMIT2 (SLC5A11) expression produces the Ha/Hc kinetics and the pharmacological inhibition observed. Such a Ha/Hc system would be advantageous for an omnivorous fish to absorb high levels of glucose presented to the gut from the diet (199).

3.5.2 Three-Kinetic SLC5A-associated Glucose Absorption in Trout

The segregation of three kinetic sodium-dependent glucose transport systems were found along the gastrointestinal tract of trout. In all the trout gut segments, the capacity for glucose transport was low in comparison to tilapia. However, the overall affinity was higher in the proximal segments of trout pyloric caeca and midgut, but drastically decreased as it reached the distal hindgut. The low capacity in all three segments of trout would protect the fish from rapid glucose absorption. Exogenous glucose ingestion in carnivorous fish has shown to induce the process of gluconeogenesis, further increasing the plasma glucose levels (121, 151). This can lead to persistent hyperglycemia (high plasma glucose levels) and high levels of plasma insulin which can hinder growth and increase liver size (110, 163). The differences in affinity explain how the proximal sections are sensitive to glucose transport when luminal glucose concentrations are low, around 1mM - 5mM, but the hindgut is sensitive to glucose transport only when the intestinal luminal glucose concentration is much higher, above 5mM.

The differences in affinity for glucose between the trout pyloric caeca and midgut may assist glucose absorption as the concentration of glucose decreases in the chyme as it moves

through the intestine (4). The Ha/Lc transport system characterized in the current study in the pyloric caeca would be efficient at absorbing most of the available glucose in the trout chyme. However, as the chyme moves to the midgut with decreasing glucose concentrations, the sHa/Lc transport system would become advantageous. A related study examining proximal intestinal glucose absorption in the carnivorous, seawater, pacific copper rockfish demonstrate similar kinetic segmental differences. (4). The uptake of ^{3}H-D-glucose in BBMVs (brush-border membrane vesicles) of pyloric caeca and upper intestine (anatomically similar to midgut) exhibited Michaelis-Menten kinetics of sodium-dependent glucose absorption (4). The Jms (Vmax) was similar between both organs (pyloric caeca and upper intestine), but the Km values were different (high Km for pyloric caeca and low Km for upper intestine) (4). The differences in the Km values indicate that pyloric caeca has lower affinity for glucose concentration than the upper intestine (midgut) (4). Similarly, we found differences in Km values between pyloric caeca and midgut, where the midgut demonstrated a super- high-affinity (sHa) for glucose compared to the pyloric caeca, with no differences in the Vmax. Ahearn *et al*. (1992) suggested that since the pyloric caeca has first access to the food, it absorbs more of the nutrients at higher concentrations (4). In contrast, the chyme that is released to the subsequent midgut section has lower nutrient content, thus needs a higher affinity transport system (4). Here we took trout intestinal segmental contributions further by characterizing glucose uptake in the hindgut as well. Interestingly, the above assertion does not hold for the trout hindgut with its Sigmoidal/Hill fit and lower affinity (La) and higher capacity than the midgut, suggesting physiological roles for this system other than nutrient absorption. Finally, the use of known mammalian SGLT inhibitors suggest a lack of contribution from trout SGLT1 (SLC5A1) and SGLT2 (SLC5A2) to the kinetic systems. However, given that the sequence similarity of trout SGLT1 (SLC5A1) and SGLT2 (SLC5A2) to human is only 58% and 66% respectively, this finding was not too surprising. Alternatively, the lack of inhibition may be attributed to the lower temperature used for trout kinetic measurements. Such temperature sensitivity of glucose transport inhibitors has previously been described (65). Thus, the three kinetic trout system was further characterized by genomic and gene expression analysis.

In trout, 5 of the known 12 SLC5A transporters where found and exhibited high SGLT1 (SLC5A1, Ha/Lc) expression in the pyloric caeca and midgut compared to the other SLC5A transporters. This data is correlated with the Michaelis-Menten Vmax values for the trout

pyloric caeca and midgut segments that exhibit Lc transport. However, the trout pyloric caeca SGLT2 (SLC5A2) and SMIT2 (SLC5A11) which are low-affinity transporters were more prominently expressed than in the midgut, possibly explaining the comparatively lower affinity detected in the pyloric caeca segment (11, 14, 42). Therefore, the kinetics of Ha/Lc in the trout pyloric caeca is likely due to the combined expression of SGLT1 (SLC5A1), SGLT2 (SLC5A2), and SMIT2 (SLC5A11), whereas the sHa/Lc kinetics in the midgut is due to a decrease in SGLT2 (SLC5A2) and SMIT2 (SLC5A11). In comparison, the decrease in trout hindgut SGLT1 (SLC5A1) expression was associated with a drastic reduction in affinity to glucose in this segment, again suggesting that the high- and super-high-affinity of the pyloric caeca and midgut is driven by SGLT1 (SLC5A1). The expression of the other SLC5A genes in the trout hindgut, which do not significantly differ from the midgut then may account for the low-capacity kinetics. Although our analysis of SLC5A gene expression does account for the kinetics defined in this study, there is still the possibility of another unidentified SGLT–like transporter that may explain the Lc paradigm in trout hindgut. Overall, our results confirm that the carnivorous trout has SGLT1 (SLC5A1), SGLT2 (SLC5A2), and SMIT2 (SLC5A11) transporters in the pyloric caeca likely driving an observed Ha/Lc system, and an increase in proportional SGLT1 (SLC5A1) expression to SGLT2 (SLC5A2) and SMIT2 (SLC5A11) driving a sHa/Lc system in the midgut. A La/Lc kinetic system in the trout hindgut is supported by low expression of all trout SLC5A genes and a significant drop in SGLT1 (SLC5A1).

3.5.3 Fish Hindgut Glucose Absorption- Different from Mammals

The presence of sodium-dependent glucose absorption in the hindgut of tilapia and trout was surprising in comparison to the mammalian models, where it is non-existent in this location (75, 84, 86, 112). However, for aquatic animals, the regulation of ionic and osmotic balances are extremely important, utilizing ionic and substrate transporters in their gills, kidneys and intestines to maintain this balance (10, 92, 190). The gut plays a role in osmoregulation by controlling the intake of dietary ions, using glucose transporters along with dietary substrates to passively contribute to ionic and osmotic balances (108, 190). Interestingly, the presence of active D-glucose uptake in the rectum was found in frugivorous avian species and was considered important to offset the fast digesta transit through their short gut (122, 123). However, the omnivorous chicken with its longer gut demonstrated high hindgut glucose uptake

(68). This suggest functions of this glucose absorption other than nutrient uptake. One possibility would be osmoregulation, especially given the proximity of the rectum and cloaca (8, 71). Together, our characterization of sodium-dependent glucose transport and associated SGLTs in the hindguts of these fish may be an unexplored mechanism that may contribute to ionic and osmotic regulation in tilapia and trout.

3.5.4 Omnivorous and Carnivorous Comparisons between Fish and Mammals

The homogenous Ha/Hc kinetic system of sodium-dependent glucose absorption that exists throughout the omnivorous tilapia differs from previously characterized omnivorous systems such as the dog, cattle, human, rat, and pig (64, 75, 84, 86, 101, 165). Generally, two types of intestinal segmental differences in sodium-dependent glucose absorption kinetic systems were identified, with Ha/Lc kinetics in the jejunum, La/Hc in the ileum, and the colon being void of transport (64, 75, 84, 86, 101, 165). Thus, tilapia have evolved to use their entire intestinal tract for Ha/Hc sodium-dependent glucose absorption, whereas omnivorous mammals only utilized their small intestinal sections (jejunum and ileum) for either Ha/Lc or La/Hc, but never show Ha/Hc sodium-dependent glucose absorption (12, 21, 75, 112). This fundamental difference suggests that tilapia may be more efficient than these other omnivorous mammals at absorbing glucose. Comparatively, trout differ from the carnivorous cat, with the cat having similar intestinal kinetic segmental segregation to omnivorous animals with Ha/Lc and La/Hc kinetics (201). The trout differs with three-kinetic, sodium-dependent glucose transport systems (Ha/Lc, sHa/Lc, La/Lc), that is overall low-capacity. This suggests trout to have a very limited capacity to absorb glucose compared to other omnivorous and carnivorous mammals.

3.6 Conclusion

In tilapia, electrogenic sodium-dependent glucose absorption was characterized as a segmentally homogenous Ha/Hc kinetic system. These finding were supported by the high expression of SGLT1 (SLC5A1) and SMIT2 (SLC5A11), and similar sensitivities to dapagliflozin and phloridzin dihydrate throughout the GI. In trout, a Ha/Lc system in the pyloric caeca was supported by the expression of SGLT1 (SLC5A1), SGLT2 (SLC5A2), and SMIT2 (SLC5A11), whereas the midgut demonstrated an sHa/Lc kinetic system, supported by the

SGLT1 (SLC5A1) expression and a decrease in SGLT2 (SLC5A2) and SMIT2 (SLC5A11) expression compared to pyloric caeca. Finally, the hindgut demonstrated a La/Lc kinetic system supported by a decrease in SGLT1 (SLC5A1) expression and a general expression of SLC5A genes. Overall, tilapia and trout demonstrate differences in transport kinetics and intestinal segmental contribution associated with SLC5A family members. Additionally, these findings highlight segmental kinetic differences between the gastrointestinal tract of fish and mammals.

3.7 Perspectives and Significance

Here, we present the first report comparing the kinetic characterization of electrogenic sodium-dependent glucose transport in the omnivorous Nile tilapia and the carnivorous rainbow trout gastrointestinal tract. The differences found suggest that omnivorous and carnivorous fish may have unique transport systems for glucose. This may have evolved to allow each species to maximize its glucose uptake from its natural diet. However, this omnivore-carnivore paradigm needs to be further tested in other mammalian and aquatic systems. Finally, in comparison to mammals, the discovery here of hindgut sodium-dependent glucose absorption in fish suggests that this process may play a greater role in osmoregulation, a homeostatic mechanism vital to aquatic species.

Chapter 4 - Sigmoidal Kinetics Define Porcine Intestinal Segregation of Electrogenic Monosaccharide Transport Systems as having Multiple Transporter Population Involvement

Marina Subramaniam[1]; Cole B. Enns[1]; Matthew E. Loewen[1b]

1. Department of Veterinary Biomedical Sciences, Western College of Veterinary Medicine, University of Saskatchewan. 52 Campus Drive. Saskatoon, Saskatchewan, Canada S7N 5B4

AUTHOR CONTRIBUTIONS

M.L. conceived and designed research; M.L., M.S., C.E. performed experiments; M.L., C.E. analyzed data; and M.L., M.S. interpreted results of experiments; M.S. prepared figures; M.L. and M.S. drafted manuscript; M.S., C.E. and M.L. edited and revised manuscript; M.S., C.E. and M.L. approved final version of manuscript.

*This manuscript has been submitted to American Journal of Physiology – Gastrointestinal and Liver Physiology.

4.1 Abstract

Kinetic characterization of electrogenic sodium-dependent transport in Ussing chambers of D-glucose and D-galactose demonstrated sigmoidal/Hill kinetics in porcine jejunum and ileum, with the absence of transport in the distal colon. In the jejunum, a high-affinity, super-low-capacity (Ha/sLc) kinetic system accounted for glucose transport, and a low-affinity, low-capacity (La/Lc) kinetic system accounted for galactose transport. In contrast, the ileum demonstrated a high-affinity, super-high-capacity (Ha/sHc) glucose transport, and a low-affinity, high-capacity (La/Hc) galactose transport systems. Jejunal glucose transport was not inhibited by dapagliflozin, but galactose transport was inhibited. Comparatively, ileal glucose and galactose transport were both sensitive to dapagliflozin. Genomic and gene expression analysis identified 10 of the 12 known SLC5A family members in the porcine jejunum, ileum, and distal colon. Dominant SGLT1 (SLC5A1) and SGLT3 (SLC5A4) expression was associated with the sigmoidal Ha/sLc glucose and La/Lc galactose transport systems in the jejunum. Comparatively, dominant expression of SGLT1 (SLC5A1) in the ileum was only associated with Ha glucose and La galactose kinetic systems. However, the sigmoidal kinetics and overall high capacity (Hc) of transport is unlikely accounted for by SGLT1 (SLC5A1) alone. Finally, the absence of transport and lack of pharmacological inhibition in the colon was associated with poor expression of SLC5A genes. Altogether, the results demonstrated intestinal segregation of monosaccharide transport fit different sigmoidal kinetic systems. This reveals multiple transporter populations in each system, supported by gene expression profiles and pharmacological inhibition. Overall, this work demonstrates a complexity to transporter involvement in intestinal electrogenic monosaccharide absorption systems not previously defined.

4.2 New and Noteworthy

Here, our work presents the first sigmoidal/Hill kinetic characterization of sodium-dependent glucose and galactose transport in the porcine jejunum and ileum. More importantly, this characterization strongly indicates the presence of multiple transporter populations in each segment. This notion of multiple transporter populations contributing to the observed kinetic transport systems has not been previously reported. Thus, this work presents a new perspective on the mechanism of electrogenic monosaccharide transport along the gastrointestinal tract.

4.3 Introduction

Sodium-dependent glucose absorption along the small intestine (jejunum and ileum) of mammals (rats, pigs, rabbits, and humans) represent a heterogeneous transport system (21, 115, 132). In particular, this has been studied extensively in porcine models that have diets similar to humans and a comparable gastrointestinal tract anatomy and physiology (13, 75). This heterogeneous system is defined by the presence of two types of sodium-dependent glucose transport kinetics in the jejunum and ileum (179, 205, 206). Specifically, the transport kinetics of glucose in the jejunum have been identified as a high-affinity, low-capacity (Ha/Lc) transport system, while the ileum demonstrates a low-affinity, high-capacity (La/Hc) glucose transport system (12, 13, 22, 53, 64, 75, 84, 112, 202-204). These systems were characterized with Michaelis-Menten kinetics (hyperbolic saturation), suggesting only one transporter involvement in each segment. (21, 75, 101, 112, 202). However, the small number of incremental increases in the glucose gradient used may have limited generating precise kinetic fits (84, 112).

Thus far, these heterogenous Michaelis-Menten systems were thought to be the product of the Ha/Lc sodium-dependent glucose transporter 1 (SGLT1), a member of the SLC5A (solute carrier family member 5A) transporter family (77, 165, 203, 204, 206). The SLC5A family is responsible for the co-transport of glucose and sodium, resulting in a measurable current (77, 165, 203, 204, 206). Recently, porcine jejunal and ileal sodium-dependent glucose transport kinetics revealed Ha kinetics in both segments, suggesting SGLT1 (SLC5A1) may be responsible in both segments (84, 112). However, it was concluded that the Hc kinetics observed in the ileum cannot be explained by SGLT1 (SLC5A1) (84, 112).

The possibility of a modified SGLT1 (SLC5A1) transporter responsible for the segregation of sodium-dependent glucose transport in the jejunum and ileum has been studied by Herrmann *et al*., as well as Klinger *et al*. (84, 112). It was concluded that the possibility of glycosylation- or phosphorylation-mediated changes to the SGLT1 (SLC5A1) transporter may compensate in situations where glucose transport is decreased, but it was not the reason for the heterogeneity of transport between the jejunum and ileum (112). Additionally, kinetic analysis only demonstrated Michaelis-Menten kinetics, suggesting only one transporter involvement (84, 112). However, the presence of a modified SGLT1 should have likely created sigmoidal kinetics.

Here, we report the first detailed kinetic description of both sodium-dependent glucose and galactose transport systems along the porcine gastrointestinal tract, with use of the dapagliflozin inhibitor and an extensive gene expression analysis of all known pig SLC5A orthologs. Overall, this description best fit sigmoidal/Hill kinetics, indicating the involvement of multiple populations of transporters in each segment. Additionally, different functional populations of transporters are present between the jejunum and ileum.

4.4 Materials and Methods

4.4.1 Animals

Twenty-two 7-9-week-old purebred Yorkshire barrows were housed in pairs and provided with a commercial, non-medicated diet and water *ad libitum*. The contents of the feed contained: crude protein (16%), crude fat (2.4%), crude fibre (5%), vitamin A (6000 IU/kg), vitamin D_3 (900 IU/kg), vitamin E (25 IU/kg), calcium (0.62%), phosphorous (0.55%), sodium (0.2%), lysine (0.83%), methionine (0.27%), and threonine (0.58%) (Whole Earth Pig Grower, Co-op Feed). Pigs were housed in the Animal Care Unit at the University of Saskatchewan, and maintained in accordance with the guidelines of the Canadian Council on Animal Care (CCAC, 2005) (33). All animal protocols were approved by the Animal Care Committee at the University of Saskatchewan (AUP#: 20130034).

4.4.2 Ex-vivo Tissue Collection

Pigs were euthanized and the gastrointestinal tract was removed. The gastrointestinal tract was separated to obtain sections of the jejunum, ileum, and distal colon. The jejunum was obtained 18 inches distal from the stomach, the ileum was sampled 2 inches proximal of the ileal-caecal junction, and the distal colon was sampled 4 inches proximal of the rectum.

4.4.3 Electrophysiology

4.4.3.1 Ussing Chamber technique. Porcine intestinal samples were examined in Ussing chambers using techniques adapted from our group (125, 126, 182). The Ussing chamber system used in this study was an EasyMount Ussing Chamber System (Physiologic Instruments Inc.,

San Diego, CA). Each segment was placed in a modified Krebs buffer containing: 114mM NaCl, 5mM KCl, 2.15mM $CaCl_2 \cdot 2H_2O$, 1.1mM $MgCl_2 \cdot 6H_2O$, 0.3mM $NaH_2PO_4 \cdot H_2O$, 1.65mM Na_2HPO_4 and 25mM $NaHCO_3$ at pH 7.4, and devoid of glucose. The lumen of the intestine was washed with buffer using a syringe and 18-gauge needle to clean the luminal membrane of any residual chyme. The serosa and longitudinal muscle layers were removed from the intestinal samples with forceps prior to mounting on $1cm^2$ Ussing chamber inserts (Slider Number: P2314, Physiologic Instruments Inc., San Diego, CA). Once mounted, tissues were inserted into the Ussing chamber, and both apical and basolateral surfaces were bathed with 5mL of Krebs buffer solution. The chambers were continuously gassed for the duration of the experiment with 5% CO_2 and 95% O_2 (40). Needle valves were also present for the adjustment of gas flow into the chambers.

The transepithelial voltage and passing current set across the tissue was measured via 3M KCl agar bridges and Ag/AgCl reference electrodes. These electrodes were connected to leads that lead to the voltage/current clamp. The short-circuit current (*Isc*) was measured by the software program LabChart (ADInstruments Pty Ltd.) in µA, and this was a result of the tissue current opposing the current induced by the electrodes. The tissues were pulsed every 30 seconds at 0.001V to determine tissue resistances from the resulting current. A recirculating water bath capable of chilling and heating was responsible for maintaining the buffer in the Ussing chambers at 36-37^oC.

The glucose gradient used was: 1-25mM, 30mM, 40mM, and 50mM in sequential order. The gradient from 1-25mM was added to the chamber in increasing 1mM increments, followed by increments of 30mM, 40mM, and 50mM. The tissues were allowed to reach a steady baseline current for 20 minutes prior to the addition of D-glucose to the apical side of the chamber. An equivalent amount of D-mannitol was added to the basal side to prevent the development of an osmotic gradient from the addition of glucose. Prior to the addition of each increment of glucose and mannitol, a wait period of 3-4 minutes was allowed between each increment for the current to reach a steady state. The experiment with D-galactose was conducted in a similar manner.

4.4.4 Chemicals. For pharmacological characterization, 0.001µM, 0.01µM, 0.1µM, 1µM, 10µM, 100µM, 200µM, and 300µM of dapagliflozin (AdooQ® Bioscience, Irvine, CA) was used in sequential order in the Ussing Chamber as final concentrations. The drug was added to

the apical side, after the jejunum, ileum, and distal colon were at final glucose/galactose and mannitol concentrations of 50mM. A wait period of 5-7 minutes was allowed between each increment for the current to reach steady state.

4.4.5 RNA extraction and cDNA synthesis using RT-PCR. Approximately 1mg samples of tissue were obtained from the dissection of the intestinal tract and stored in RNA*later*® RNA Stabilization Solution (Thermo Fisher Scientific, Baltics) at -80ºC. RNA was isolated using the TRIzol reagent (Ambion *Life* Technologies, Van Allen Way, CA), and cDNA was synthesized through reverse transcription PCR using the qScript™ cDNA SuperMix (Quanta Biosciences, Maryland, USA) according to the manufacturer's protocol. The cDNA samples were stored at -80ºC for subsequent use in quantitative PCR.

4.4.6 Genomic Identification of SLC5A Genes. A detailed BLAST+ (Basic Local Alignment Search Tool) application was used to identify all of the annotated porcine SLC5A transporters. The twelve human SLC5A transporter sequences retrieved from the National Center for Biotechnology Information (NCBI) website (http://www.ncbi.nlm.nih.gov/) were used in a "blastn" command to search for similar mRNA sequences in the porcine genome (204). The expect value (e-value) was used to assess the significance of the match, where an e-value close to zero was considered significant and an e-value higher than 10^-15 was considered as a non-significant match. Once SLC5A transporters were identified, phylogenic trees were generated using the alignment program CLUSTAL W and MEGA7 (www.megasoftware.net) software.

4.4.7 Gene transcript expression levels by quantitative polymerase chain reaction.

Quantitative PCR was performed by RT-qPCR reaction using the GoTaq®qPCR Master Mix containing SYBR®Green1 (Promega, Madison USA). The Bio-Rad QPCR system (CFX96™ Bio-Rad Laboratories, Inc) was used to perform these reactions. The total volume of the PCR reaction was 12.5µL. A total of 40 cycles of qPCR was performed, with each cycle consisting of GoTaq® Hot Start Polymerase activation at 95ºC for 2 minutes, and then denaturation at 95ºC for 15 seconds, followed by annealing/extension at the primer's hybridization temperature for 1 minute. The dissociation step was at 60-95ºC. Serial dilutions of cDNA were also used to

generate a standard curve for each target gene, where the efficiency of each primer was calculated. The efficiencies for the primers ranged from 1.8-2.0. Porcine β-actin (Beta-actin) was used as the housekeeping gene and was used to normalize the relative mRNA expression levels of SGLTs in the pig. The method of analysis used to represent the relative expression levels was calculated using delta CT, where the amount of gene of interest was normalized to the amount of β-actin in that sample (173).

The primers for the porcine SLC5A genes and housekeeping gene were designed through the Integrated DNA Technologies website (https://www.idtdna.com/site), where the sequences and their accession numbers are presented in Table 4.1.

Table 4.1 Pig Primer Sequences used for quantitative PCR

Gene	Forward Primer (5`-3`)	Reverse Primer (5`-3`)	Accession Number
SGLT1	CTGTGGTGTGCACTACTT	GGTCAATACGCTCCTCTTT	NM_001164021.1
SGLT2	CTGGGCTGGAACATCTAC	CGTAACCCATGAGGATGAA	XM_021086375.1
SMIT1	TCTGAGATGCAGTGAGAATAG	CTGAATGACCCAAGGAAGA	XM_005657149.3
SGLT3	ATTGTGTGGGTCCCATTAG	GAAGGCTCCCTGTTCATT	NM_214182.1
NIS	GTTAGATCCTCTCTGGACAAC	CCACCTGTAAAGTGGGTATAG	NM_214410.1
SMVT	CAGCAATCAGCATCTTTGG	GGCCATGTTGGTCACTAT	XM_013996254.2
CHT	AGCAGTTGCAGGTGTAATA	GTAGACACACTCAGAGGAAC	XM_021087111.1
SMCT1	CCTCACTGCCAGCTTTAT	TCGTAGGTGCTGGTAAATC	NM_001291414.1
SGLT4	GGAACCTTTACCTCTCCAC	CTCCTGAAAGCCCAGAAA	XM_021096677.1
SGLT5	TCCAGATCGAGAACCTCA	AGAAGAGGTTGACACACAC	NM_001012297.1
SMIT2	CCCTCACCTCCATCTTTAAC	TGGAGACCAGCACTAGAA	NM_001110422.1
SMCT2	CACTGGGTAAGGAGGAAAG	CAGGTGTGAGCTGAATGA	XM_003122908.4
β-ACTIN	CACCACTGGCATTGTCAT	GTGGTGGTGAAGCTGTAG	XM_021086047

4.4.8 Designating Affinities (Ha or La) and Capacities (sHc, Hc, sLc, or Lc). After the Km and Vmax values were calculated from Hill/sigmoidal fits (preferred model) using GraphPad Prism 8 (GraphPad Software, Inc.), the affinities, high-affinity (Ha) or low-affinity (La), and the capacities, super-high-capacity (sHc), high-capacity (Hc), super-low-capacity (sLc), and low capacity (Lc) were designated to the transport systems. To denote whether a system was Ha or La, the Km values were statistically compared between jejunum and ileal glucose and galactose transport. If Km values were low and non-significant from each other, they were characterized as high-affinity, Ha. In Tables 4.2 and 4.3, the Km values for the jejunum and ileum glucose transport were low and non-significant from each other, which designated as Ha. If Km values were higher and significantly different from the low Km values, then those were designated as low-affinity, La. In Tables 4.2 and 4.3, the Km values for the jejunum and ileum galactose transport were non-significant from each other and higher than the corresponding glucose transport, thus they were designated as La. Similarly, if the Vmax values were low and significantly different from the high Vmax values, then those were denoted as low-capacity, Lc (Tables 4.2 and 4.3). Additionally, if the low Vmax values were significantly different from each other, then it was further designated as Lc and sLc (Tables 4.2 and 4.3). If the Vmax values were high, and significantly different from the low Vmax values, then those would be designated as high-capacity, Hc (Table 4.2). Additionally, if the high Vmax values were significantly different from each other, then they were further designated as Ha and sHc (Tables 4.2 and 4.3). Altogether in this study, the characterization of Ha/sLc, La/Lc, Ha/sHc, and La/Hc were determined by statistically comparing Km and Vmax values between monosaccharide transport and segments.

Table 4.2 Vmax and Km Values for D-Glucose and D-Galactose Electrogenic Absorption

D-Glucose			D-Galactose			Glucose Vs. Galactose	
Tissue	**Km ± SEM (mM)**	**Vmax ± SEM ($\mu A/cm^2$)**	**Tissue**	**Km ± SEM (mM)**	**Vmax ± SEM ($\mu A/cm^2$)**	**Km**	**Vmax**
Jejunum	4.6 ± 0.4^{A}	11.1 ± 2.3^{A}	Jejunum	19.1 ± 1.2^{A}	30.0 ± 5.0^{A}	*	*
Ileum	6.3 ± 0.9^{A}	100.7 ± 9.3^{B}	Ileum	17.4 ± 2.1^{A}	60.3 ± 7.1^{B}	*	*
Distal Colon	nd	nd	Distal colon	nd	nd	nd	nd

Vmax (µA) and Km (mM) represented for sodium-dependent electrogenic D-glucose and D-galactose absorption for each tissue type in pig. ND represents non-detectable transport of those substrates. Area of intestinal segment was $1cm^2$. Data are presented as means ± SEM. Different letter superscripts represent significance between each intestinal segment for Vmax and Km within each substrate (Student's t-test, $P < 0.05$). Asterisks represent significances for Vmax and Km between substrates for the same intestinal segment (Student's t-test, $P < 0.05$).

Table 4.3 Final Designations of Transport Systems for each Segment

Tissue	D-Glucose	D-Galactose
Jejunum	High-affinity, super-low-capacity (Ha/sLc)	Low-affinity, low-capacity (La/Lc)
Ileum	High-affinity, super-high-capacity (Ha/sHc)	Low-affinity, high-capacity (La/Hc)
Distal Colon	ND	ND

Kinetic transport systems defined for each porcine intestinal segment for D-glucose and D-galactose sodium-dependent transport. These designations are further defined in the Material and Methods Section. ND represents non-detectable kinetic characterization of sodium-dependent transport.

4.4.9 Statistical Analyses. D-glucose and D-galactose gradients in the jejunum and ileum demonstrated sigmoidal saturation kinetics, with hill coefficients greater than 1. This was determined from conducting an F-test between the traditionally used Michaelis-Menten fit and a sigmoidal/Hill fit to confirm the preferred model using GraphPad Prism 8 (GraphPad Software, Inc.) (119, 145). The sigmoidal/Hill fit was determined as the preferred model, with a $P < 0.001$. Generally, sigmoidal/Hill fits indicate the presence of more than one binding site/transporter, with hill coefficients usually greater than 1 (104, 135). The Vmax (represented in $\mu A/cm^2$) and Km (represented in mM) values for glucose and galactose transport were calculated using the equation for "One Site-Specific Binding with Hill slope" for jejunum and ileum using GraphPad Prism 8. The equation used for the Sigmoidal Hill kinetics was:

Equation 4.1

Sigmoidal Hill fit: $Y=Vmax*X^h/(Kd^h + X^h)$

All data met parametric assumptions, being normally distributed and exhibited homogeneity of variance. A student's t-test was performed between jejunum and ileum Vmax and Km values for glucose and galactose to determine significance (210). Similarly, a student's t-test was performed between jejunal glucose and galactose transport for Vmax and Km, as well as ileal glucose and galactose transport for Vmax and Km to determine significance. A $P < 0.05$ was considered to be significantly different.

For the inhibitor dapagliflozin, the percent activity remaining was calculated from the division of the 50mM increment short-circuit current (the concentration where the transporter is 100% saturated and it is 100% un-inhibited) and the resulting drop in current from the addition of each drug concentration. These calculations were performed for both glucose and galactose inhibitor data. The Ki values for the dapagliflozin response were calculated for jejunum and ileum using the "One-Site Fit logIC50" from GraphPad Prism 8 (GraphPad Software, Inc.). This fit follows the equation: $Y = Bottom + (Top-Bottom)/(1+10^{(X-LogIC50)})$. Parametric 1-way ANOVA's were performed on the three intestinal sections to determine significance for inhibition. After ANOVA, pairwise comparisons were made using Tukey's posteriori tests, as appropriate. A Student's t-test was performed between Ki values to determine significance. For the qPCR analyses, relative expressions were determined by the BioRad system, where the threshold cycle was established using the housekeeping gene, β-actin. A 2-way ANOVA (two factors: intestinal segment and gene) was conducted on the gene expressions. After ANOVA,

pairwise comparisons were made using Tukey's posteriori tests, as appropriate. All statistical analyses were performed on SigmaPlot (Systat Software Inc., San Jose, CA).

4.5 Results

4.5.1 Jejunum

4.5.1.1 Ha/sLc Glucose and La/Lc Galactose Kinetic Transport Systems

The electrogenic sodium-dependent glucose and galactose transport followed sigmoidal/Hill kinetics in the porcine jejunum, with Hill coefficients greater than 1 (Figures 4.1A and 4.2A). An F-test was conducted to confirm that the sigmoidal/Hill fit was preferred over a Michaelis-Menten, hyperbolic fit ($P< 0.001$). Jejunal glucose transport became saturated around 14 – 15mM glucose and resulted in very low Vmax and Km values (Table 4.2 and Figure 4.1A). In contrast, jejunal glucose transport revealed a significantly lower Vmax compared to the galactose transport system (Table 4.2, $P < 0.001$). The Km values between jejunal glucose and galactose transport revealed significantly higher Km in jejunal galactose transport (Table 4.2, $P < 0.001$). Thus, these findings support a Ha/sLc (low Km, very low Vmax) glucose transport system and a La/Lc (high Km, low Vmax) galactose transport system in the porcine jejunum (Tables 4.2 and 4.3). Additionally, the sigmoidal kinetics observed suggests the involvement of more than one transporter population in the jejunal monosaccharide transport. Sodium-dependency of glucose transport in the jejunum was demonstrated by replacement of sodium with choline creating a sodium-free Krebs buffer, which eliminated the glucose-mediated current (Figures 4.1A and 4.1B) (147).

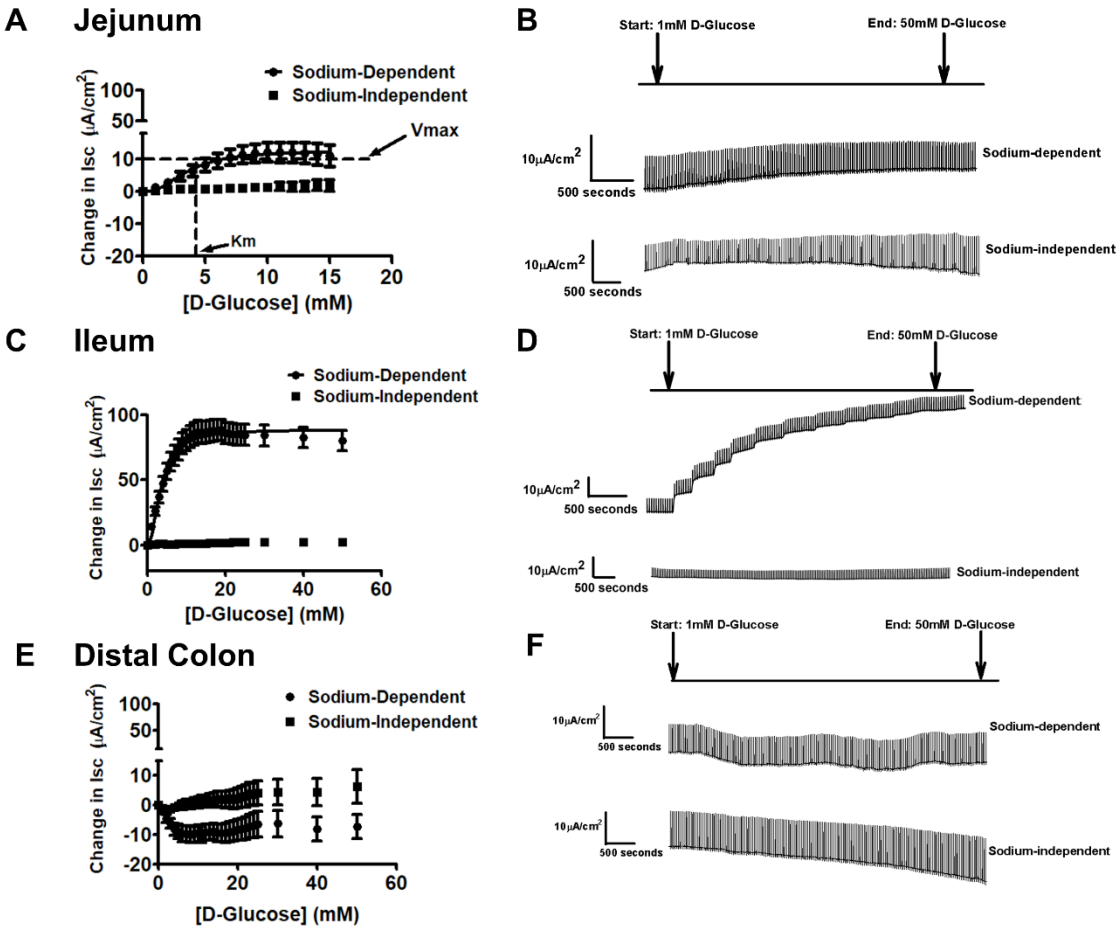

Figure 4.1 Kinetics of sodium-dependent glucose transport in pig.

Sigmoidal kinetics for sodium-dependent electrogenic glucose transport in **A)** jejunum, illustrated with representative traces on the right side **(B)** (Sodium-dependent: Pig N = 11; Sodium-independent: Pig N = 3), **C)** ileum, illustrated with representative traces on the right side **(D)** (Sodium-dependent: Pig N = 13; Sodium-independent: Pig N = 3), and **E)** no kinetics observed in distal colon, illustrated with representative traces on the right side **(F)** (Sodium-dependent: Pig N = 13; Sodium-independent: Pig N = 3). The Vmax and Km is represented in **A)** jejunum for illustration purposes. Data are represented as means ± SEM.

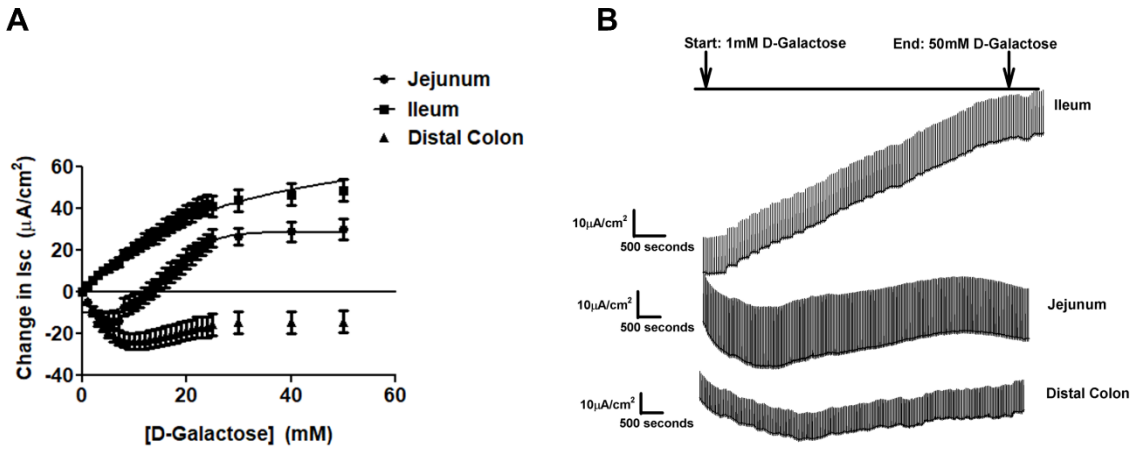

Figure 4.2 Kinetics of sodium-dependent galactose transport in pig.

Sigmoidal kinetics for sodium-dependent electrogenic galactose transport in **A)** jejunum, ileum and colon, illustrated with representative traces on the right side **(B)** (Pig: Jejunum: N = 5, Ileum: N = 6, Distal Colon: N = 6). Data are represented as means ± SEM.

4.5.1.2 Inhibition of Ha/sLc Glucose and La/Lc Galactose Systems

Dapagliflozin, a selective inhibitor for SGLT2 (sodium/glucose cotransporter 2) was used, and did not inhibit glucose-induced electrogenic current in the porcine jejunum (Figures 4.3A and B) (116, 170). Interestingly, dapagliflozin did cause significant inhibition (about 20-25%) of the galactose-induced electrogenic current at the higher concentrations (100-300μM) (Figures 4.4A and B, $P < 0.001$). The Ki value for inhibition of jejunal galactose transport by dapagliflozin is presented in Table 4.4.

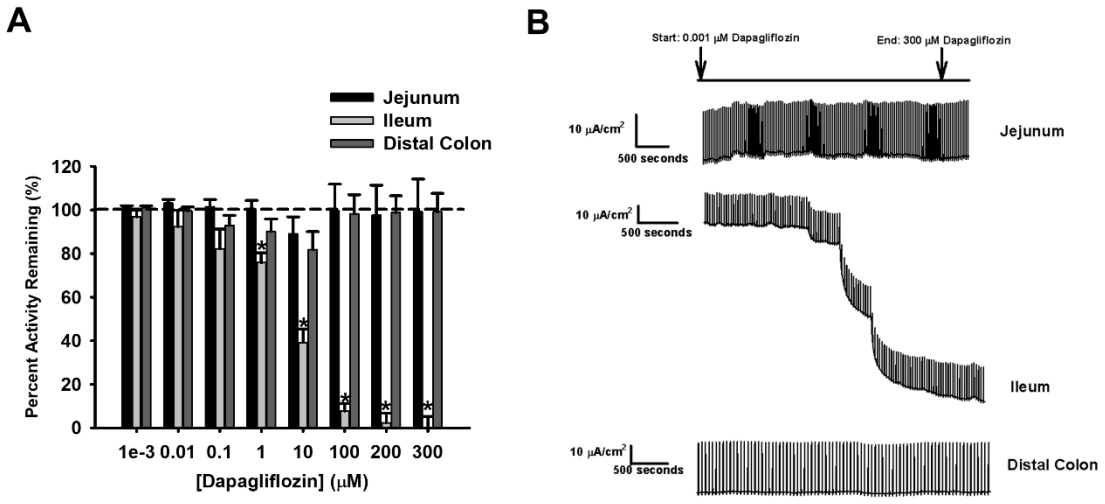

Figure 4.3 Pharmacological inhibition of glucose transport.

Percent activity remaining of short-circuit current (Isc) in response to D-glucose transport by **A)** dapagliflozin (0.001, 0.01, 0.1,10, 100, 200, and 300μM) in pig intestinal tissues (Jejunum: N=12, Ileum: N=12, Distal Colon: N=11). **B)** Representative traces for all intestinal tissues are presented for illustration purposes. Data are represented as means ± SEM. Asterisks represent significance from 100% transporter activity before inhibition, which is presented as the dotted line (1-way ANOVA, $P < 0.05$).

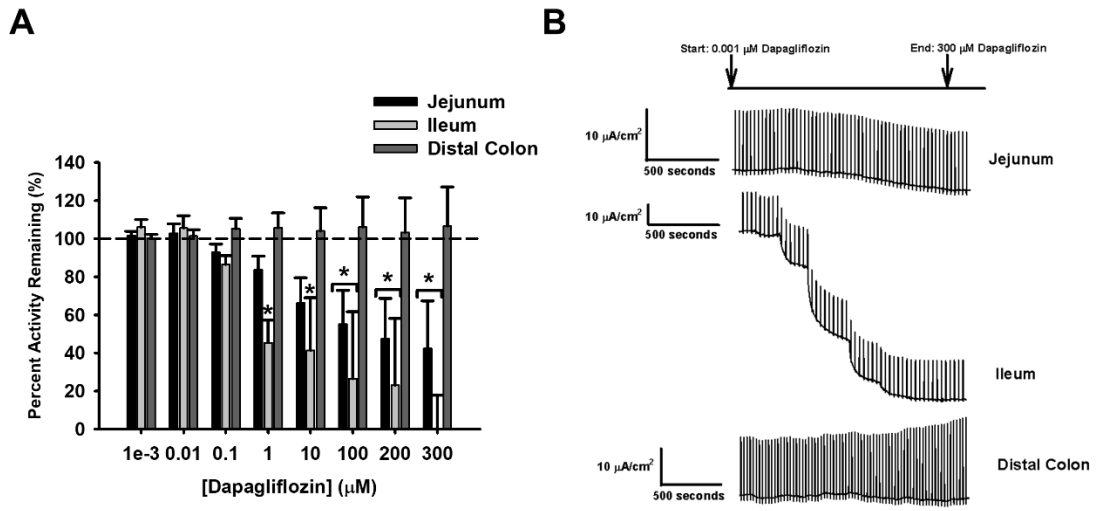

Figure 4.4 Pharmacological inhibition of galactose transport.

Percent activity remaining of short-circuit current (Isc) in response to D-galactose transport by **A)** dapagliflozin (0.001, 0.01, 0.1,10, 100, 200, and 300μM) in pig intestinal tissues (All tissues: N = 6). **B)** Representative traces for all intestinal tissues are presented for illustration purposes. Data are represented as means ± SEM. Asterisks represent significance from 100% transporter activity before inhibition, which is presented as the dotted line (1-way ANOVA, $P < 0.05$).

Table 4.4 Ki Values for D-Glucose and D-Galactose Electrogenic Absorption

D-Glucose		D-Galactose	
Tissue	**Ki ± SEM (µM)**	**Tissue**	**Ki ± SEM (µM)**
Jejunum	nd	Jejunum	4.6 ± 0.9 [A]
Ileum	6.0 ± 1.0	Ileum	1.8 ± 0.6 [B]
Distal Colon	nd	Distal colon	nd

Ki (µM) values represented for dapagliflozin inhibition of sodium-dependent electrogenic D-glucose (Jejunum: N=12, Ileum: N=12, Distal Colon: N=11) and D-galactose (All tissues: N = 6) absorption for each tissue type in pig. ND represents non-detectable inhibition. Data are presented as means ± SEM. Different letter superscripts represent significance between each intestinal segment (Student's t-test, $P < 0.05$).

4.5.1.3 SLC5A Gene Identification Affirms Kinetics in Jejunum

To identify gene product candidates that could contribute to the observed kinetics in the porcine jejunum, BLAST+ was utilized to probe the known SLC5A gene family. Our findings revealed 12 porcine SLC5A members in the genome (Table 4.1). However, quantitative real-time PCR only identified 10 porcine SLC5A members in the intestine. The SLC5A transporters identified with qPCR were SGLT1 (SLC5A1, sodium/glucose cotransporter 1), SGLT2 (SLC5A2, sodium/glucose cotransporter 2), SMIT1 (SLC5A3, sodium/myoinositol cotransporter 1), SGLT3 (SLC5A4, sodium/glucose cotransporter 3), SMVT (SLC5A6, sodium/multivitamin cotransporter), CHT (SLC5A7, sodium/choline cotransporter), SMCT1 (SLC5A8, sodium/monocarboxylate cotransporter 1), SGLT5 (SLC5A10, sodium/glucose cotransporter 5), SMIT2 (SLC5A11, sodium/myoinositol cotransporter 2), and SMCT2 (SLC5A12, sodium/monocarboxylate cotransporter 2). The genes NIS (SLC5A5, sodium/iodide cotransporter) and SGLT4 (SLC5A9, sodium/mannose cotransporter) were not detected by qPCR in the pig jejunum.

More specifically, porcine SGLT1 (SLC5A1) expression was significantly greater than the other 9 identified SLC5A isoforms in the jejunum, supporting the Ha/sLc glucose and La/Lc galactose transport systems (Figure 4.5A, $P < 0.001$ for transporter type). In addition, SGLT3 (SLC5A4) expression in the jejunum was significantly greater than the expression in the ileum and distal colon (Figure 4.5A, $P < 0.05$ for transporter type). Both gene candidates support the observed kinetics and inhibitor data found in the porcine jejunum. Sequence similarities between pig SLC5A transporters were compared in a phylogenic tree (Figure 4.5B). In a CLUSTAL W analysis, the nucleotide identities relative to pig SGLT1 (SLC5A1) were 57.5% SGLT2 (SLC5A2), 48.1% SMIT1 (SLC5A3), 72.8% SGLT3 (SLC5A4), 40.3% NIS (SLC5A5), 39.8% SMVT (SLC5A6), no sequence similarity with CHT (SLC5A7), 37.3% SMCT1 (SLC5A8), 51.7% SGLT4 (SLC5A9), 56.6% SGLT5 (SLC5A10), 56.1% SMIT2 (SLC5A11), and 35.3% SMCT2 (SLC5A12), revealing highest nucleotide sequence similarity between SGLT1 (SLC5A1) and SGLT3 (SLC5A4).

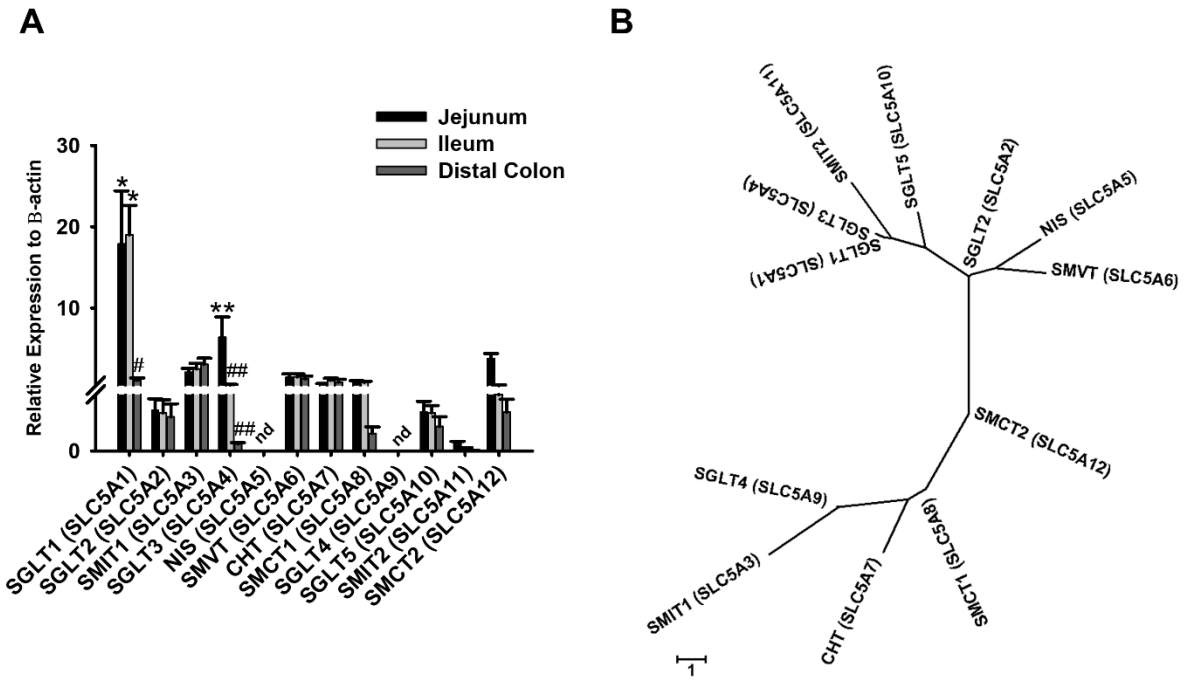

Figure 4.5 Genomic and gene expression analyses in pig.

A) Relative expression levels of SLC5A transporters (Jejunum: N = 8-10, Ileum: N = 7-10, Distal Colon: N = 7-10) using quantitative PCR. Expression levels were normalized against β-actin housekeeping gene. Letters represent significance between genes and tissues (2-way ANOVA, $P < 0.05$). ND represents non-detectable expression of those genes. **B)** Phylogenic tree of the 12 members of the SLC5A family of cotransporters in pig. The alignment program CLUSTAL W and the phylogenic display program MEGA7 were used to generate the tree.

4.5.2 Ileum

4.5.2.1 Ha/sHc Glucose and La/Hc Galactose Kinetic Transport Systems

In the porcine ileum, glucose and galactose gradients followed sigmoidal/Hill kinetics for both substrates, with hill coefficients greater than 1 (Figures 4.1C and 4.2A). An F-test was conducted to confirm that the sigmoidal/Hill fit was preferred over a Michaelis-Menten, hyperbolic fit ($P < 0.001$). A Ha/sHc glucose transport system was demonstrated, which saturated around 30-40 mM glucose and resulted in a similarly low Km and a significantly higher Vmax compared to the glucose transport system in the jejunum (Km: $P = 0.1$, Vmax: $P < 0.001$; Table 4.2 and Figure 4.1C). Specifically, ileal glucose transport kinetics had 9 times higher capacity than jejunal glucose transport kinetics (Table 4.2; Compare ileum: 100.7 ± 9.3 $\mu A/cm^2$ versus jejunum: 11.1 ± 2.3 $\mu A/cm^2$, $P < 0.001$).

The galactose-induced gradient in the ileum resulted in a La/Hc transport kinetic system, becoming saturated around 40-50 mM, with a significantly higher Km and a lower Vmax compared to glucose transport (Tables 4.2 and 4.3, and Figure 4.2A, Vmax: $P = 0.02$ for both substrates, Km: $P < 0.001$ for both substrates). Ileal glucose transport had a significantly higher Vmax than ileal galactose transport, resulting in sHc and Hc kinetics, respectively (Tables 4.2 and 4.3). Similarly, to the jejunum, the sigmoidal kinetics observed in the ileum suggests the involvement of more than one transporter. Sodium-dependency of glucose transport in the ileum was demonstrated by replacement of sodium with choline creating a sodium-free Krebs buffer, which eliminated the glucose stimulated current (Figures 4.1C and D).

4.5.2.2 Inhibition of Ha/sHc Glucose and La/Hc Galactose Transport Systems

In the ileum, dapagliflozin significantly inhibited glucose sodium-dependent electrogenic current from 1-300µM dosages, resulting in 20-90% inhibition (Figures 4.3A and B, $P < 0.05$). Similarly, in the galactose-induced electrogenic current, dapagliflozin significantly inhibited from 1-300µM dosages, resulting in approximately 40-80% inhibition (Figures 4.4A and B, $P < 0.001$). The Ki values for inhibition of ileal glucose and galactose transport are presented in Table 4.4. Finally, the significant difference in Ki values observed between jejunal and ileal galactose inhibition, as well as the absence of inhibition in jejunal glucose transport, suggest different multiple transporter populations between segments (Table 4.4).

4.5.2.3 SLC5A Gene Profiling in Ileum

To identify gene product candidates that could contribute to the observed kinetics in the porcine ileum, BLAST+ was utilized to probe the known SLC5A gene family. Similar to the findings in the jejunum, only 10 SLC5A members were identified by qPCR in the ileum, with no detection of NIS (SLC5A5) and SGLT4 (SLC5A9).

Gene expression in the ileum revealed significantly greater expression of SGLT1 (SLC5A1) when compared to the other 9 SLC5A isoforms (Figure 4.5A, $P < 0.001$). In contrast to the jejunum, SGLT3 (SLC5A4) expression was not significantly different between the ileum and distal colon (Figure 4.5A). Sequence similarities between pig SLC5A transporters were compared in a phylogenic tree (Figure 4.5B). Overall, sigmoidal kinetics of monosaccharide transport demonstrated in the ileum raises the possibility of another transporter in addition to SGLT1 (SLC5A1), which is either a modified SGLT1 (SLC5A1) different than the jejunum, or another transporter.

4.5.3 Distal Colon

4.5.3.1 Lack of Electrogenic Monosaccharide Transport in Distal Colon

The addition of glucose and galactose in the colon did not generate any observable sodium-dependent saturation kinetics, preventing the calculation of Vmax or Km values (Tables 4.2 and 4.3, Figures 4.1E and 4.2A). A lack of inhibition with dapagliflozin for glucose- and galactose-induced electrogenic currents confirmed the non-detectable kinetic transport system (Figures 4.3A and 4.4A). Identification of 10 SLC5A transporters in the distal colon by qPCR resulted in low expression of all genes in comparison to the jejunum and ileum, supporting the absence of electrogenic monosaccharide transport in this segment (Figure 4.5A).

4.6 Discussion

In terms of porcine sodium-dependent glucose transport, our results mirror studies presented previously that represent an overall low-capacity of transport in the jejunum and an overall high-capacity of transport in the ileum (75, 84, 112). In addition to these studies, we have presented sodium-dependent galactose transport following a similar pattern of low-capacity

jejunal transport and high-capacity ileal transport, which has not been characterized before. However, in contrast to previous studies, this study presents both glucose and galactose sodium-dependent transport following sigmoidal/Hill kinetic systems, instead of previously characterized Michaelis-Menten systems (75, 84, 112). This kinetic characterization of glucose and galactose transport was demonstrated by both the jejunum and ileum. Therefore, this strongly suggests the involvement of multiple transporter populations contributing to the kinetic systems observed in each segment, which is contrary to previous studies (75, 84, 112). Finally, pharmacological inhibition and gene expression analysis support the presence of different multiple transporter populations in each segment.

4.6.1 Jejunum

4.6.1.1 Sigmoidal Kinetics Support Multiple Transporter Involvement in the Jejunum

In this study, the porcine jejunum electrogenic glucose absorption is defined as a Ha/sLc system following sigmoidal/Hill kinetics, which becomes saturated at 14-15mM glucose (Figure 4.1A, and Tables 4.2 and 4.3). Comparatively, jejunal galactose transport revealed a La/Lc system, with 4 times lower affinity than glucose transport (Tables 4.2 and 4.3). Previous studies that have characterized glucose transport systems revealed a Ha/Lc transport system following a Michaelis-Menten model (21, 75, 80, 97, 112, 203, 206, 207). The use of Michaelis-Menten fits in these studies may be due to a smaller number of glucose increments used (21, 75, 80, 97, 112, 203, 206, 207). However, the results in this study reveal both glucose and galactose transport following a sigmoidal/Hill fit. This may be due to the techniques used, the increased number of glucose increments, as well as a larger glucose/galactose range (Figures 4.1 and 4.2). Nonetheless, with both jejunal glucose and galactose transport following sigmoidal/Hill fits, it strongly suggests the possibility of multiple transporter populations contributing to these kinetic transport systems.

Pharmacological inhibition with dapagliflozin lacked effect on jejunal sodium-dependent glucose transport, but inhibited jejunal galactose transport at concentrations greater than 100µM (Figures 4.3A and 4.4A, respectively). The lack of inhibition on glucose transport is not surprising given the low expression of SGLT2 (SLC5A2) in the jejunum, since dapagliflozin is a specific, competitive inhibitor for SGLT2 (SLC5A2) (Figure 4.5A) (93, 116, 143). In contrast,

the inhibition of galactose-induced transport by dapagliflozin may be explained by the lower affinity for galactose by a transporter such as SGLT1 (SLC5A1), thus allowing for competitive inhibition by dapagliflozin. Alternatively, it may also suggest the presence of another transporter such as SGLT3 (SLC5A4) that may be sensitive to dapagliflozin inhibition with galactose transport.

Following inhibitor characterization, a genomic and gene expression analysis of all porcine SLC5A genes revealed that SGLT1 (SLC5A1) and SGLT3 (SLC5A4) had the greatest expression in the porcine jejunum (Figure 4.5A). The high SGLT1 (SLC5A1) expression mirror those from previous studies that found SGLT1 (SLC5A1) as the dominant ortholog in guinea pig and porcine jejunal BBMVs, supporting a Ha/Lc system in this segment (21, 75, 80, 97, 112, 203, 206, 207). Additionally, studies in rats, mice, horses, rabbits, and beef steers found that SGLT1 (SLC5A1) expression was greater in the jejunum than ileum, which affirmed SGLT1 (SLC5A1) as a contributor to the Ha/Lc system (21, 75, 80, 84, 97, 112, 203, 206, 207). SGLT1 (SLC5A1) is known to absorb both glucose and galactose, but with a lower affinity for galactose (204).

However, the sigmoidal kinetic systems for jejunal glucose and galactose transport, strongly suggest the presence of multiple transporter populations in this segment. Therefore, the high expression of SGLT3 (SLC5A4) may be the other transporter involved in the jejunum (Figure 4.5A). In pigs, SGLT3 (SLC5A4) was first identified as SAAT1 (low-affinity sodium-dependent amino acid transporter) in the porcine kidney, which was mistakenly identified as SGLT2 in the porcine intestine, and finally confirmed as SGLT3 (SLC5A4) as a low-affinity glucose transporter (53, 203, 204). It has a lower affinity for glucose and galactose compared to SGLT1 (SLC5A1) (53). Overall, SGLT1 (SLC5A1) and SGLT3 (SLC5A4), or secondary modifications of these transporters, may contribute to the sigmoidal Ha/sLc and La/Lc glucose and galactose transport systems respectively, further supporting the notion of multiple transporter populations in the porcine jejunum.

4.6.2 Ileum

4.6.2.1 Multiple Transporter Populations involved in Ileal Monosaccharide Transport which Differ from Jejunum

A Ha/sHc glucose transport system following sigmoidal/Hill kinetics was characterized in the porcine ileum with significant differences in kinetics and pharmacological inhibition compared to the jejunum. The kinetics revealed a similar affinity, but a 9 times higher capacity in the ileum compared to jejunal glucose transport (Tables 4.2 and 4.3). Previous studies comparing glucose transport between porcine jejunal and ileal BBMVs found that the ileum had a higher Vmax than the jejunum, but similar Km values, supporting findings in the current study (75, 84, 112). For the first time, our study also revealed sodium-dependent galactose transport had a La/Hc kinetic system following sigmoidal/Hill kinetics in the ileum, but at a higher capacity than the jejunum (Tables 4.2 and 4.3). Finally, similarly to the jejunum, the sigmoidal/Hill kinetics for glucose and galactose transport in the ileum strongly suggest the presence of multiple transporter populations contributing to these kinetic systems. Additionally, pharmacological inhibition and gene expression analysis further support these results.

Dapagliflozin inhibited both glucose and galactose transport at concentrations 1-300μM in the ileum (Figures 4.3A and 4.4A). These results are different from the jejunum, where dapagliflozin inhibition was only observed with jejunal galactose transport. Additionally, the Ki value between jejunal and ileal galactose transport were significantly different, suggesting different multiple transporter populations (Table 4.4). Therefore, this strongly suggests the presence of another transporter in the ileum that is not similar to either SGLT1 (SLC5A1) or SGLT3 (SLC5A4) identified in the jejunum due to different patterns of inhibition.

Gene expression analysis determined that SGLT1 (SLC5A1) was the dominant SLC5A ortholog expressed in the porcine ileum. This is similarly described in other mammalian species such as rabbits, mice, and rats, where high expression of SGLT1 (SLC5A1) was found in the ileum (75, 83, 84, 112, 115, 191). These findings suggest that SGLT1 (SLC5A1) may contribute to the Ha glucose transport system and the La galactose transport system in the porcine ileum. This is supported by previous studies indicating SGLT1 (SLC5A1) has a higher affinity for glucose than galactose (204). However, SGLT1 (SLC5A1) alone does not explain the sHc and Hc kinetics observed with glucose and galactose transport, as well as the dapagliflozin inhibition to the glucose- and galactose-induced currents. Additionally, it has been concluded previously that SGLT1 (SLC5A1), although having dominant expression in the ileum, was not wholly responsible for the overall high-capacity glucose transport in the ileum (112). Thus, suggesting more than one transport involved in ileal glucose transport, although only Michaelis-Menten

kinetics were found (84, 112). Here, more importantly, the sigmoidal/Hill fits observed with ileal monosaccharide transport strongly suggest the involvement of another transporter.

4.6.3 Distal Colon

4.6.3.1 Lack of Electrogenic Monosaccharide Transport

The distal colon demonstrated a lack of glucose and galactose sodium-dependent transport. Our findings are supported by previous studies that have suggested that the colon lacks glucose transport (150, 203). During neonatal development in pigs, mice, and rats, the colon possess villus-like structures that assist in carbohydrate absorption, but this property disappears soon after birth (150). The pigs used in the current study were weaned and 7-9 weeks of age, thus having a mature colon lacking monosaccharide absorptive properties, producing the observed results (Figures 4.1E and 4.2A). Additionally, the lack of dapagliflozin inhibition and the poor expression of all SLC5A genes further support the absence of sodium-dependent glucose and galactose transport in the colon.

4.7 Conclusion

Electrogenic sodium-dependent glucose and galactose absorption in the jejunum and ileum followed sigmoidal/Hill kinetics, suggesting the presence of multiple transporter populations in each segment. In support of this, the jejunum had dominant expression of SGLT1 (SLC5A1) and SGLT3 (SLC5A4), possibly contributing to the Ha/sLc glucose and the La/Lc galactose transport systems. In contrast, the ileum presents itself with Ha/sHc glucose and La/Hc galactose transport systems, with dominant expression of SGLT1 (SLC5A1). However, the sigmoidal kinetics in the ileum likely suggests the involvement of another transporter along with SGLT1 (SLC5A1). Additionally, pharmacological inhibition demonstrates differences in inhibition patterns between jejunum and ileum supporting different multiple transporter populations in each segment. Finally, this detailed kinetic analysis provides a substantial burden of proof for not one but multiple transporter populations that differ between jejunum and ileum in the electrogenic absorption of glucose and galactose not previously reported.

Chapter 5 - Small Intestinal Tissue ^{14}C 3-O-Methyl D-Glucose Absorptive Flux Reveals Species Differences between the Mammalian Pig and Aquatic Species Tilapia and Trout

Marina Subramaniam[1]; Cole B. Enns[1]; Lynn P. Weber[1]; Matthew E. Loewen[1b]

1. Department of Veterinary Biomedical Sciences, Western College of Veterinary Medicine, University of Saskatchewan. 52 Campus Drive. Saskatoon, Saskatchewan, Canada S7N 5B4

M.L. conceived and designed research; M.L., M.S. and C.E. performed experiments; M.S. and C.E. analyzed data; and M.L., M.S. interpreted results of experiments; M.S. prepared figures; M.L. and M.S. drafted manuscript; M.S., C.E., L.W., and M.L. edited and revised manuscript; M.S., C.E., L.W., and M.L. approved final version of manuscript.

*This manuscript will be submitted for publication in American Journal of Physiology - Regulatory, Integrative, and Comparative Physiology.

5.1 Abstract

The mucosal to serosal flux of ^{14}C 3-O-Methyl D-glucose across the proximal small intestine was compared between Nile tilapia (*Oreochromis niloticus*), rainbow trout (*Oncorhynchus mykiss*), and the pig (*Sus scrofa*) in Ussing chambers. A 1mM to 8000mM D-glucose gradient revealed a high-affinity, high-capacity (Ha/Hc) total glucose transport system in tilapia, a high-affinity, low-capacity (Ha/Lc) total glucose transport system in trout, and a low-affinity, low-capacity (La/Lc) total glucose transport system in pig. The overall La glucose transport in the pig suggested a different mechanism of total glucose absorption compared to tilapia and trout. This was supported by responses to inhibitors of sodium-dependent glucose transporters (SGLTs), glucose transporter type 2 (GLUT2), and aquaporins (AQPs) on the apical side demonstrating major differences between the three species. In tilapia, glucose flux was inhibited by SGLT and AQP inhibitors, but not with the GLUT2 inhibitor. In trout, none of the inhibitors caused inhibition of total glucose transport. However, the pig responded to inhibition by both SGLT and AQP inhibitors, as well as the GLUT2 inhibitor. Genomic and gene expression analysis of GLUT2 supported this finding with the highest expression in the pig jejunum compared to tilapia and trout. Altogether, the Ha/Hc total tissue glucose absorption in tilapia is associated with a combination of SGLT and AQP transporters. In contrast, the La/Lc total tissue glucose transport system in the pig seems to be associated with a combination of SGLTs, AQPs, and apical GLUT2 contributing to continuing absorption at higher concentration.

5.2 Introduction

In the 1960s, the mechanism of glucose transport across the brush-border membrane (BBM) of mammalian enterocytes was first proposed (106, 107). Since then, this model developed to include both the entry of glucose through the sodium-dependent glucose transporter type 1 (SGLT1) by secondary active transport, followed by exit across the basolateral membrane via the facilitative glucose transporter type 2 (GLUT2) (44, 106, 107, 110). However, 11 more sodium-dependent glucose transporters have been identified and characterized that may also contribute to glucose movement across the intestinal BBM in addition to SGLT1 (13, 17, 18, 53, 112, 124). (13, 17, 18, 53, 112, 124, 204).

Generally, it is thought that SGLTs saturated around 30-50mM glucose, reaching their maximum transport capacity (105-107, 120, 213). However, luminal glucose concentrations in mammals are often in excess of 50mM (thought to be around 300 – 400mM), especially after a meal (105, 120). Therefore, the luminal glucose concentration will exceed the maximum saturation capacity of SGLTs (105, 120, 213). Thus, this leads to the question of whether SGLT transporters are the only ports of glucose entry present along the apical membrane of enterocytes, especially when luminal glucose concentrations exceed 30 – 50mM.

Therefore, the proposed theory of apical glucose absorption was modified to suggest the involvement of two components (105, 107, 213). This includes the SGLTs and a diffusive component that saturates at higher concentrations than SGLTs (105-107). This diffusive component has been argued to follow different pathways, including a "paracellular solvent drag" pathway, and a "GLUT2 translocation" pathway (106, 107, 213). However, evidence gathered was in stronger support of the "GLUT2 translocation" pathway, that suggested GLUT2 was responsible for the majority of glucose absorption once luminal glucose concentrations exceeded the capacities of SGLTs (107, 213). This pathway was initiated after SGLT1 reached maximum saturation capacity, which then activates protein kinase C βII (PKC βII) that activates downstream pathways leading to GLUT2 translocation to the BBM of enterocytes (107, 213). Once situated on the apical side, GLUT2 assists in glucose absorption at high luminal glucose concentrations (107). However, this has not been confirmed outside of the mouse.

Aside from GLUT2 possibly being the diffusive component of total glucose absorption, other types of transporters may contribute to glucose absorption as well. These include aquaporins (AQPs), which have about 13 members and have recently been suggested to transport other types of solutes apart from water (186). More specifically, aquaporin 9 (AQP 9) in humans have been found to transport non-charged solutes like carbamides, polyols, purines, and pyrimidines, in addition to their well known ability to transport urea and water (186). Therefore, AQPs may have the ability to transport solutes like glucose, especially when luminal glucose concentrations drastically increase.

Here, we present the mucosal to serosal flux (Jms) of ^{14}C 3-O-Methyl D-glucose (non-metabolizable form of D-glucose) across the proximal intestinal segments of Nile tilapia, rainbow trout, and pig in Ussing chambers. Overall, our data suggest that all species use SGLTs and AQPs in the total absorption of glucose, supported by inhibitor and gene expression data. In

trout, the data suggests most of the glucose transport occurs through SGLTs. However, it would appear that the pig differs with its low-affinity (La) total glucose absorption system, suggesting apical GLUT2 transporter involvement, supported by inhibitor and gene expression analysis. Together, there are similarities of total glucose absorption between the aquatic and mammalian species, but also drastic differences.

5.3 Materials and Methods

5.3.1 Maintenance of Animals

All fish and pigs were maintained in accordance with the guidelines of the Canadian Council on Animal Care (CCAC, 2005) (33). All animal protocols were approved by the Animal Care Committee at the University of Saskatchewan (AUP#: 19980142 – Fish, 20130034 - Pig).

5.3.1.1 Pigs. Eight 7-9-week-old purebred Yorkshire barrows were obtained from a finishing farm. They were housed in pairs in the Animal Care Unit at the University of Saskatchewan, and provided with a commercially prepared, non-medicated, pellet starter diet *ad libitum*. The contents of the feed contained: crude protein (16%), crude fat (2.4%), crude fibre (5%), vitamin A (6000 IU/kg), vitamin D_3 (900 IU/kg), vitamin E (25 IU/kg), calcium (0.62%), phosphorous (0.55%), sodium (0.2%), lysine (0.83%), methionine (0.27%), and threonine (0.58%) (Whole Earth Pig Grower, Co-op Feed).

5.3.1.2 Nile Tilapia. Nile tilapia were obtained from AmeriCulture Inc. (New Mexico, USA) as fingerlings. They were housed in 360L tanks filtered via a biological filtration system. Photoperiod was kept constant at 14h light/10h dark, and the water temperature maintained at 27 ± 2^{o}C. Fish were fed a standard ration of commercial feed by hand twice per day to visual satiety. The contents of the feed contained: crude protein (54%), crude fat (16%), crude fibre (1%), vitamin A (15000 IU/kg), vitamin D_3 (5000 IU/kg), vitamin E (400 IU/kg), calcium (2.3%), phosphorous (1.5%), and sodium (0.2%) (EWOS). The average weight of fish at the time of study was 700 grams.

5.3.1.3 Rainbow Trout. Triploid female rainbow trout were obtained from Wild West Steelhead (Lucky Lake, Saskatchewan, CA). The fish were housed in standard 1000-4000L density tanks, provided with biologically-filtered recirculation systems. They were housed in municipal, dechlorinated water at temperatures between 11 ± 2^{o}C, with a photoperiod at 12h light/12h dark. They were fed a standard ration of commercial feed at 2-5% of their body weight. The contents of the feed contained: crude protein (53%), crude fat (20%), crude fibre (1%), vitamin A (15000 IU/kg), vitamin D_3 (5000 IU/kg), vitamin E (300 IU/kg), calcium (2.3%), phosphorous (1.6%), and sodium (0.2%) (EWOS). At the time of study, the average weight of fish used was 300 grams.

5.3.2 Ex-vivo Tissue Collection

5.3.2.1 Tilapia and Trout. Fish were euthanized by blunt trauma to the head and the entire intestinal section was dissected out of both fish. In Nile tilapia, its intestinal section was separated to obtain proximal intestinal tissue (2 inches distal from the stomach). In rainbow trout, the intestine was separated to obtain the midgut section (located right after the pyloric caeca, 2 inches from the stomach).

5.3.2.2 Pig. Pigs were euthanized and the entire gastrointestinal section was removed for further dissections. The intestine was separated to obtain sections of the jejunum, which was obtained 18 inches distal from the stomach.

5.3.3 Electrophysiology

5.3.3.1 Ussing Chamber technique. The fish intestinal sections (tilapia proximal intestinal and trout midgut) were examined in Ussing chambers using techniques adapted from this group (125, 126, 164, 182). The Ussing chamber system used in this study was an EasyMount Ussing Chamber System (Physiologic Instruments Inc., San Diego, CA). Sections were washed in teleost saline: 118mM NaCl, 2.9mM KCl, 2.0mM $CaCl_2 \cdot 2H_2O$, 1.0mM $MgSO_4 \cdot 7H_2O$, 0.1mM $NaH_2PO_4 \cdot H_2O$, 2.5mM Na_2HPO_4 and 1.9mM $NaHCO_3$ at pH 7.9 (63). This physiological buffer was used for both tilapia proximal intestine and trout midgut. No glucose was added to the buffer. The lumen of the intestine for both fish was also washed with buffer using an 18gage needle, to clean the luminal membrane of any residual chyme.

The pig intestinal section (jejunum) was examined in Ussing chambers similarly as described for the fish. The jejunal segment was placed in Krebs buffer containing: 114mM NaCl, 5mM KCl, 2.15mM $CaCl_2 \cdot 2H_2O$, 1.1mM $MgCl_2 \cdot 6H_2O$, 0.3mM $NaH_2PO_4 \cdot H_2O$, 1.65mM Na_2HPO_4 and 25mM $NaHCO_3$ at pH 7.4, similar to the buffer used in a mice study done by Clarke (40). No glucose was added to the buffer. The lumen of the intestine was washed with buffer using an 18gage needle to clean the luminal membrane of any residual chyme. The muscularis mucosal layer was also stripped from the intestine prior to mounting.

The dissected tissue sections were exposed as a flat sheet between two sliders of inserts. The available tissue area for tilapia and trout was constant and equal to 0.3 cm^2 (Slider Number: P2304, Physiologic Instruments Inc., San Diego, CA). The available tissue area for pig intestinal tissue was 1cm^2 (Slider Number: P2314, Physiologic Instruments Inc., San Diego, CA). For trout and tilapia, the teleost saline buffer solutions bathing the apical and basal sides of the intestine had a buffer volume of 5ml, and were continuously gassed throughout the experiment with 1% CO_2 and 99% O_2 for the fish (40). For the pig jejunum sections, the Krebs buffer solution bathing the apical and basal sides of the intestine had a buffer volume of 5ml, and were continuously gassed throughout the experiment with 5% CO_2 and 95% O_2 (40).

The transepithelial voltage and passing current set across the tissue was measured via agar bridges and Ag/AgCl reference electrodes. These electrodes were connected to leads that lead to the voltage/current clamp. The pulse was kept constant at 0.001V. A recirculating bath capable of chilling and heating controlled the temperature of the jacketed chambers, with tissues examined at fish housing temperatures. The temperature used was matched to housing temperature for fish and body temperature for pigs; tilapia was 25ºC-26ºC, trout was 11ºC-12ºC, and pigs was 36-37ºC. Needle valves were also present for the adjustment of gas flow into the chambers.

Once mounted, the intestinal sections were allowed to reach a steady baseline current for 30-40 minutes, followed by addition of 1µCi of ^{14}C-3-*O*-Methyl D-glucose and 1µCi ^{3}H-inulin to the apical side of the intestinal tissues. An initial 100uL "hot" sample was taken from the apical ("hot") side for ^{14}C-3-*O*-Methyl D-glucose and ^{3}H-inulin. An isotope equilibration period was performed after, with a 70 minute time period for tilapia and trout, and a 60 minute time period for pig. Following the isotope equilibration period, a non-labeled D-glucose gradient from 1mM to 8000mM was used to assess saturation of transport, with equivalent amounts of non-labeled

D-mannitol additions to the basal side to control for osmotic drift. ^{3}H-inulin was used as a control to measure tissue integrity through the duration of the experiment. After every increment of D-glucose, there was a wait period of 10 minutes after which a 500µL sample was taken from the basolateral/ "cold" side. The radioactive samples were placed into 6mL liquid scintillation vials (LSVs) that contained 4.3mL of UltimaGold cocktail solution (PerkinElmer®, Waltham, MA). The radioactive samples were counted in a Beckman scintillation β-counter for ^{14}C and ^{3}H emission (PerkinElmer®, Waltham, MA).

5.3.4 Chemicals. For pharmacological characterization, 0.000001mM, 0.00001mM, 0.0001mM, 0.001mM, 0.01mM, 0.1mM, 0.2mM, and 0.3mM of dapagliflozin (AdooQ® Bioscience, Irvine, CA), followed by 0.001mM, 0.01mM, 0.1mM, 1mM, and 2mM of phloridzin dihydrate (AdooQ® Bioscience, Irvine, CA), followed by 1mM, 2mM, 3mM, 4mM, and 5mM of phloretin (AdooQ® Bioscience, Irvine, CA), followed by 1mM, 2mM, 3mM, 4mM, and 5mM tetraethyl ammonium (TEA) (Sigma-Aldrich Co., St. Louis, MO), and finally with 1mM, 2mM, 3mM, 4mM, and 5mM nickel chloride ($NiCl_2$) (FisherScientific Ottawa, Ontario) were used in sequential order in the Ussing Chamber as final concentrations. The inhibitors were added to the apical side once D-glucose and D-mannitol concentrations in the chambers reached 8000mM.

5.3.5 Radioisotopes. 1µCi of ^{14}C-3-*O*-Methyl D-glucose (non-metabolizable analogue of glucose) and 1µCi of ^{3}H-inulin, obtained from PerkinElmer® (Waltham, MA) were used.

5.3.6 RNA extraction and cDNA synthesis using RT-PCR. Approximately 1mg samples of tissue were obtained from the dissection of the intestinal tract, and stored in RNA*later*® RNA Stabilization Solution at -80^{o}C. RNA was isolated using the TRIzol reagent, and cDNA was synthesized through reverse transcription PCR using the qScript™ cDNA SuperMix (Quanta Biosciences, Maryland, USA). The reaction was run as: incubation for 5 minutes at 25^{o}C, then 30 minutes at 42^{o}C, and the final 5 minutes at 85^{o}C. The cDNA samples were stored at -80^{o}C for subsequent use in quantitative PCR.

5.3.7 Genomic Identification of SLC5A Genes. A detailed BLAST+ (Basic Local Alignment Search Tool) application was used to identify all of the annotated GLUT2 transporters in both tilapia, trout, and pig. The human GLUT2 transporter sequence retrieved from the National Center for Biotechnology Information (NCBI) website (http://www.ncbi.nlm.nih.gov/) were used in a "blastn" command to search for similar mRNA sequences in the tilapia, trout, and pig genome (204). The expect value (e-value) was used to assess the significance of the match, where an e-value close to zero was considered significant and an e-value higher than 10^-15 was considered as a non-significant match. Once GLUT2 transporters were identified from tilapia, trout, and pig, phylogenetic trees were generated using the alignment program CLUSTAL W and MEGA7 (www.megasoftware.net) software.

5.3.8 Gene transcript expression levels by quantitative polymerase chain reaction.

Quantitative PCR was performed on the RT-PCR reaction using the GoTaq®qPCR Master Mix containing SYBR®Green1 (Promega, Madison USA). The BioRad QPCR system was used to perform these reactions. The total volume of the PCR reaction was 12.5µL. A total of 40 cycles of qPCR was performed, with each cycle consisting of GoTaq® Hot Start Polymerase activation at 95^{o}C for 2 minutes, and then denaturation at 95^{o}C for 15 seconds, followed by annealing/extension at the primer's hybridization temperature (59^{o}C) for 1 minute. The dissociation step was at 60-95^{o}C. Serial dilutions of cDNA were also used to generate a standard curve for each target gene, where the efficiency of each primer was calculated. The efficiencies for the tilapia, trout, and pig primers ranged from 1.9-2.1. Tilapia, trout, and pig EFα1 (α-elongation factor 1) was used as the house-keeping gene, and was used to normalize the relative mRNA expression levels of GLUT2 for each species. The method of analysis used to represent the relative expression levels was calculated using delta CT, where the amount of the gene of interest was normalized to the amount of EFα1 in that sample (173).

The primers for pig, trout, and tilapia were designed using the Integrated DNA Technologies website (https://www.idtdna.com/site), where the sequences and their accession numbers are presented in Table 5.1.

Table 5.1 Nile Tilapia, Rainbow Trout, and Pig Primer Sequences used for quantitative PCR

Species	Gene	Forward Primer (5`-3`)	Reverse Primer (5`-3`)	Accession Number
Nile Tilapia	**GLUT2**	CCTCCTTCTTGGTTGGATTT	CAGACGTCAGACCACAATAG	XM_003442884.5
	EFα1	CTCTTCTACCGTCGGATTAC	ATTGACTCCCTCGTAGAAAC	XM_005476483.3
Rainbow Trout	**GLUT2**	CAACCATTGGAGTAGGAGTTC	ACATAGGACATCCAGGAGTAG	XM_021610908.1
	EFα1	AGCGAGCTCAAGAAGAAG	GACCAAGAGGAGGGTATTC	NM_001124339.1
Pig	**GLUT2**	GGACTTGTGCTACTGGATAA	CGTGGTCCTTGACTGAAA	NM_001097417.1
	EFα1	GCGAGTGGGATTCTGTTA	GGTGCCTGTCATCTTCTT	XM_013987376.1

5.3.9 Statistical Analyses. The mucosal to serosal flux (Jms) of 3-O-Methyl-D-Glucose was calculated from the protocol adapted from Schultz *et al*. (174). The ^{14}C and ^{3}H emissions from the 500µL cold samples taken after each concentration increment and inhibitor concentration were recorded as counts per minute (cpm). The Jms was calculated as follows:

Equation 5.1

Φ_{ms}^{C} (Jms) = $\nu_s(p_s2 - cp_s1)/(\Delta tp_m*A)$

p_s = cpm/cm^3 in the serosal reservoir

ν_s = volume of buffer in the serosal side in cm^3

A = area of tissue exposed

Δt = time interval between samples in hours

p_m* = specific activity of ^{14}C-3-*O*-methylD-glucose in the mucosal solution in cpm/µmol

Φ_{ms}^{C} = unidirectional ^{14}C flux from mucosa to serosa in µmol/cm^2/hour

Vmax (represented in µmol/cm^2/hr) and Km (represented in mM) values were determined for each species' intestinal sections using GraphPad Prism 8 (GraphPad Software, Inc.). All three sections followed Michaelis-Menten kinetics (F-test with Sigmoidal/Hill fit, $P < 0.05$ for Michaelis-Menten fit), where the equation for Michaelis-Menten is:

Equation 5.2

Michaelis-Menten fit: $Y = Vmax*X/(Km + X)$

A 1-way ANOVA was performed between each species to determine significant differences between Vmax and Km values. All data met parametric assumptions, being normally distributed and exhibited homogeneity of variance so ANOVA analyses were used. After ANOVA, pairwise comparisons were made using Tukey's posteriori tests, as appropriate. A $P < 0.05$ was considered significantly different. The percentage increase of Jms from the 50mM increment to the 5-8M increments were calculated for each species, and a 1-way ANOVA was performed to determine significance between the compared increments. After ANOVA, pairwise comparisons were made using Tukey's posteriori tests, as appropriate. A $P < 0.05$ was considered significantly different.

For the inhibitors, the percent activity remaining was calculated from the division of the last previous drug increment (the concentration where the transporter is 100% un-inhibited by that specific inhibitor) and the resultant drop in mucosal to serosal flux (Jms) from the addition of each drug concentration. Parametric 1-way ANOVA's were performed between the 100%

and each drug response to determine significance. After ANOVA, pairwise comparisons were made using Tukey's posteriori tests, as appropriate. Again, $P < 0.05$ was considered significant. The Ki values for the inhibitor responses were calculated using the "One-Site Fit long IC50" from GraphPad Prism 8 (GraphPad Software, Inc.). This fit follows the equation: $Y = Bottom + (Top-Bottom)/(1+10^{(X-LogIC50)})$. Student's t-test were performed to determine significance between Ki values for that inhibitor between species.

For the qPCR analyses, relative expressions were determined by the BioRad system, where the threshold cycle was established using the housekeeping gene, EFα1. A 1-way ANOVA (one factor: species) was conducted on the gene expressions. After ANOVA, pairwise comparisons were made using Tukey's posteriori tests, as appropriate. A $P < 0.05$ was considered significant. All statistical analyses were performed on SigmaPlot (Systat Software Inc., San Jose, CA).

5.4 Results

5.4.1 Kinetic Characterization of ^{14}C 3-O-Methyl D-glucose in Nile Tilapia, Rainbow Trout, and Pig

In tilapia, trout, and pig, the mucosal to serosal flux (Jms) of ^{14}C 3-O-Methyl D-glucose was measured in Ussing chambers, and followed Michaelis-Menten kinetics in all three species. Tilapia demonstrated a significantly higher capacity (higher Vmax) of glucose flux compared to trout and pig (Table 5.2 and Figure 5.1; $P < 0.001$). There were no significant differences in Vmax values between trout and pig, indicating similar capacities in overall whole tissue glucose absorption. However, the Km value in pig was significantly higher (over 400 fold) compared to tilapia and trout, with no significant differences between tilapia and trout Km values (Table 5.2 and Figure 5.1; $P < 0.001$). The higher Km value in pig suggests an overall dominating low-affinity glucose transport system. Altogether, the kinetic values present a Ha/Hc total glucose transport system in tilapia, a Ha/Lc total glucose transport system in trout, and a La/Lc total glucose transport system in the pig (Table 5.2).

Finally, the percentage increase of Jms in response to glucose increments was assessed in each species (Figure 5.1D). No significant differences in Jms increase occurred for tilapia and

trout, but significant increases from 50mM to 5000, 6000, 7000, and 8000mM were observed for pig (above 300%; Figure 5.1D, $P < 0.001$).

Table 5.2 Vmax and Km Values for Nile Tilapia, Rainbow Trout, and Pig

Species	Intestinal Section	Vmax ± SEM (µmol/cm^2/hr)	Km ± SEM (mM)
Nile Tilapia	Proximal Intestine	$0.009 \pm 0.001^{\mathbf{A}}$	$1.6 \pm 0.4^{\mathbf{A}}$
Rainbow Trout	Midgut	$0.002 \pm 0.0003^{\mathbf{B}}$	$3.3 \pm 0.7^{\mathbf{A}}$
Pig	Jejunum	$0.004 \pm 0.0005^{\mathbf{B}}$	$1561.4 \pm 185.6^{\mathbf{B}}$

Vmax (µA) and Km (mM) values represented for Nile Tilapia, rainbow Trout, and pig. Area of intestinal segment was 0.3cm^2 for both fish and 1cm^2 for pig. Data are presented as means ± SEM. Significant differences for Vmax values found between species: A, Nile Tilapia vs. B, rainbow Trout, and A, Nile Tilapia vs. B, Pig, with no significant differences between rainbow Trout and pig (Tukey's test after 1-way ANOVA, $P < 0.05$). Significant differences for Km values found between species: A, Nile Tilapia vs. B, Pig, and A, rainbow Trout vs. B, Pig, with no significant differences between Nile Tilapia and rainbow Trout (Tukey's test after 1-way ANOVA, $P < 0.05$).

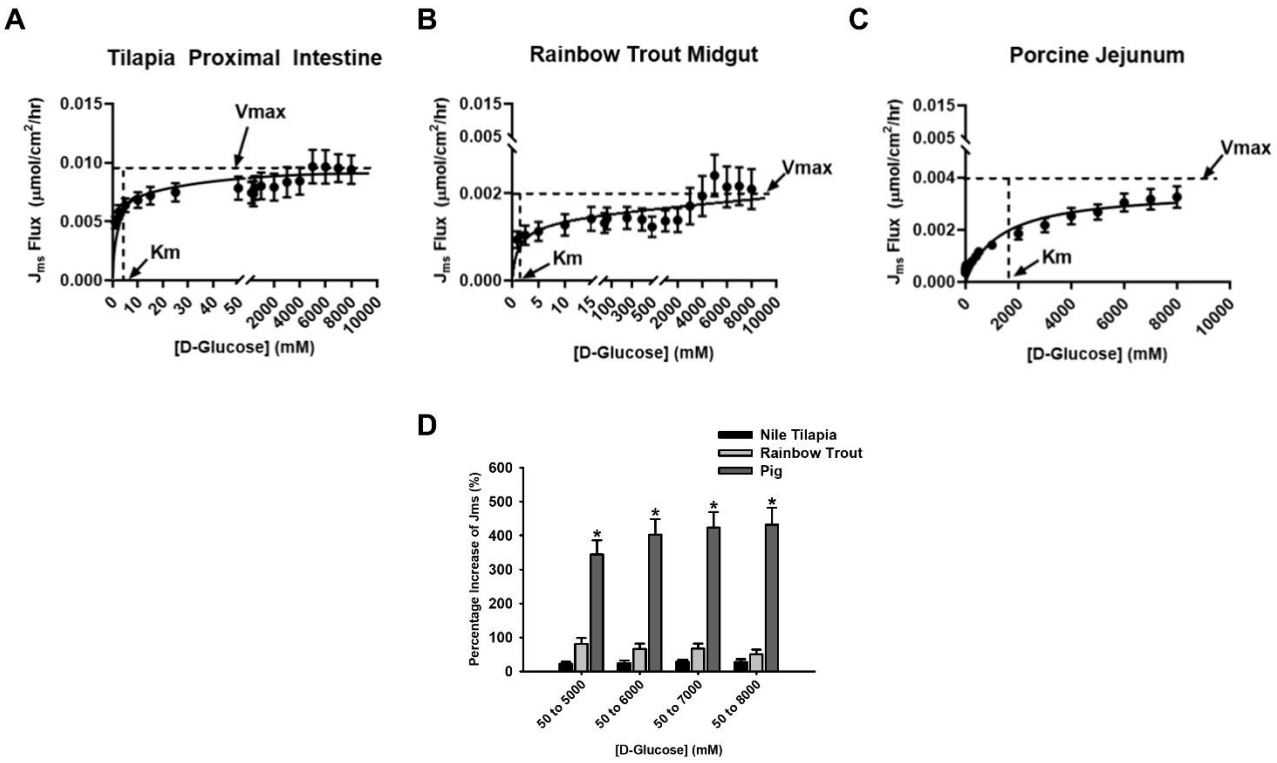

Figure 5.1 Kinetics of total tissue glucose absorption in tilapia, trout, and pig.

Michaelis-Menten kinetics for mucosal to serosal (Jms) 3-O-Methyl D-glucose flux for **A)** tilapia proximal intestine (Fish N = 15) with Vmax and Km represented for illustration, **B)** trout midgut intestinal section (Fish N = 17) with Vmax and Km represented for illustration, and **C)** pig jejunum (Pig N = 6) with Vmax and Km represented for illustration. **D)** The percentage increase of Jms for the represented concentration comparisons between species. Single asterisk represents significant differences for those concentration comparisons within pig (1-Way ANOVA, $P < 0.05$). Data are represented as means ± SEM.

5.4.2 Inhibition of Whole Intestinal Tissue Glucose Flux

A series of inhibitors for sodium-dependent glucose transporters (SGLTs), glucose transporter type 2 (GLUT2), and aquaporins (AQPs) were used in succession to inhibit total glucose flux across the intestinal segments of tilapia, trout, and pig. Dapagliflozin, specific for sodium-dependent glucose transporter type 2 (SGLT2), and phloridzin dihydrate, specific for sodium-dependent glucose transporter type 1 (SGLT1) were both used cumulatively to inhibit SGLTs (116, 143, 170). Phloretin is an inhibitor specifically for the GLUT2 transporter, and tetraethylammonium (TEA) and nickel (II) chloride ($NiCl_2$) inhibit aquaporins (50, 107, 211). The cumulative addition of each inhibitor was in the order of dapagliflozin, phloridzin dihydrate, phloretin, TEA, and $NiCl_2$ after glucose flux reached 8000mM in all three species. A dose response was performed for each inhibitor. Figures 5.2, 5.3, and 5.4 illustrate the percent activity remaining after successive addition of each inhibitor in each species.

5.4.2.1 Nile tilapia Flux inhibition

Tilapia had significant inhibition with dapagliflozin from 0.001 to 0.3mM, with about 60% activity remaining by 0.3mM dapagliflozin (Figure 5.2A, $P < 0.05$). Similarly, significant inhibition was observed with phloridzin dihydrate, with about 70% activity remaining by the 2mM concentration (Figure 5.2B, $P < 0.05$). Following phloridzin dihydrate, phloretin did not reveal significant inhibition with any of its concentrations (Figure 5.2C). However, TEA did reveal significant inhibition at 3mM and 5mM concentrations (Figure 5.2D, $P < 0.05$). At the 3mM and 5mM TEA inhibitor concentrations, about 70% activity remained (Figure 5.2D). Finally, $NiCl_2$ did not reveal significant inhibition at any concentrations (Figure 5.2E). A significant difference between the Ki value of $NiCl_2$ was observed between tilapia and pig (Table 5.3, $P < 0.05$).

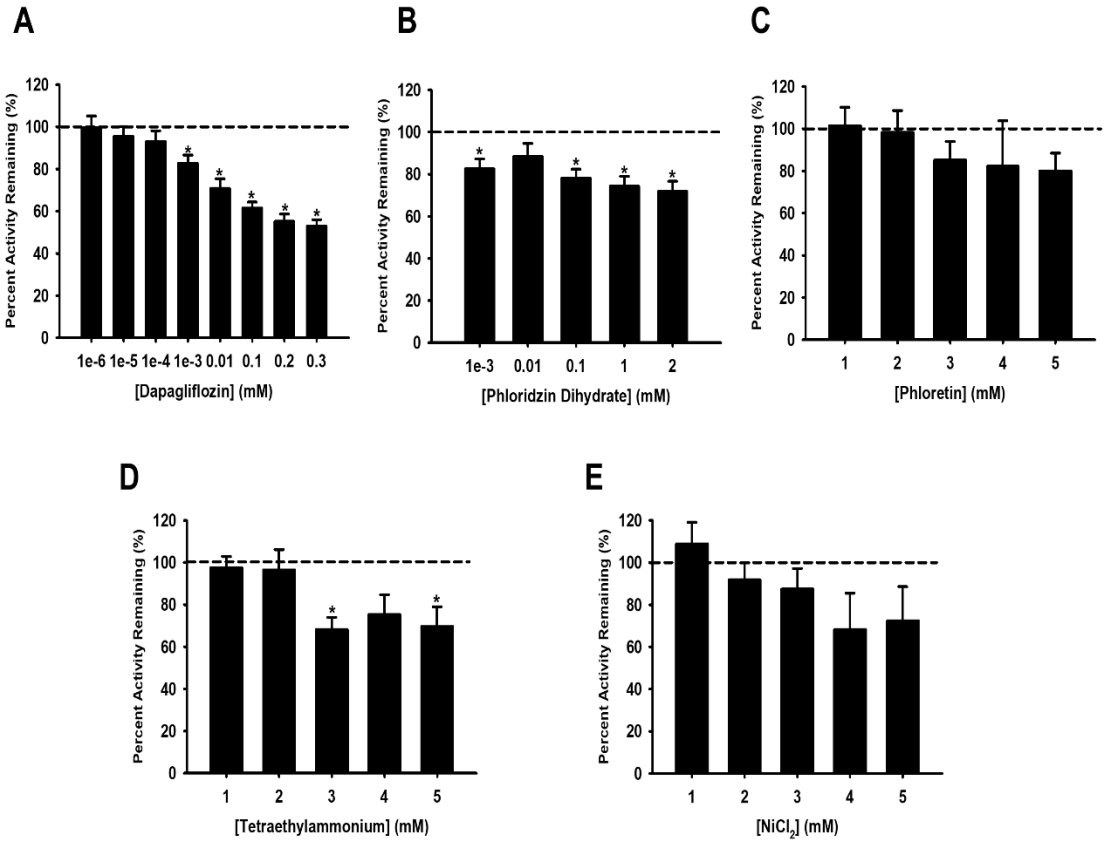

Figure 5.2 Pharmacological inhibition in tilapia.

Percent activity remaining of Jms in Nile tilapia by **A)** dapagliflozin (0.000001, 0.00001, 0.0001, 0.001, 0.01, 0.1, 0.2, and 0.3mM) (Fish N = 11), followed by addition of **B)** phloridzin dihydrate (0.001, 0.01, 0.1, 1, and 2mM) (Fish N = 14), followed by **C)** phloretin (1, 2, 3, 4, and 5mM) (Fish N = 8), followed by **D)** tetraethylammonium (1, 2, 3, 4, and 5mM) (Fish N = 9), and finally by **E)** $NiCl_2$ (1, 2, 3, 4, and 5mM) (Fish N = 6). Single asterisks represent significance from 100% (where 100% represents transport is 100% un-inhibited by that inhibitor), which is presented as the dotted line (1-way ANOVA, $P < 0.05$).

Table 5.3 Ki Values for Nile Tilapia, Rainbow Trout, and Pig

Species	Inhibitor	Ki ± SEM (mM)
Nile Tilapia	Dapagliflozin	0.007 ± 0.002
	Phloridzin Dihydrate	1.2 ± 0.7
	Phloretin	4.7 ± 1.0
	Tetraethylammonium (TEA)	4.5 ± 1.5
	Nickel Chloride ($NiCl_2$)	4.7 ± 1.1^{A}
Rainbow Trout	Dapagliflozin	nd
	Phloridzin Dihydrate	nd
	Phloretin	nd
	Tetraethylammonium (TEA)	nd
	Nickel Chloride ($NiCl_2$)	nd
Pig	Dapagliflozin	0.004 ± 0.001
	Phloridzin Dihydrate	0.5 ± 0.3
	Phloretin	3.6 ± 1.6
	Tetraethylammonium (TEA)	6.1 ± 2.0
	Nickel Chloride ($NiCl_2$)	1.6 ± 0.7^{B}

Ki (mM) values represented for Nile Tilapia, rainbow Trout, and pig. Data are presented as means ± SEM. Different letter superscripts indicate significances for $NiCl_2$: A, Nile tilapia vs. B, pig (Student's t-test, $P < 0.05$). ND represents non-detectable data.

5.4.2.2 Rainbow Trout Flux inhibition

No significant inhibition was observed for dapagliflozin, phloridzin dihydrate, phloretin, TEA, and $NiCl_2$ (Figure 5.3A, B, C, D, and E). Additionally, no Ki values were detected for any of the inhibitors (Table 5.3).

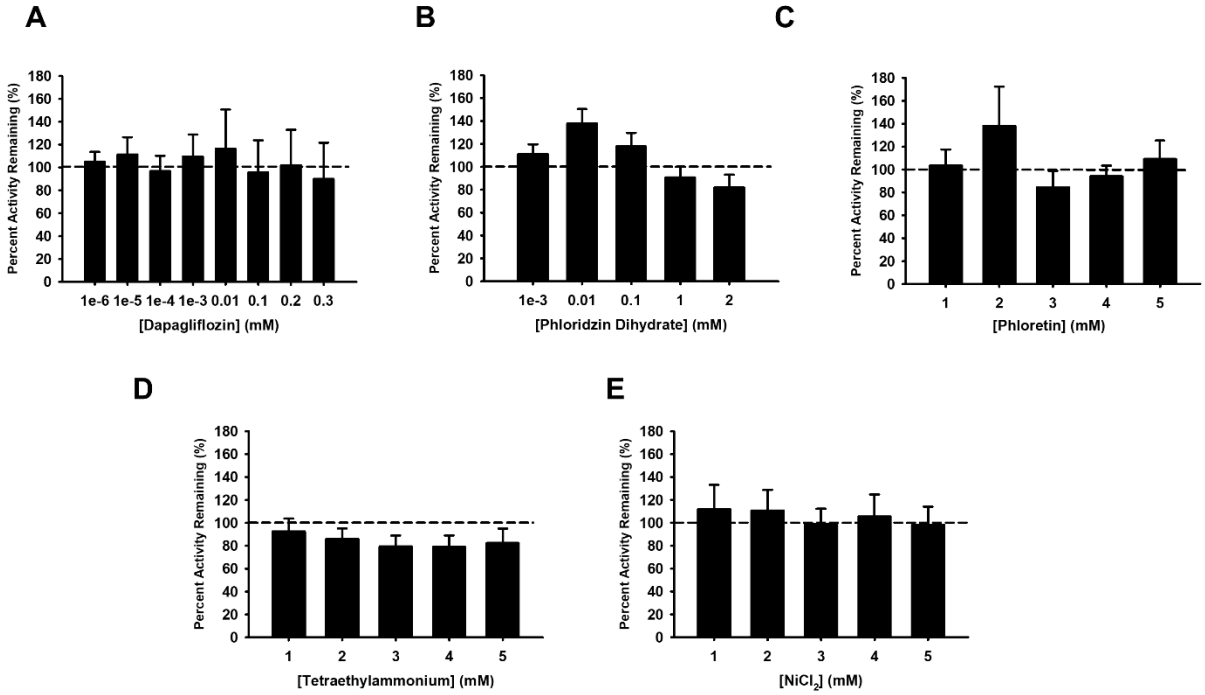

Figure 5.3 Lack of pharmacological inhibition in trout.

Percent activity remaining of Jms in rainbow trout by **A)** dapagliflozin (0.000001, 0.00001, 0.0001, 0.001, 0.01, 0.1, 0.2, and 0.3mM) (Fish N = 12), followed by addition of **B)** phloridzin dihydrate (0.001, 0.01, 0.1, 1, and 2mM) (Fish N = 9), followed by **C)** phloretin (1, 2, 3, 4, and 5mM) (Fish N = 15), followed by **D)** tetraethylammonium (1, 2, 3, 4, and 5mM) (Fish N = 13), and finally by **E)** $NiCl_2$ (1, 2, 3, 4, and 5mM) (Fish N = 5). The 100% represents transporter is 100% not inhibited by that inhibitor, which is presented as the dotted line.

5.4.2.3 Pig Flux inhibition

Dapagliflozin revealed significant inhibition from 0.0001mM to 0.3mM concentrations, with about 50% activity remaining at 0.3mM (Figure 5.4A, $P < 0.05$). Similarly, phloridzin dihydrate revealed significant inhibition from 0.01mM to 2mM concentrations, demonstrating about 60% activity remaining at 2mM phloridzin dihydrate (Figure 5.4B, $P < 0.05$). In contrast to tilapia, pig revealed significant inhibition with phloretin, from 3 to 5mM (Figure 5.4C, $P < 0.05$). Additionally, about 70% activity remained with phloretin at 5mM (Figure 5.4C). Both TEA and $NiCl_2$ revealed significant inhibition, with TEA demonstrating inhibition at concentrations from 3mM to 5mM, leaving about 50-60% activity remaining (Figure 5.4D, $P < 0.05$). The inhibitor $NiCl_2$ revealed significant responses at 1mM and 5mM, yielding about 70-75% activity remaining (Figure 5.4E, $P < 0.05$). A significant difference between the Ki value of $NiCl_2$ was observed with tilapia (Table 5.3, $P < 0.05$).

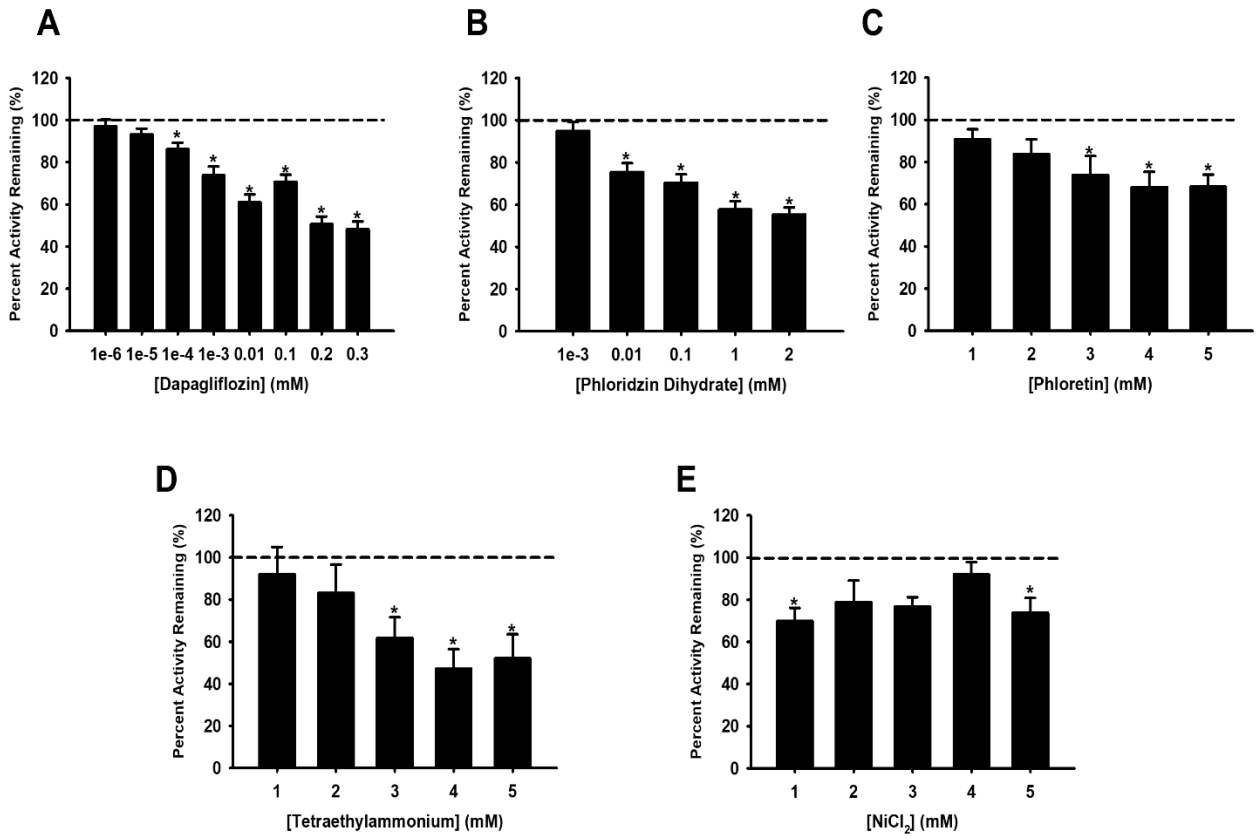

Figure 5.4 Pharmacological inhibition in pig.

Percent activity remaining of Jms in pig by **A)** dapagliflozin (0.000001, 0.00001, 0.0001, 0.001, 0.01, 0.1, 0.2, and 0.3mM) (Pig N = 6), followed by addition of **B)** phloridzin dihydrate (0.001, 0.01, 0.1, 1, and 2mM) (Pig N = 5), followed by **C)** phloretin (1, 2, 3, 4, and 5mM) (Pig N = 4), followed by **D)** tetraethylammonium (1, 2, 3, 4, and 5mM) (Pig N = 4), and finally by **E)** $NiCl_2$ (1, 2, 3, 4, and 5mM) (Pig N = 4). Single asterisks represent significance from 100% (where 100% represents transport is 100% un-inhibited by that inhibitor), which is presented as the dotted line (1-way ANOVA, $P < 0.05$).

5.4.3 Genomic and Gene Expression Analysis

The GLUT2 (SLC2A2) transporter was identified for tilapia, trout and pig genome using the BLAST+ application (Table 5.1). The expression levels of GLUT2 were compared among the different species using quantitative real-time PCR.

Pig revealed significantly higher GLUT2 expression (over 100 fold higher) compared to tilapia and trout (Figure 5.5A, $P < 0.05$). The significantly higher GLUT2 expression in pig jejunum is supported by its kinetic characterization and the inhibitor response of phloretin. Both tilapia and trout had similar expression of GLUT2 (Figure 5.5A). The low expression of GLUT2 in tilapia was supported by the kinetic characterization and the lack of inhibition by phloretin (Figure 5.2C). Sequence similarities of GLUT2 between tilapia, trout, and pig were compared in a phylogenetic tree (Figure 5.5B). In a CLUSTAL W analysis, the nucleotide identity of GLUT2 was compared between the three species, and relative to tilapia GLUT2 (SLC2A2) were 70% GLUT2 (SLC2A2) in trout, and 62% GLUT2 (SLC2A2) in pig. Sequence similarities of AQPS in tilapia, trout, and pig were compared in a phylogenetic tree as well (Figures 5.6A, B, and C). It revealed the number of AQPs present in each species, possibly suggesting contribution of these transporters to total glucose flux.

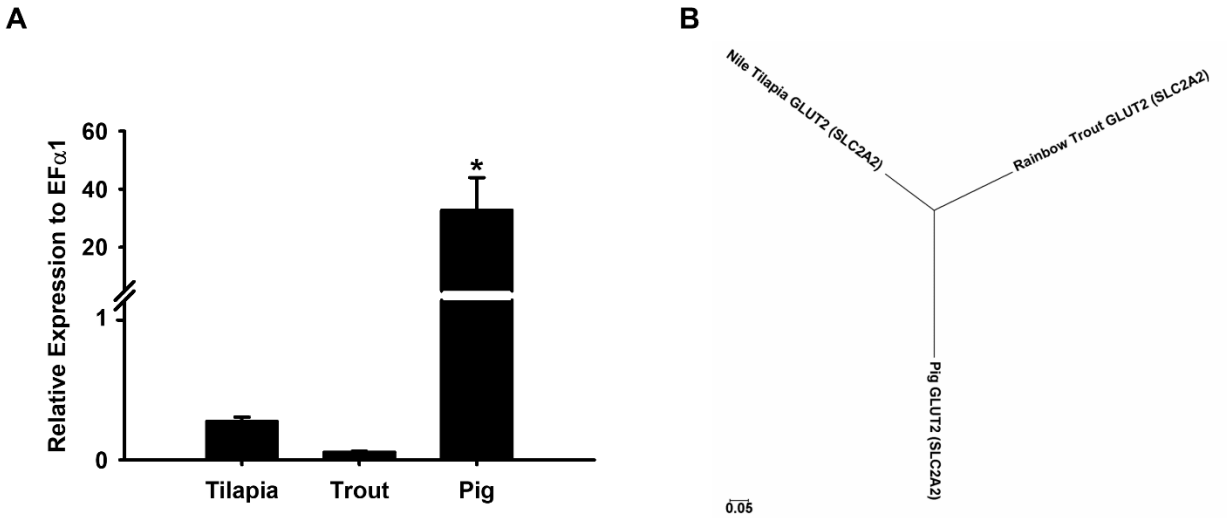

Figure 5.5 Genomic and gene expression analyses in tilapia, trout, and pig.

A) Relative expression levels of GLUT2 transporters in Nile tilapia proximal intestine (N = 10), rainbow trout midgut intestinal section (N = 10), and pig jejunum (N = 10) using quantitative PCR. Expression levels were normalized against EFα1 housekeeping gene. Asterisk represents significance between species (1-way ANOVA, $P < 0.05$). **B)** Phylogenetic tree of GLUT2 in each species. The alignment program CLUSTAL W and the phylogenetic display program MEGA7 were used to generate the tree.

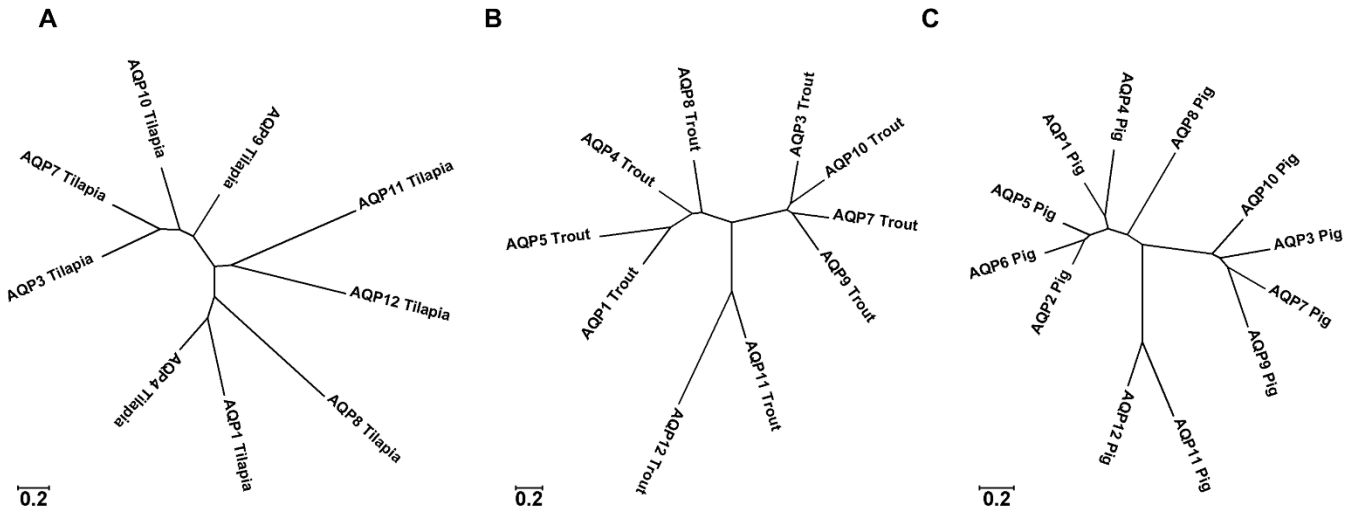

Figure 5.6 Genomic analyses of AQPs in tilapia, trout, and pig.

A) Phylogenetic tree of AQPs in tilapia. **B)** Phylogenetic tree of AQPs in trout. **C)** Phylogenetic tree of AQPs in pig. The alignment program CLUSTAL W and the phylogenetic display program MEGA7 were used to generate the tree.

5.5 Discussion

For the first time, we characterized the total tissue glucose transport systems in tilapia, trout, and pig, using a D-glucose gradient ranging from 1mM to 8000mM. Along with inhibitor and genomic analyses, we demonstrate SGLT involvement and the potential involvement of AQPs that may contribute to glucose absorption in all species. Additionally, important species differences between the mammalian pig and the aquatic species here suggest apical GLUT2 transporter involvement in the pig, but not in tilapia and trout. It would appear apical GLUT2 transporter involvement likely contributes to continued glucose absorption above the capacity of SGLTs.

5.5.1 Ha/Hc Tilapia, Ha/Lc Trout and La/Lc Pig total glucose transport systems

Kinetic characterization of total intestinal glucose absorption between tilapia, trout, and pig revealed an overall Ha/Hc transport system in tilapia, a Ha/Lc transport system in trout, and a La/Lc transport system in pig (Table 5.2). The Hc transport in tilapia is similar to the Hc sodium-dependent glucose transport system (~47μA/cm^2; data presented in Chapter 1), which has a higher Vmax value compared to sodium-dependent glucose transport in trout (~1.7μA/cm^2; data presented in Chapter 1). This suggests the majority of glucose transport in tilapia is predominantly through sodium-dependent glucose transporters. However, the affinity for total glucose absorption is similar between both aquatic species presented here, suggesting similar transporters may be responsible in both species. The high Km values for tilapia and trout in the millimolar range indicate that transporters involved in total glucose absorption are generally high affinity. Even though tilapia exhibits a higher Vmax value for glucose flux, both tilapia and trout demonstrate saturation of glucose transport around 50mM glucose (Figures 5.1A and B, and Table 5.2). This is further emphasized as a lack of percentage increase in Jms after 50mM glucose for both aquatic species (Figure 5.1D).

The low saturation of the transporters in both fish species could have evolved due to the lower use of glucose by fish species, previously described (82, 151). This is particularly true for carnivorous fish like rainbow trout, where glucose use is not the primary energy source compared to omnivorous fish and mammals (121, 161). This is reflected by the lower Vmax in total glucose absorption in trout compared to tilapia. It has also been demonstrated in

omnivorous fish like the black bullhead catfish that glucose usage is lower than mammals, which may also be true for the omnivorous tilapia (110, 161). Therefore, the possibility of apical GLUT2 absorption for tilapia and trout may not exist or is not needed. The low saturation of the transporters in both aquatic species, as well as the very low Km values in comparison to the pig, support this notion.

In contrast, the pig total glucose transport is a La/Lc total glucose absorption system, with a Km in the molar range that is over 400 fold higher than both tilapia and trout (Table 5.2). This very low-affinity for total glucose transport has been similarly described in other mammals, such as mice and rats (107). This system was attributed to apical GLUT2 insertion that allowed for higher glucose absorption, thus increasing the overall Km value of total glucose transport (106, 107, 192). However, the Km values for GLUT2 reported in these studies ranged from 17mM to 56mM, and were dependent on the glucose range and techniques used (44, 107). These Km values are over 20 fold lower than the Km value presented in this study, possibly due to differences in techniques such as glucose range, type of assay, and species used (rodents versus pig) (107). The total glucose transport in the pig which continued after 50mM glucose, in comparison to tilapia and trout, exhibited a significant percentage increase of Jms at the higher concentrations (Figure 5.1D). Therefore, the presence of apical GLUT2 transporters may explain the higher saturation of total glucose transport present in the pig, shifting the Km value away from SGLTs. The presence of GLUT2 was supported by pharmacological inhibition.

5.5.2 Inhibition of Glucose Flux defines Different Transport Mechanism between Species

Inhibitor responses from dapagliflozin, phloridzin dihydrate, phloretin, TEA, and $NiCl_2$ demonstrated differences between the aquatic species here and the mammalian pig (Figures 5.2, 5.3, and 5.4). Dapagliflozin and phloridzin dihydrate in tilapia defined the involvement of SGLTs for total tissue glucose absorption (Figures 5.2A and B). This has been similarly demonstrated in a previous study that focused on sodium-dependent glucose transport in tilapia and found inhibition with both dapagliflozin and phloridzin (180). Since most of inhibition was achieved by SGLT inhibitors, it suggests that majority of transport in tilapia is through SGLTs. Additionally, the lack of phloretin response in tilapia suggests a lack of GLUT2 involvement with total glucose absorption (Figure 5.2C). However, significant inhibition with TEA, but less

than the SGLT inhibitors in tilapia suggests the possible involvement of AQPs. Transport through AQPs may explain the Michaelis-Menten kinetics observed in this study, where the Km of AQPs for glucose may sit between the two previously described SGLTs associated with the electrogenic transport in tilapia (see Chapter 1). In contrast, trout did not exhibit any significant responses to any of the inhibitors (Figure 5.3). The lack of significant inhibition to total tissue glucose absorption in trout may be due to the low temperature used to conduct the flux experiments (~11-12^{o}C), some of which have been previously described (180). These low temperatures may have hindered the effects of the inhibitors that have previously been used on mammalian systems (temperatures ~ 37^{o}C), thus producing no measurable effect on trout total glucose absorption (Figure 5.3).

Similarly to tilapia, the pig responded to inhibition by dapagliflozin and phloridzin dihydrate, indicating the involvement of SGLTs in total tissue glucose absorption (Figures 5.4A and B). However, in contrast to tilapia and trout, significant inhibition with phloretin was observed. GLUT2 phloretin sensitivity has been shown in rat jejunum and *Xenopus laevis* oocyte expression systems (81, 106, 189, 213). This supports GLUT2 involvement in the pig, giving insight into the large shifted Km in comparison to the aquatic species here. Additionally, it was found that SGLT1 was not sensitive to phloretin, further supporting the fact that GLUT2 transporters may be present in pig jejunum (107, 120). Finally, the AQP inhibitors, TEA and $NiCl_2$, were found to produce significant inhibition, suggesting that AQPs are involved in total tissue glucose absorption in the pig (Figures 5.4D and E) (50, 211). Similar to tilapia, the lack of sigmoidal kinetic fit in the pig may be attributed to AQP transport with a Km that is between previously described SGLT transporters (see Chapter 2).

The involvement of AQPs in both tilapia and pig to total tissue glucose absorption is plausible as AQPs are known to have substrate transport promiscuity of AQPs (50, 186). It was demonstrated in human AQP isoform 9 (AQP9) that in addition to transporting water and urea, it could also transport non-charged solutes such as carbamides and polyols (186). Other researchers have defined AQPs as aqua-glycerol-porins, that allow passive diffusion of other solutes in addition to water (50). Therefore, given the response to TEA and $NiCl_2$, AQPs contributing to total tissue glucose absorption in tilapia and pig is plausible.

5.5.3 Gene Expression support a dominant GLUT2-transporter involvement in Pig

Genomic and gene expression analysis of GLUT2 in all three species revealed significantly higher GLUT2 expression in the pig, compared to tilapia and trout (Figure 5.5A). This result supports the kinetic and inhibitor analyses in the pig, suggesting a large contribution of GLUT2 to total glucose absorption. This plausible GLUT2 contribution to total glucose absorption may indicate that the pig also has a GLUT2 apical translocation mechanism, which has been shown previously to assist with high glucose absorption in mice and rats (106, 107). In addition to GLUT2 transporters, the pig jejunum also involves SGLT and AQP transporters, based on the responses to the inhibitors. In the pig jejunum, SGLT1 (SLC5A1) and SGLT3 (SLC5A4) may contribute to the La/Lc total tissue glucose transport system (Chapter 2). Additionally, 12 AQPs members have been identified in the pig genome, some possibly contributing to overall glucose flux in the pig (Figure 5.6C).

In contrast, the low expression of GLUT2 in both fish species is supported by the kinetic and inhibitor analyses (in tilapia), suggesting a lack of apical GLUT2 contribution to total glucose absorption. Thus, the SGLTs are likely responsible for the majority of transport, which have been identified in Chapter 1. Therefore, for tilapia, possible SGLT1 (SLC5A1) and SMIT2 (SLC5A11) transporters may contribute to the overall Ha/Hc total tissue glucose transport system, and SGLT1 (SLC5A1) in trout may contribute to the overall Ha/Lc total tissue glucose transport system (Chapter 1) (180). Interestingly in tilapia, responses to the AQP inhibitors suggest the possible involvement of AQPs contributing to total tissue glucose absorption, possibly shifting the kinetic fit from a sigmoidal/Hill to Michaelis-Menten. With a phylogenetic analysis, AQPs were identified in both tilapia and trout, with 9 members identified in tilapia and 10 members identified in trout, possibly suggesting AQPs may contribute to overall glucose flux (Figures 5.6A and B).

5.6 Conclusion

Total tissue glucose flux presents a Ha/Hc total glucose transport system in tilapia, a Ha/Lc total glucose transport system in trout, and a La/Lc total glucose transport system in pig. The Ha/Hc total glucose transport system in tilapia is most likely attributed to SGLTs, with some AQP contribution, and lack of apical GLUT2 involvement. The Ha/Lc total glucose transport system in trout is most likely attributed to SGLTs, given similarities to the electrogenic kinetics (Chapter 1). In contrast, the pig jejunum is a La/Lc total glucose transport system, which may be

attributed to SGLTs, GLUT2, and AQP transporters. Given these differences in transporter involvement, this study demonstrates continued glucose absorption at higher concentrations in the mammalian pig, whereas this is not observed in the aquatic tilapia and trout species. These transport mechanisms observed in the mammalian pig may be an evolutionary adaptation different from fish, which may not be exposed to a diet high enough in free glucose to allow non-facilitative glucose absorption.

Chapter 6 – General Discussion

6.1 Implications

Overall, we characterized sodium-dependent and total tissue glucose transport kinetic systems in the mammalian pig (omnivore), the omnivorous tilapia, and the carnivorous trout. We found that the transport mechanism for glucose is different between species. We assume that these differences exist to meet the specific needs of that species, depending on many factors such as environmental influences and their natural diets.

Specifically, in chapter 3, we discovered different kinetic sodium-dependent glucose transport systems between tilapia and trout, which has not been previously characterized or compared. Overall, we demonstrated that electrogenic sodium-dependent glucose transport was much higher in tilapia than trout, which was not surprising as tilapia is an omnivorous fish with higher amounts of carbohydrates in its natural diet. However, we also demonstrated that trout can absorb high concentrations of glucose, especially in its hindgut intestinal section, which is interesting as they are known to be poorly tolerant of high carbohydrate levels in their diet (69). Finally, the hindgut glucose absorption that exists in both fish species is different from mammals, where colonic glucose absorption is little to none. This presents a divergent adaptation from mammals, where both tilapia and trout have evolved to absorb glucose along their hindgut, implicating this segment and the glucose transporters in other physiological roles. We speculated it may have to do with osmoregulation, which has been studied in avian species (68). Interestingly, even though sodium-dependent glucose absorption has been extensively studied in mammalian species in comparison to their aquatic counterparts, there are still undefined mechanisms, especially in the pig. Therefore, our next chapter focuses on sodium-dependent glucose absorption in the pig, revealing interesting insights into its glucose transport mechanisms.

Thus, in chapter 4, the kinetic characterization of sodium-dependent glucose absorption was investigated along the porcine jejunum, ileum, and distal colon. Here, for the first time, we demonstrated that the jejunum and ileum follow sigmoidal/Hill kinetics, instead of the previously characterised Michaelis-Menten kinetics. This result changes the perspective of porcine sodium-dependent glucose transport, since this kinetic fit strongly suggests that multiple transporters are involved in each segment. Previous studies have characterized sodium-dependent glucose

transport in both segments following Michaelis-Menten models, suggesting only one-transporter involvement (75). However, our characterization reveals that this is not the case. Therefore, our kinetic work strongly supports the involvement of multiple transporters in each segment contributing to overall glucose absorption in the porcine jejunum and ileum. This is supported by the expression of multiple SLC5A isoforms identified here and previously described secondary modifications of SGLT1 along the GI tract.

Finally, in chapter 5, we studied total tissue glucose absorption, to include sodium-dependent and sodium-independent absorption. Our results described surprising differences between the mammalian pig and the aquatic species tilapia and trout. The sodium-independent component of total tissue glucose absorption along the BBM is generally assumed to be associated with the GLUT2 transporter, at least in rodents (213). Interestingly, this was not found in tilapia and trout. In fact, the majority of transport in these fish species seemed to occur predominantly through SGLTs, saturating at around 50mM glucose. However, the pig demonstrated continued glucose absorption past 50mM glucose, with a strong GLUT2 presence based on pharmacological inhibition, as well as gene expression analyses. Therefore, the pig demonstrated glucose absorption through SGLTs, as well as through GLUT2 transporters. This is interesting, suggesting that mammals adapted to increase the efficiency of their glucose absorption, seeing as they have much higher carbohydrates in their natural diets compared to both omnivorous and carnivorous fish species (1). Finally, this chapter revealed the possible contribution of AQPs to total glucose absorption in tilapia and pig. With pharmacological inhibition of AQP transporters in both species, we revealed that AQPs may contribute to total glucose transport, an area not yet investigated in these species.

Glucose absorption, whether it is sodium-dependent or a combination of sodium-dependent and sodium-independent, revealed different kinetic glucose transport systems in the species presented in the above chapters. We demonstrated and provided reasons as to why different kinetic glucose transport systems may exist along the GI tract of these species. However, there is still no concrete answer as to why these systems are needed.

6.2 Limitations

Each chapter contains limitations, as with all studies based on techniques and assays used. These limitations are presented below.

In chapter 3, there are a few limitations in this study based on the techniques used. The assumption of mRNA expression of the SLC5A transporters directly correlating with protein function does not always hold. However, identifying these fish SLC5A proteins using Western blots is not currently possible as there are no available fish SLC5A antibodies. Another technical limitation in this study involves the possibility of contamination of other tissues when collecting whole intestinal segments for RT-qPCR. Avoiding contamination by scraping cells off the epithelial lumen was not possible, given the very thin intestinal tissue which would tear upon scraping, thus not completely eliminating contamination. Another limitation addresses the higher absorptive capacity seen in tilapia, which could be due to other structural and functional adaptations. The current study expressed absorptive capacity in terms of intestinal segment area exposed by the insert in the Ussing chamber (0.3 cm^2). However, while the tissue area was constant, the epithelial surface area may have differed between the two species, depending on the size of villi and microvilli structures. Additionally, the higher SGLT1 expression in tilapia compared to trout may contribute to the higher Vmax values as the coupling ratio of sodium to glucose for SGLT1 is known to be 2:1 (13, 16, 53, 58, 75, 83, 84, 90, 112). Finally, the definition of Km in this study is collectively termed as affinity, where the assumption is made that the rate of transport and binding is similar. This assumption is supported by the fact that our technique requires the simultaneous binding and transport of glucose to generate a current.

In chapter 4, there are limitations as well. As said previously in chapter 3, we acknowledge that mRNA and protein expression are not directly correlative, therefore the gene expression results presented in this chapter only suggest the possible involvement of these transporters. Additionally, we have assumed that the SLC5A family, secondary modifications of family members, or another family of sodium-dependent glucose transporters may be responsible for the observed glucose transport kinetic differences between the jejunum and ileum. Investigating these different mechanisms would be beyond the scope of the study presented in this chapter.

In Chapter 5, as mentioned previously in Chapter 3, one of the limitations addresses the fact that the results obtained from the gene expression analyses represents assumptions, since

mRNA and protein expression are not always correlated. However, performing Western blots using fish and pig antibodies for SGLTs, GLUT2, and AQPs is not possible, as fish and pig antibodies are not available. Additionally, GLUT2 expression was conducted using whole intestinal tissues, rather than scraping the apical portion of the intestine. Therefore, possible GLUT2 expression from the basolateral membrane may also contribute to the overall expression. However, our conclusions of GLUT2 presence on the apical side of the pig jejunum is based on the support of using inhibitors only on the apical side of the intestine and observing significant inhibition.

6.3 Future Research

In our first study, we have shown that the omnivorous tilapia absorbs higher amounts of glucose than the carnivorous trout. Additionally, the aquatic species here demonstrated major differences in sodium-dependent glucose transport systems, with different patterns of intestinal segregation. Therefore, we speculate whether these results may mirror other omnivorous and carnivorous fish species, such as the carnivorous salmon, or the omnivorous black bullhead catfish. Studying sodium-dependent glucose absorption in other types of fish can allow for broader conclusions to be made between omnivorous and carnivorous fish species. We have also demonstrated that both tilapia and trout absorb glucose across the entirety of their GI tract, especially in their hindgut segments. This finding has also been demonstrated in avian and other fish species (Tambaqui, black Piranha, and Pacu), which may all suggest a unique evolutionary adaptation to glucose absorption, similar to tilapia and trout (68, 99, 156). Therefore, specifically exploring the absorption of glucose in the hindgut of these species can reveal important evolutionary adaptational mechanisms in these species. Finally, the sodium-dependent glucose transporters responsible for hindgut glucose absorption in trout were not identified. Thus, future studies can focus on identifying potential sodium-dependent glucose transporters from other solute carrier families that may contribute to the observed kinetics in the trout hindgut.

In the pig, the heterogeneous system of sodium-dependent glucose absorption in the jejunum and ileum has been demonstrated in other mammalian species, but has yet to be fully characterized. More specifically, the second transporter involved in ileal sodium-dependent

glucose absorption has not been identified. Investigating the identity of this transporter from other solute carrier families, or producing knockdowns of existing transporters may provide answers. Additionally, heterogeneous systems of glucose transport have been discovered in other species like bovine, equine, and rodents, where characterization is incomplete. Therefore, further investigating these systems can possibly introduce similar or different mechanisms of glucose transport in these species.

Finally, total tissue glucose absorption can be expanded to study other mammalian species, to see similar transport mechanisms to the pig. Additionally, the other intestinal sections in both the pig and the aquatic species can be used to study total tissue glucose absorption as well. The GLUT2 presence in the pig and its lack thereof in tilapia and trout is very interesting as this difference has not been presented before. Therefore, studying total tissue glucose absorption in other aquatic species is important to see if similar results are observed in comparison to tilapia and trout. Additionally, studying the importance of GLUT2 in pig or other mammalian models by running different assays (sodium-independent Ussing chamber experiments, knockdowns, etc.) can allow us to better understand the difference in glucose transport mechanisms between mammalian species.

REFERENCES

1. *The Nutrient Requirements of Pigs: Technical review*. Slough, U.K: Commonwealth Agricultural Bureaux, 1981.
2. **A.M. Bakke-McKellep SN, A. Krogdahl and R.K. Buddington**. Absorption of glucose, amino acids, and dipeptides by the intestines of Atlantic Salmon (*Salmo salar* L.). *Fish Physiology and Biochemistry* 22: 33-44, 2000.
3. **Agyekum AK, Sands JS, Regassa A, Kiarie E, Weihrauch D, Kim WK, and Nyachoti CM**. Effect of supplementing a fibrous diet with a xylanase and beta-glucanase blend on growth performance, intestinal glucose uptake, and transport-associated gene expression in growing pigs. *Journal of Animal Science* 93: 3483-3493, 2015.
4. **Ahearn GA, Behnke RD, Zonno V, and Storelli C**. Kinetic heterogeneity of Na-D-glucose cotransport in teleost gastrointestinal tract. *American Journal of Physiology* 263: R1018-1023, 1992.
5. **Ahearn RPFaGA**. Intestinal glucose transport in carnivorous and herbivorous marine fishes. *Journal of comparative physiology* 152: 79-90, 1983.
6. **Aleksei Krasnov HT, Hannu Molsa**. Rainbow Trout (*Onchorhynchus mykiss*) hepatic glucose transporter. *Biochimica et Biophysica Acta* 1520: 174-178, 2001.
7. **Althoff T, Hentschel H, Luig J, Schutz H, Kasch M, and Kinne RK**. Na(+)-D-glucose cotransporter in the kidney of Squalus acanthias: molecular identification and intrarenal distribution. *American Journal of Physiology - Regulatory, Integrative, and Comparative Physiology* 290: R1094-1104, 2006.
8. **Anderson GL, and Braun EJ**. Postrenal modification of urine in birds. *American Journal of Physiology-Regulatory, Integrative and Comparative Physiology* 248: R93-R98, 1985.
9. **Anderson J, Jackson AJ, Matty AJ, and Capper BS**. Effects of dietary carbohydrate and fibre on the tilapia Oreochromis niloticus (Linn.). *Aquaculture* 37: 303-314, 1984.
10. **Anderson WG, Dasiewicz PJ, Liban S, Ryan C, Taylor JR, Grosell M, and Weihrauch D**. Gastro-intestinal handling of water and solutes in three species of elasmobranch fish, the white-spotted bamboo shark, Chiloscyllium plagiosum, little skate, Leucoraja erinacea and the clear nose skate Raja eglanteria. *Comparative Biochemistry and Physiology A Molecular and Integrative Physiology* 155: 493-502, 2010.
11. **Aouameur R, Da Cal S, Bissonnette P, Coady MJ, and Lapointe JY**. SMIT2 mediates all myo-inositol uptake in apical membranes of rat small intestine. *American Journal of Physiology - Gastrointestinal and Liver Physiology* 293: G1300-1307, 2007.
12. **Arai T, Washizu T, Sagara M, Sako T, Nigi H, Matsumoto H, Sasaki M, and Tomoda I**. D-glucose transport and glycolytic enzyme activities in erythrocytes of dogs, pigs, cats, horses, cattle and sheep. *Research in Veterinary Sciences* 58: 195-196, 1995.
13. **Aschenbach JR, Steglich K, Gabel G, and Honscha KU**. Expression of mRNA for glucose transport proteins in jejunum, liver, kidney and skeletal muscle of pigs. *Journal of Physiology and Biochemistry* 65: 251-266, 2009.
14. **Augustin R, and Mayoux E**. *Mammalian Sugar Transporters*. 2014, p. 3-36.
15. **Axelsson E, Ratnakumar A, Arendt M-L, Maqbool K, Webster MT, Perloski M, Liberg O, Arnemo JM, Hedhammar Å, and Lindblad-Toh K**. The genomic signature of dog domestication reveals adaptation to a starch-rich diet. *Nature* 495: 360, 2013.
16. **Balen D, Ljubojevic M, Breljak D, Brzica H, Zlender V, Koepsell H, and Sabolic I**. Revised immunolocalization of the Na+-D-glucose cotransporter SGLT1 in rat organs with an improved antibody. *American Journal of Physiology - Cell Physiology* 295: C475-489, 2008.
17. **Bianchi L, and Diez-Sampedro A**. A single amino acid change converts the sugar sensor SGLT3 into a sugar transporter. *PLoS One* 5: e10241, 2010.

18. **Blanco AM, Bertucci JI, Ramesh N, Delgado MJ, Valenciano AI, and Unniappan S**. Ghrelin Facilitates GLUT2-, SGLT1- and SGLT2-mediated Intestinal Glucose Transport in Goldfish (Carassius auratus). 7: 45024, 2017.
19. **Breque FBaJ**. Digestibility of Starch by Rainbow Trout: Effects of the Physical State of Starch and of the Intake Level. *Aquaculture* 34: 203-212, 1983.
20. **Breves G, Kock J, and Schröder B**. Transport of nutrients and electrolytes across the intestinal wall in pigs. *Livestock Science* 109: 4-13, 2007.
21. **Brot-Laroche E, Dao MT, Alcalde AI, Delhomme B, Triadou N, and Alvarado F**. Independent modulation by food supply of two distinct sodium-activated D-glucose transport systems in the guinea pig jejunal brush-border membrane. *Proceedings of the National Academy of Sciences U S A* 85: 6370-6373, 1988.
22. **Brot-Laroche E, Serrano MA, Delhomme B, and Alvarado F**. Temperature sensitivity and substrate specificity of two distinct Na+-activated D-glucose transport systems in guinea pig jejunal brush border membrane vesicles. *Journal of Biological Chemistry* 261: 6168-6176, 1986.
23. **Bucke D**. The anatomy and histology of the alimentary tract of the carnivorous fish the pike Esox lucius L. *Journal of Fish Biology* 3: 421-431, 1971.
24. **Buddington RK**. Intestinal nutrient transport during ontogeny of vertebrates. *American Journal of Physiology* 263: R503-509, 1992.
25. **Buddington RK, Chen JW, and Diamond JM**. Dietary regulation of intestinal brush-border sugar and amino acid transport in carnivores. *American Journal of Physiology-Regulatory, Integrative and Comparative Physiology* 261: R793-R801, 1991.
26. **Buhler DR, and Halver JE**. Nutrition of Salmonoid FishesIX. Carbohydrate Requirements of Chinook Salmon. *The Journal of Nutrition* 74: 307-318, 1961.
27. **Burnstock G**. The Morphology of the Gut of the Brown Trout (*Salmo trutta*). *Quarterly Journal of Microscopical Science* 100: 183-198, 1959.
28. **Byrne FL, Olzomer EM, Brink R, and Hoehn KL**. Knockout of glucose transporter GLUT6 has minimal effects on whole body metabolic physiology in mice. *American Journal of Physiology - Endocrinology and Metabolism* 315: E286-e293, 2018.
29. **Caccia S, Casartelli M, Grimaldi A, Losa E, de Eguileor M, Pennacchio F, and Giordana B**. Unexpected similarity of intestinal sugar absorption by SGLT1 and apical GLUT2 in an insect (Aphidius ervi, Hymenoptera) and mammals. *American Journal of Physiology - Regulatory, Integrative, and Comparative Physiology* 292: R2284-2291, 2007.
30. **Caceci T, El-Habback HA, Smith SA, and Smith BJ**. The stomach of Oreochromis niloticus has three regions. *Journal of Fish Biology* 50: 939-952, 1997.
31. **Caceci T, El-Habback HA, Smith SA, and Smith BJ**. The stomach of Oreochromis niloticus has three regions. *Journal of Fish Biology* 50: 939-952, 1997.
32. **Carciofi AC, Takakura FS, de-Oliveira LD, Teshima E, Jeremias JT, Brunetto MA, and Prada F**. Effects of six carbohydrate sources on dog diet digestibility and post-prandial glucose and insulin response. *Journal of Animal Physiology and Animal Nutrition (Berl)* 92: 326-336, 2008.
33. **Care CCoA**. Canadian Council on Animal Care Guidelines on: The Care and Use of Fish in Research, Teaching and Testing. 2005.
34. **Carr KE, and Toner PG**. Morphology of the Intestinal Mucosa. In: *Pharmacology of Intestinal Permeation I*, edited by Csáky TZ. Berlin, Heidelberg: Springer Berlin Heidelberg, 1984, p. 1-50.
35. **Chao EC, and Henry RR**. SGLT2 inhibition--a novel strategy for diabetes treatment. *Nature Reviews Drug Discovery* 9: 551-559, 2010.
36. **Charalampopoulos D, Rastall R, and ebrary Inc.** *Prebiotics and probiotics science and technology*. New York, NY: Springer, 2009, p. 1 online resource.

37. **Cheeseman C**. GLUT7: a new intestinal facilitated hexose transporter. *American Journal of Physiology - Endocrinology and Metabolism* 295: E238-241, 2008.
38. **Chen YJ, Zhang TY, Chen HY, Lin SM, Luo L, and Wang DS**. Simultaneous stimulation of glycolysis and gluconeogenesis by feeding in the anterior intestine of the omnivorous GIFT tilapia, Oreochromis niloticus. *Biology Open* 6: 818-824, 2017.
39. **Chou T-C**. Derivation and properties of Michaelis-Menten type and Hill type equations for reference ligands. *Journal of Theoretical Biology* 59: 253-276, 1976.
40. **Clarke LL**. A guide to Ussing chamber studies of mouse intestine. *American Journal of Physiology - Gastrointestinal and Liver Physiology* 296: G1151-G1166, 2009.
41. **Coady MJ, Wallendorff B, Bourgeois F, Charron F, and Lapointe J-Y**. Establishing a definitive stoichiometry for the Na+/monocarboxylate cotransporter SMCT1. *Biophysical journal* 93: 2325-2331, 2007.
42. **Coady MJ, Wallendorff B, Gagnon DG, and Lapointe JY**. Identification of a novel Na+/myo-inositol cotransporter. *Journal of Biological Chemistry* 277: 35219-35224, 2002.
43. **Coelho AI, Berry GT, and Rubio-Gozalbo ME**. Galactose metabolism and health. *Current Opinion in Clinical Nutrition and Metabolic Care* 18: 422-427, 2015.
44. **Colville CA, Seatter MJ, Jess TJ, Gould GW, and Thomas HM**. Kinetic analysis of the liver-type (GLUT2) and brain-type (GLUT3) glucose transporters in Xenopus oocytes: substrate specificities and effects of transport inhibitors. *Biochemistry Journal* 290 (Pt 3): 701-706, 1993.
45. **D.L. Thiessen GLCaPDA**. Digestibility and growth performance of juvenile rainbow trout (*Oncorhynchus mykiss*) fed with pea and canola products. *Aquaculture Nutrition* 9: 67-75, 2003.
46. **Dawson PA, Mychaleckyj JC, Fossey SC, Mihic SJ, Craddock AL, and Bowden DW**. Sequence and functional analysis of GLUT10: a glucose transporter in the Type 2 diabetes-linked region of chromosome 20q12-13.1. *Molecular Genetics and Metabolism* 74: 186-199, 2001.
47. **de-Oliveira LD, Carciofi AC, Oliveira MC, Vasconcellos RS, Bazolli RS, Pereira GT, and Prada F**. Effects of six carbohydrate sources on diet digestibility and postprandial glucose and insulin responses in cats. *Journal of Animal Science* 86: 2237-2246, 2008.
48. **De La Vieja A, Dohan O, Levy O, and Carrasco N**. Molecular analysis of the sodium/iodide symporter: impact on thyroid and extrathyroid pathophysiology. *Physiological Reviews* 80: 1083-1105, 2000.
49. **Debosch BJ, Chen Z, Saben JL, Finck BN, and Moley KH**. Glucose transporter 8 (GLUT8) mediates fructose-induced de novo lipogenesis and macrosteatosis. *Journal of Biological Chemistry* 289: 10989-10998, 2014.
50. **Detmers FJM, de Groot BL, Müller EM, Hinton A, Konings IBM, Sze M, Flitsch SL, Grubmüller H, and Deen PMT**. Quaternary Ammonium Compounds as Water Channel Blockers: SPECIFICITY, POTENCY, AND SITE OF ACTION. *Journal of Biological Chemistry* 281: 14207-14214, 2006.
51. **Diamond JM, Karasov WH, Cary C, Enders D, and Yung R**. Effect of dietary carbohydrate on monosaccharide uptake by mouse small intestine in vitro. *Journal of Physiology* 349: 419-440, 1984.
52. **Diamond RKBaJM**. Aristotle revisited: The function of pyloric caeca in fish. *Proceedings in the National Academy of Sciences* 83: 8012-8014, 1986.
53. **Diez-Sampedro A, Eskandari S, Wright EM, and Hirayama BA**. Na+-to-sugar stoichiometry of SGLT3. *American Journal of Physiology - Renal Physiology* 280: F278-282, 2001.
54. **Doege H, Bocianski A, Scheepers A, Axer H, Eckel J, Joost HG, and Schürmann A**. Characterization of human glucose transporter (GLUT) 11 (encoded by SLC2A11), a novel sugar-transport facilitator specifically expressed in heart and skeletal muscle. *The Biochemical journal* 359: 443-449, 2001.

55. **Dorando FC, and Crane RK**. Studies of the kinetics of Na+ gradient-coupled glucose transport as found in brush-border membrane vesicles from rabbit jejunum. *Biochimica et Biophysica Acta (BBA) - Biomembranes* 772: 273-287, 1984.
56. **Drochner W**. Digestion of carbohydrates in the pig. *Arch Tierernahr* 43: 95-116, 1993.
57. **Dunham I, Shimizu N, Roe BA, Chissoe S, Hunt AR, Collins JE, Bruskiewich R, Beare DM, Clamp M, Smink LJ, Ainscough R, Almeida JP, Babbage A, Bagguley C, Bailey J, Barlow K, Bates KN, Beasley O, Bird CP, Blakey S, Bridgeman AM, Buck D, Burgess J, Burrill WD, O'Brien KP, and et al.** The DNA sequence of human chromosome 22. *Nature* 402: 489-495, 1999.
58. **Dyer J, Al-Rammahi M, Waterfall L, Salmon KS, Geor RJ, Boure L, Edwards GB, Proudman CJ, and Shirazi-Beechey SP**. Adaptive response of equine intestinal Na+/glucose co-transporter (SGLT1) to an increase in dietary soluble carbohydrate. *Pflugers Arch* 458: 419-430, 2009.
59. **Edwards DJ, Austreng E, Risa S, and Gjedrem T**. Carbohydrate in rainbow trout diets. I. Growth of fish of different families fed diets containing different proportions of carbohydrate. *Aquaculture* 11: 31-38, 1977.
60. **Enes P, Panserat S, Kaushik S, and Oliva-Teles A**. Nutritional regulation of hepatic glucose metabolism in fish. *Fish Physiology and Biochemistry* 35: 519-539, 2009.
61. **Erik K, Knudsen B, Lærke HN, and Jørgensen H**. Carbohydrates and Carbohydrate Utilization in Swine. *Sustainable Swine Nutrition* 2012.
62. **Eskandari S, Loo DD, Dai G, Levy O, Wright EM, and Carrasco N**. Thyroid Na+/I- symporter. Mechanism, stoichiometry, and specificity. *Journal of Biological Chemistry* 272: 27230-27238, 1997.
63. **Farrell SASaAP**. Vascular Reactivity of the Coronary Artery in Steelhead Trout (*Oncorhynchus mykiss*). *Comparative Biochemistry and Physiology* 97C: 59-63, 1990.
64. **Ferraris RP, and Diamond JM**. A method for measuring apical glucose transporter site density in intact intestinal mucosa by means of phlorizin binding. *Journal of Membrane Biology* 94: 65-75, 1986.
65. **Forsling ML, and Widdas WF**. The effect of temperature on the competitive inhibition of glucose transfer in human erythrocytes by phenolphthalein, phloretin and stilboestrol. *Journal of Physiology* 194: 545-554, 1968.
66. **Fromm RMSaPO**. Glucose Absorption and Metabolism by the Gut of Rainbow Trout. *Comparative Biochemistry and Physiology* 13: 53-69, 1964.
67. **Fujimura K, and Okada N**. Development of the embryo, larva and early juvenile of Nile tilapia Oreochromis niloticus (Pisces: Cichlidae). Developmental staging system. *Development, Growth & Differentiation* 49: 301-324, 2007.
68. **Garriga C, Rovira N, Moreto M, and Planas JM**. Expression of Na+-D-glucose cotransporter in brush-border membrane of the chicken intestine. *American Journal of Physiology* 276: R627-631, 1999.
69. **Gary H. Thorgaard GSB, David Williams, Donald R. Buhler, Stephen L, Kaatari, Sandra S. Ristow, John D. Hansen, James R. Winton, Jerri L. Bartholomew, James J. Nagler, Patrick J. Walsh, Matt M. Vijayan, Robert H. Devlin, Ronald W. Hardy, Kenneth E. Overturf, William P. Young, Barrie D. Robison, Caird Rexroad, Yniv Palti**. Status and opportunities for genomics research with rainbow trout. *Comparative Biochemistry and Physiology* 133: 609-646, 2002.
70. **Girniene J, Tatibouët A, Sackus A, Yang J, Holman GD, and Rollin P**. Inhibition of the d-fructose transporter protein GLUT5 by fused-ring glyco-1,3-oxazolidin-2-thiones and -oxazolidin-2-ones. *Carbohydrate Research* 338: 711-719, 2003.
71. **Goldstein DL, and Braun EJ**. Contributions of the kidneys and intestines to water conservation, and plasma levels of antidiuretic hormone, during dehydration in house sparrows (Passer domesticus). *Journal of Comparative Physiology B* 158: 353-361, 1988.
72. **Gopal E, Umapathy NS, Martin PM, Ananth S, Gnana-Prakasam JP, Becker H, Wagner CA, Ganapathy V, and Prasad PD**. Cloning and functional characterization of human SMCT2 (SLC5A12) and expression pattern of the transporter in kidney. *Biochim Biophys Acta* 1768: 2690-2697, 2007.

73. **Grempler R, Augustin R, Froehner S, Hildebrandt T, Simon E, Mark M, and Eickelmann P**. Functional characterisation of human SGLT-5 as a novel kidney-specific sodium-dependent sugar transporter. *FEBS Lett* 586: 248-253, 2012.
74. **Guilloteau P, Zabielski R, Hammon HM, and Metges CC**. Nutritional programming of gastrointestinal tract development. Is the pig a good model for man? *Nutrition Research Reviews* 23: 4-22, 2010.
75. **Halaihel N, Gerbaud D, Vasseur M, and Alvarado F**. Heterogeneity of pig intestinal D-glucose transport systems. *American Journal of Physiology* 277: C1130-1141, 1999.
76. **Hall JR, Richards RC, MacCormack TJ, Ewart KV, and Driedzic WR**. Cloning of GLUT3 cDNA from Atlantic cod (Gadus morhua) and expression of GLUT1 and GLUT3 in response to hypoxia. *Biochim Biophys Acta* 1730: 245-252, 2005.
77. **Harada N, and Inagaki N**. Role of sodium-glucose transporters in glucose uptake of the intestine and kidney. *Journal of Diabetes Investigation* 3: 352-353, 2012.
78. **Hecker J, and Grovum W**. Rates of Passage of Digesta and Water Absorption along the Large Intestines of Sheep, Cows and Pigs. *Australian Journal of Biological Sciences* 28: 161-168, 1975.
79. **Heli Teerijoki AK, Tiina I. Pitkanen, Hannu Molsa**. Cloning and characterization of glucose transporter in teleost fish rainbow trout (*Oncorhynchus mykiss*). *Biochimica et Biophysica Acta* 1494: 290-294, 2000.
80. **Helliwell GLKaPA**. The diffusive component of intestinal glucose absorption is mediated by the glucose-induced recruitment of GLUT2 to the brush-border membrane. *Biochemical Journal* 350: 155-162, 2000.
81. **Helliwell PA, Richardson M, Affleck J, and Kellett GL**. Stimulation of fructose transport across the intestinal brush-border membrane by PMA is mediated by GLUT2 and dynamically regulated by protein kinase C. *The Biochemical journal* 350 Pt 1: 149-154, 2000.
82. **HEMRE G-I, MOMMSEN TP, and KROGDAHL Å**. Carbohydrates in fish nutrition: effects on growth, glucose metabolism and hepatic enzymes. *Aquaculture Nutrition* 8: 175-194, 2002.
83. **Herrmann J, Möller N, Lange P, and Breves G**. Different phlorizin binding properties to porcine mucosa of the jejunum and ileum in relation to SGLT1 activity. *Journal of Animal Science* 94: 238-242, 2016.
84. **Herrmann J, Schroder B, Klinger S, Thorenz A, Werner AC, Abel H, and Breves G**. Segmental diversity of electrogenic glucose transport characteristics in the small intestines of weaned pigs. *Comparative Biochemistry and Physiology A Molecular and Integrative Physiology* 163: 161-169, 2012.
85. **Hilton JW, and Atkinson JL**. Response of rainbow trout (Salmo gairdneri) to increased levels of available carbohydrate in practical trout diets. *British Journal of Nutrition* 47: 597-607, 1982.
86. **Hirayama BA, Lostao MP, Panayotova-Heiermann M, Loo DD, Turk E, and Wright EM**. Kinetic and specificity differences between rat, human, and rabbit Na+-glucose cotransporters (SGLT-1). *American Journal of Physiology* 270: G919-926, 1996.
87. **Hoenig M, Clark M, Schaeffer DJ, and Reiche D**. Effects of the sodium-glucose cotransporter 2 (SGLT2) inhibitor velagliflozin, a new drug with therapeutic potential to treat diabetes in cats. *Journal of Veterinary Pharmacology Therapeutics* 2017.
88. **Hofer R, and Sturmbauer C**. Inhibition of trout and carp α-amylase by wheat. *Aquaculture* 48: 277-283, 1985.
89. **Horaci Osorio MF, Rocio Bautista, Hilda Vargas-Robles, Bruno Escalante, Abraham Arellano, Eunice Romo, and Amelia Rios**. Effect of phlorizin on SGLT2 expression in the kidney of diabetic rats. *JN EPHROL* 23: 541-546, 2010.
90. **Horiba N, Masuda S, Takeuchi A, Takeuchi D, Okuda M, and Inui K**. Cloning and characterization of a novel Na+-dependent glucose transporter (NaGLT1) in rat kidney. *Journal of Biological Chemistry* 278: 14669-14676, 2003.

91. **Hrytsenko O, Pohajdak B, Xu BY, Morrison C, van Tol B, and Wright JR, Jr.** Cloning and molecular characterization of the glucose transporter 1 in tilapia (Oreochromis niloticus). *General and Comparative Endocrinology* 165: 293-303, 2010.
92. **Hwang PP, Lee, T-H., Lin, L-Y.** Ion regulation in fish gills: recent progress in the cellular and molecular mechanisms. *American Journal of Physiology - Regulatory, Integrative, and Comparative Physiology* 301: R28 - R47, 2011.
93. **Isaji M**. SGLT2 inhibitors: molecular design and potential differences in effect. *Kidney International* 79: S14-S19, 2011.
94. **J. Dyer EF-CM, K. S. H. Salmon, C. J. Proudman, G. B. Edwards, and S. P. Shirazi-Beechey**. Molecular Characterisation of carbohydrate digestion and absorption in equine small intestine. *Equine Veterinary Journal* 34: 349-358, 2002.
95. **James R. Wright J, Wael O'Hali, Hua Yan, Xiao-Xia Han, and Arend Bonen**. GLUT-4 Deficiency and Severe Peripheral Resistance to Insulin in the Teleost Fish Tilapia. *General and Comparative Endocrinology* 111: 20-27, 1998.
96. **John R. White J**. Apple trees to Sodium Glucose Co-transporter Inhibitors: A review of SGLT2 inhibition. *Clinical Diabetes* 28: 5-10, 2010.
97. **Kanwal A, Singh SP, Grover P, and Banerjee SK**. Development of a cell-based nonradioactive glucose uptake assay system for SGLT1 and SGLT2. *Analytical Biochemistry* 429: 70-75, 2012.
98. **Kararli TT**. Comparison of the Gastrointestinal Anatomy, Physiology, and Biochemistry of Humans and Commonly used Laboratory Animals. *Biopharmaceutics and Drug Disposition* 16: 351-380, 1995.
99. **Karasov WH, Duong P, Diamond JM, and Carpenter FL**. Food Passage and Intestinal Nutrient Absorption in Hummingbirds. *The Auk* 103: 453-464, 1986.
100. **Karasov WH, Rio CMd, and Caviedes-Vidal E**. Ecological Physiology of Diet and Digestive Systems. *Annual Review of Physiology* 73: 69-93, 2011.
101. **Kaunitz JD, and Wright EM**. Kinetics of sodiumd-glucose cotransport in bovine intestinal brush border vesicles. *Journal of Membrane Biology* 79: 41-51, 1984.
102. **Kaushik JDKaSJ**. Contribution of digestible energy from carbohydrates and estimation of protein/energy requirements for growth of rainbow trout (*Oncorhynchus mykiss)*. *Aquaculture* 106: 161-169, 1992.
103. **Kayano T, Fukumoto H, Eddy RL, Fan YS, Byers MG, Shows TB, and Bell GI**. Evidence for a family of human glucose transporter-like proteins. Sequence and gene localization of a protein expressed in fetal skeletal muscle and other tissues. *Journal of Biological Chemistry* 263: 15245-15248, 1988.
104. **Kekuda R, Wang H, Huang W, Pajor AM, Leibach FH, Devoe LD, Prasad PD, and Ganapathy V**. Primary Structure and Functional Characteristics of a Mammalian Sodium-coupled High Affinity Dicarboxylate Transporter. *Journal of Biological Chemistry* 274: 3422-3429, 1999.
105. **Kellet GL**. Topical Review: The facilitated component of intestinal glucose absorption. *Journal of Physiology* 531: 585-595, 2001.
106. **Kellett GL, Brot-Laroche E, Mace OJ, and Leturque A**. Sugar absorption in the intestine: the role of GLUT2. *Annual Review of Nutrition* 28: 35-54, 2008.
107. **Kellett GL, and Helliwell PA**. The diffusive component of intestinal glucose absorption is mediated by the glucose-induced recruitment of GLUT2 to the brush-border membrane. *The Biochemical journal* 350 Pt 1: 155-162, 2000.
108. **Kevin M. McGowan SDLaPHP**. Glucose Transporter Gene Expression: Regulation of Transcription and mRNA stability. *Pharmacology and Therapeutics* 66: 465-505, 1995.
109. **Kienzle E**. Effect of Carbohydrates on Digestion in the Cat. *American Institute of Nutrition Journal of Nutrition* 124: 2568S-2571S, 1994.

110. **Kirchner S, Panserat S, Lim PL, Kaushik S, and Ferraris RP**. The role of hepatic, renal and intestinal gluconeogenic enzymes in glucose homeostasis of juvenile rainbow trout. *Journal of Comparative Physiology B* 178: 429-438, 2008.
111. **Klaus F, Palmada M, Lindner R, Laufer J, Jeyaraj S, Lang F, and Boehmer C**. Up-regulation of hypertonicity-activated myo-inositol transporter SMIT1 by the cell volume-sensitive protein kinase SGK1. *Journal of Physiology* 586: 1539-1547, 2008.
112. **Klinger S, Lange P, Brandt E, Hustedt K, Schroder B, Breves G, and Herrmann J**. Degree of SGLT1 phosphorylation is associated with but does not determine segment-specific glucose transport features in the porcine small intestines. *Physiological Reports* 6: 2018.
113. **Klinger S, Zurich M, Schröder B, and Breves G**. Effects of dietary starch source on electrophysiological intestinal epithelial properties and intestinal glucose uptake in growing goats. *Archives of Animal Nutrition* 67: 289-300, 2013.
114. **Knudsen K, Lærke H, Ingerslev A, Hedemann M, Nielsen T, and Theil P**. *Carbohydrates in pig nutrition – Recent advances*. 2016, p. 1–11.
115. **Koepsell H, and Spangenberg J**. Function and presumed molecular structure of Na+-D-glucose cotransport systems. *Journal of Membrane Biology* 138: 1-11, 1994.
116. **Komoroski B, Vachharajani N, Boulton D, Kornhauser D, Geraldes M, Li L, and Pfister M**. Dapagliflozin, a novel SGLT2 inhibitor, induces dose-dependent glucosuria in healthy subjects. *Clinical Pharmacology and Therapeutics* 85: 520-526, 2009.
117. **Kristjansson MM**. Purification and characterization of trypsin from the pyloric caeca of rainbow trout (Oncorhynchus mykiss). *Journal of Agricultural and Food Chemistry* 39: 1738-1742, 1991.
118. **Krogdahl Å, Hemre GI, and Mommsen TP**. Carbohydrates in fish nutrition: digestion and absorption in postlarval stages. *Aquaculture Nutrition* 11: 103-122, 2005.
119. **Kuehl GE, Lampe JW, Potter JD, and Bigler J**. Glucuronidation of nonsteroidal anti-inflammatory drugs: identifying the enzymes responsible in human liver microsomes. *Drug Metabolism and Disposition* 33: 1027-1035, 2005.
120. **Kwon O, Eck P, Chen S, Corpe CP, Lee JH, Kruhlak M, and Levine M**. Inhibition of the intestinal glucose transporter GLUT2 by flavonoids. *FASEB J* 21: 366-377, 2007.
121. **Legate NJ, Bonen A, and Moon TW**. Glucose tolerance and peripheral glucose utilization in rainbow trout (Oncorhynchus mykiss), American eel (Anguilla rostrata), and black bullhead catfish (Ameiurus melas). *General and Comparative Endocrinology* 122: 48-59, 2001.
122. **Levey DJ, and Duke GE**. How Do Frugivores Process Fruit? Gastrointestinal Transit and Glucose Absorption in Cedar Waxwings (Bombycilla cedrorum). *The Auk* 109: 722-730, 1992.
123. **Levey DJ, and Karasov WH**. Digestive modulation in a seasonal frugivore, the American robin (Turdus migratorius). *American Journal of Physiology* 262: G711-718, 1992.
124. **Lin X, Ma L, Fitzgerald RL, and Ostlund RE, Jr.** Human sodium/inositol cotransporter 2 (SMIT2) transports inositols but not glucose in L6 cells. *Arch Biochem Biophys* 481: 197-201, 2009.
125. **Loewen ME, Bekar LK, Walz W, Forsyth GW, and Gabriel SE**. pCLCA1 lacks inherent chloride channel activity in an epithelial colon carcinoma cell line. *American Journal of Physiology - Gastrointestinal and Liver Physiology* 287: G33-41, 2004.
126. **Loewen ME, Smith NK, Hamilton DL, Grahn BH, and Forsyth GW**. CLCA protein and chloride transport in canine retinal pigment epithelium. *American Journal of Physiology - Cell Physiology* 285: C1314-1321, 2003.
127. **Low AG**. Nutrient absorption in pigs. *Journal of the Science of Food and Agriculture* 31: 1087-1130, 1980.
128. **Mackenzie B, Loo DD, Panayotova-Heiermann M, and Wright EM**. Biophysical characteristics of the pig kidney Na+/glucose cotransporter SGLT2 reveal a common mechanism for SGLT1 and SGLT2. *Journal of Biological Chemistry* 271: 32678-32683, 1996.

129. **Mackenzie B, Panayotova-Heiermann M, Loo DD, Lever JE, and Wright EM**. SAAT1 is a low affinity Na+/glucose cotransporter and not an amino acid transporter. A reinterpretation. *Journal of Biological Chemistry* 269: 22488-22491, 1994.
130. **Maffia M, Acierno R, Cillo E, and Storelli C**. Na(+)-D-glucose cotransport by intestinal BBMVs of the Antarctic fish Trematomus bernacchii. *American Journal of Physiology-Regulatory, Integrative and Comparative Physiology* 271: R1576-R1583, 1996.
131. **Mallee JJ, Atta MG, Lorica V, Rim JS, Kwon HM, Lucente AD, Wang Y, and Berry GT**. The structural organization of the human Na+/myo-inositol cotransporter (SLC5A3) gene and characterization of the promoter. *Genomics* 46: 459-465, 1997.
132. **Malo C**. Separation of two distinct Na+/d-glucose cotransport systems in the human fetal jejunum by means of their differential specificity for 3-O-methylglucose. *Biochimica et Biophysica Acta (BBA) - Biomembranes* 1022: 8-16, 1990.
133. **McGowan KM, Long SD, and Pekala PH**. Glucose transporter gene expression: regulation of transcription and mRNA stability. *Pharmacology and Therapeutics* 66: 465-505, 1995.
134. **Merchant HA, McConnell EL, Liu F, Ramaswamy C, Kulkarni RP, Basit AW, and Murdan S**. Assessment of gastrointestinal pH, fluid and lymphoid tissue in the guinea pig, rabbit and pig, and implications for their use in drug development. *European Journal of Pharmaceutical Sciences* 42: 3-10, 2011.
135. **Miyauchi S, Gopal E, Babu E, Srinivas SR, Kubo Y, Umapathy NS, Thakkar SV, Ganapathy V, and Prasad PD**. Sodium-coupled electrogenic transport of pyroglutamate (5-oxoproline) via SLC5A8, a monocarboxylate transporter. *Biochimica et Biophysica Acta (BBA) - Biomembranes* 1798: 1164-1171, 2010.
136. **Moriarty DJW**. The physiology of digestion of blue-green algae in the cichlid fish, Tilapia nilotica. *Journal of Zoology* 171: 25-39, 1973.
137. **Morrison CM, Pohajdak B, Tam J, and Wright JR, Jr.** Development of the islets, exocrine pancreas, and related ducts in the Nile tilapia, Oreochromis niloticus (Pisces: Cichlidae). *Journal of Morphology* 261: 377-389, 2004.
138. **Morrison CM, and Wright JR**. A study of the histology of the digestive tract of the Nile tilapia. *Journal of Fish Biology* 54: 597-606, 1999.
139. **Mosenthin R**. Physiology of Small and Large Intestine of Swine - Review. *Asian-Australas Journal of Animal Science* 11: 608-619, 1998.
140. **Mueckler M, Caruso C, Baldwin SA, Panico M, Blench I, Morris HR, Allard WJ, Lienhard GE, and Lodish HF**. Sequence and structure of a human glucose transporter. *Science* 229: 941-945, 1985.
141. **Nagase G**. *Contribution to the physiology of digestion in Tilapia mossambica Peters: Digestive enzymes and the effects of diets on their activity*. 1964, p. 270-284.
142. **Newsome SD, Fogel ML, Kelly L, and del Rio CM**. Contributions of direct incorporation from diet and microbial amino acids to protein synthesis in Nile tilapia. *Functional Ecology* 25: 1051-1062, 2011.
143. **Obermeier M, Yao M, Khanna A, Koplowitz B, Zhu M, Li W, Komoroski B, Kasichayanula S, Discenza L, Washburn W, Meng W, Ellsworth BA, Whaley JM, and Humphreys WG**. In vitro characterization and pharmacokinetics of dapagliflozin (BMS-512148), a potent sodium-glucose cotransporter type II inhibitor, in animals and humans. *Drug Metabolism and Disposition* 38: 405-414, 2010.
144. **Obi IE, Sterling KM, and Ahearn GA**. Transepithelial D-glucose and D-fructose transport across the American lobster, Homarus americanus, intestine. *Journal of Experimental Biology* 214: 2337-2344, 2011.
145. **Obi IE, Sterling KM, and Ahearn GA**. Transepithelial d-glucose and d-fructose transport across the American lobster, Homarus americanus, intestine. *Journal of Experimental Biology* 214: 2337-2344, 2011.

146. **Okuda T, Haga T, Kanai Y, Endou H, Ishihara T, and Katsura I**. Identification and characterization of the high-affinity choline transporter. *Nature Neuroscience* 3: 120-125, 2000.
147. **Olivier Delezey BV, Kamel Mabrouk, Jurphaas van Rietschoten, Jacques Fantini, Jean Mauchamp, and Corinne Gerard**. Characterization of an Electrogenic Sodium/Glucose Cotransporter in a Human Colon Epithelial Cell Line. *Journal of Cellular Physiology* 163: 120-128, 1995.
148. **Osorio H, Bautista R, Rios A, Franco M, Arellano A, Vargas-Robles H, Romo E, and Escalante B**. Effect of phlorizin on SGLT2 expression in the kidney of diabetic rats. *Journal of Nephrology* 23: 541-546, 2010.
149. **P. Bergot JMB, and A.M. Escaffre**. Relationship between number of pyloric caeca and growth in rainbow trout (*Salmo gairdneri* Richardson). *Aquaculture* 22: 81-96, 1981.
150. **Pácha J**. Development of Intestinal Transport Function in Mammals. *Physiological Reviews* 80: 1633-1667, 2000.
151. **Palmer TN, and Ryman BE**. Studies on oral glucose intolerance in fish. *Journal of Fish Biology* 4: 311-319, 1972.
152. **Pappenheimer JR**. On the coupling of membrane digestion with intestinal absorption of sugars and amino acids. *American Journal of Physiology-Gastrointestinal and Liver Physiology* 265: G409-G417, 1993.
153. **Pasha SMK**. The Anatomy and Histology of the Alimentary Canal of a Herbivorous Fish *Tilapia Mossambica* (Peters). *Proceedings of the Indian Academy of Sciences* L1X: 340-349, 1964.
154. **Pattanawongsa A, Chau N, Rowland A, and Miners JO**. Inhibition of Human UDP-Glucuronosyltransferase Enzymes by Canagliflozin and Dapagliflozin: Implications for Drug-Drug Interactions. *Drug Metabolism and Disposition* 43: 1468-1476, 2015.
155. **Patton KT, and Thibodeau GA**. *Anatomy & Physiology*. Elsevier Science Health Science Division, 2010.
156. **Pelster B, Wood CM, Speers-Roesch B, Driedzic WR, Almeida-Val V, and Val A**. Gut transport characteristics in herbivorous and carnivorous serrasalmid fish from ion-poor Rio Negro water. *Journal of Comparative Physiology B* 185: 225-241, 2015.
157. **Peng S-YSaC-Y**. Protein-sparing effect by carbohydrates in diets for tilapia, *Oreochromis niloticus* X *O. aureus*. *Aquaculture* 117: 327-334, 1993.
158. **Persson B, Bengtsson G, Gentz J, Hakkarainen J, and Hellström R**. Plasma Levels of FFA, Glycerol, β-Hydroxybutyrate and Blood Glucose during the Postnatal Development of the Pig. *The Journal of Nutrition* 97: 311-315, 1969.
159. **Pfeffer APaE**. Studies on the Comparative Efficiency of Utilization of Gross Energy from some Carbohydrates, Proteins and Fats by Rainbow Trout (*Salmo Gairdneri,* R.). *Aquaculture* 20: 323-332, 1980.
160. **Plantikow LSaH**. Studies on Carbohydrate Digestion in Rainbow Trout. *Aquaculture* 30: 95-108, 1983.
161. **Polakof S, Alvarez R, and Soengas JL**. Gut glucose metabolism in rainbow trout: implications in glucose homeostasis and glucosensing capacity. *American Journal of Physiology - Regulatory, Integrative, and Comparative Physiology* 299: R19-32, 2010.
162. **Polakof S, Panserat S, Soengas JL, and Moon TW**. Glucose metabolism in fish: a review. *Journal of Comparative Physiology B* 182: 1015-1045, 2012.
163. **Polakof S, and Soengas JL**. Evidence of sugar sensitive genes in the gut of a carnivorous fish species. *Comparative Biochemistry and Physiology Part B: Biochemistry and Molecular Biology* 166: 58-64, 2013.
164. **Polentarutti BI, Peterson AL, Sjoberg AK, Anderberg EK, Utter LM, and Ungell AL**. Evaluation of viability of excised rat intestinal segments in the Ussing chamber: investigation of morphology, electrical parameters, and permeability characteristics. *Pharmaceutical Research* 16: 446-454, 1999.

165. **Poulsen SB, Fenton RA, and Rieg T**. Sodium-glucose cotransport. *Current opinion in nephrology and hypertension* 24: 463-469, 2015.
166. **Preitner F, Bonny O, Laverrière A, Rotman S, Firsov D, Da Costa A, Metref S, and Thorens B**. Glut9 is a major regulator of urate homeostasis and its genetic inactivation induces hyperuricosuria and urate nephropathy. *Proceedings of the National Academy of Sciences U S A* 106: 15501-15506, 2009.
167. **Ramsay PT, and Carr A**. Gastric acid and digestive physiology. *Surgical Clinics of North America* 91: 977-982, 2011.
168. **Refstie S, Korsøen ØJ, Storebakken T, Baeverfjord G, Lein I, and Roem AJ**. Differing nutritional responses to dietary soybean meal in rainbow trout (Oncorhynchus mykiss) and Atlantic salmon (Salmo salar). *Aquaculture* 190: 49-63, 2000.
169. **Roll P, Massacrier A, Pereira S, Robaglia-Schlupp A, Cau P, and Szepetowski P**. New human sodium/glucose cotransporter gene (KST1): identification, characterization, and mutation analysis in ICCA (infantile convulsions and choreoathetosis) and BFIC (benign familial infantile convulsions) families. *Gene* 285: 141-148, 2002.
170. **Ronaldo P. Ferraris aJMD**. Use of Phlorizin binding to Demonstrate Induction of Intestinal Glucose Transporters. *Journal of Membrane Biology* 94: 77-82, 1986.
171. **Sabolic I, Vrhovac I, Eror DB, Gerasimova M, Rose M, Breljak D, Ljubojevic M, Brzica H, Sebastiani A, Thal SC, Sauvant C, Kipp H, Vallon V, and Koepsell H**. Expression of Na+-D-glucose cotransporter SGLT2 in rodents is kidney-specific and exhibits sex and species differences. *American Journal of Physiology - Cell Physiology* 302: C1174-1188, 2012.
172. **Sala-Rabanal M, Gallardo MA, Sanchez J, and Planas JM**. Na-dependent D-glucose transport by intestinal brush border membrane vesicles from gilthead sea bream (Sparus aurata). *Journal of Membrane Biology* 201: 85-96, 2004.
173. **Sasaki T, Mori IC, Furuichi T, Munemasa S, Toyooka K, Matsuoka K, Murata Y, and Yamamoto Y**. Closing plant stomata requires a homolog of an aluminum-activated malate transporter. *Plant Cell Physiology* 51: 354-365, 2010.
174. **Schultz SG, and Zalusky R**. Ion Transport in Isolated Rabbit Ileum. *The Journal of General Physiology* 47: 567, 1964.
175. **Sergio Polakof RA, and Jose L. Soengas**. Gut glucose metabolism in rainbow trout: implications in glucose homeostasis and glucosensing capacity. *American Journal of Physiology - Regulatory, Integrative, and Comparative Physiology* 299: R19-R32, 2010.
176. **Shiau SY**. Utilization of carbohydrates in warmwater fish - with particular reference to tilapia, *Oreochromis niloticus* X *O. aureus*. *Aquaculture* 151: 79-96, 1997.
177. **Soengas JL, and Moon TW**. Transport and metabolism of glucose in isolated enterocytes of the black bullhead ictalurus melas: effects of diet and hormones. *Journal of Experimental Biology* 201 (Pt 23): 3263-3273, 1998.
178. **Stone DAJ**. Dietary Carbohydrate Utilization by Fish. *Reviews in Fisheries Science* 11: 337-369, 2003.
179. **Stumpel F, Burcelin R, Jungermann K, and Thorens B**. Normal kinetics of intestinal glucose absorption in the absence of GLUT2: evidence for a transport pathway requiring glucose phosphorylation and transfer into the endoplasmic reticulum. *Proceedings in the National Academy of Sciences U S A* 98: 11330-11335, 2001.
180. **Subramaniam M, Weber LP, and Loewen ME**. Intestinal Electrogenic Sodium-Dependent Glucose Absorption In Tilapia And Trout Reveal Species Differences In SLC5A-associated Kinetic Segmental Segregation. *American Journal of Physiology - Regulatory, Integrative, and Comparative Physiology* 2019.

181. **Suzuki K, and Kono T**. Evidence that insulin causes translocation of glucose transport activity to the plasma membrane from an intracellular storage site. *Proceedings in the National Academy of Sciences U S A* 77: 2542-2545, 1980.
182. **Tarran R, Loewen ME, Paradiso AM, Olsen JC, Gray MA, Argent BE, Boucher RC, and Gabriel SE**. Regulation of murine airway surface liquid volume by CFTR and Ca2+-activated Cl- conductances. *Journal of General Physiology* 120: 407-418, 2002.
183. **Tazawa S, Yamato T, Fujikura H, Hiratochi M, Itoh F, Tomae M, Takemura Y, Maruyama H, Sugiyama T, Wakamatsu A, Isogai T, and Isaji M**. SLC5A9/SGLT4, a new Na+-dependent glucose transporter, is an essential transporter for mannose, 1,5-anhydro-D-glucitol, and fructose. *Life Sciences* 76: 1039-1050, 2005.
184. **Teerijoki H, Krasnov A, Pitkänen TI, and Mölsä H**. Monosaccharide uptake in common carp (Cyprinus carpio) EPC cells is mediated by a facilitative glucose carrier. *Comparative Biochemistry and Physiology Part B: Biochemistry and Molecular Biology* 128: 483-491, 2001.
185. **Thurston JH, Sherman WR, Hauhart RE, and Kloepper RF**. myo-inositol: a newly identified nonnitrogenous osmoregulatory molecule in mammalian brain. *Pediatric Research* 26: 482-485, 1989.
186. **Tsukaguchi H, Weremowicz S, Morton CC, and Hediger MA**. *Functional and molecular characterization of the human neutral solute channel aquaporin-9*. 1999, p. F685-F696.
187. **Turk E, Martin MG, and Wright EM**. Structure of the human Na+/glucose cotransporter gene SGLT1. *Journal of Biological Chemistry* 269: 15204-15209, 1994.
188. **Turner RJ, and Moran A**. Further studies of proximal tubular brush border membrane D-glucose transport heterogeneity. *Journal of Membrane Biology* 70: 37-45, 1982.
189. **Uldry M, and Thorens B**. The SLC2 family of facilitated hexose and polyol transporters. *Pflugers Arch* 447: 480-489, 2004.
190. **Verri T, Barca A, Pisani P, Piccinni B, Storelli C, and Romano A**. Di- and tripeptide transport in vertebrates: the contribution of teleost fish models. *Journal of Comparative Physiology B* 187: 395-462, 2017.
191. **Vrhovac I, Balen Eror D, Klessen D, Burger C, Breljak D, Kraus O, Radovic N, Jadrijevic S, Aleksic I, Walles T, Sauvant C, Sabolic I, and Koepsell H**. Localizations of Na(+)-D-glucose cotransporters SGLT1 and SGLT2 in human kidney and of SGLT1 in human small intestine, liver, lung, and heart. *Pflugers Arch* 467: 1881-1898, 2015.
192. **Waeber G, Thompson N, Haefliger JA, and Nicod P**. Characterization of the murine high Km glucose transporter GLUT2 gene and its transcriptional regulation by glucose in a differentiated insulin-secreting cell line. *Journal of Biological Chemistry* 269: 26912-26919, 1994.
193. **Waller AP, George M, Kalyanasundaram A, Kang C, Periasamy M, Hu K, and Lacombe VA**. GLUT12 functions as a basal and insulin-independent glucose transporter in the heart. *Biochim Biophys Acta* 1832: 121-127, 2013.
194. **Walthall K, Cappon GD, Hurtt ME, and Zoetis T**. Postnatal development of the gastrointestinal system: a species comparison. *Birth Defects Research B Dev Reprod Toxicol* 74: 132-156, 2005.
195. **Wang H, Huang W, Fei YJ, Xia H, Yang-Feng TL, Leibach FH, Devoe LD, Ganapathy V, and Prasad PD**. Human placental Na+-dependent multivitamin transporter. Cloning, functional expression, gene structure, and chromosomal localization. *Journal of Biological Chemistry* 274: 14875-14883, 1999.
196. **Wang Y, Aun R, and Tse FL**. Absorption of D-glucose in the rat studied using in situ intestinal perfusion: a permeability-index approach. *Pharmaceutical Research* 14: 1563-1567, 1997.
197. **Weinreb EL, and Bilstad NM**. Histology of the Digestive Tract and Adjacent Structures of the Rainbow Trout, Salmo gairdneri irideus. *Copeia* 1955: 194-204, 1955.
198. **Wielert-Badt S, Lin J-T, Lorenz M, Fritz S, and Kinne RKH**. Probing the Conformation of the Sugar Transport Inhibitor Phlorizin by 2D-NMR, Molecular Dynamics Studies, and Pharmacophore Analysis. *Journal of Medicinal Chemistry* 43: 1692-1698, 2000.

199. **Wilson RP**. Utilization of dietary carbohydrate by fish. *Aquaculture* 124: 67-80, 1994.
200. **Wittenberger C, Coprean D, and Morar L**. Studies on the carbohydrate metabolism of the lateral muscles in carp (influence of phloridzin, insulin and adrenaline). *Journal of comparative physiology* 101: 161-172, 1975.
201. **Wolffram S, Eggenberger E, and Scharrer E**. Kinetics of d-glucose transport across the intestinal brush-border membrane of the cat. *Comparative Biochemistry and Physiology Part A: Physiology* 94: 111-115, 1989.
202. **Wolffram S, Eggenberger E, and Scharrer E**. Kinetics of D-glucose transport across the intestinal brush-border membrane of the cat. *Comparative Biochemistry and Physiology A Comparative Physiology* 94: 111-115, 1989.
203. **Wood IS, and Trayhurn P**. Glucose transporters (GLUT and SGLT): expanded families of sugar transport proteins. *British Journal of Nutrition* 89: 3-9, 2003.
204. **Wright EM**. Glucose transport families SLC5 and SLC50. *Molecular Aspects of Medicine* 34: 183-196, 2013.
205. **Wright EM**. Renal Na(+)-glucose cotransporters. *American Journal of Physiology - Renal Physiology* 280: F10-18, 2001.
206. **Wright EM, Loo DD, and Hirayama BA**. Biology of human sodium glucose transporters. *Physiological Reviews* 91: 733-794, 2011.
207. **Wright EM, Loo DD, Hirayama BA, and Turk E**. Surprising versatility of Na+-glucose cotransporters: SLC5. *Physiology (Bethesda)* 19: 370-376, 2004.
208. **Wright JR, Jr, Bonen A, Michael Conlon J, and Pohajdak B**. Glucose Homeostasis in the Teleost Fish Tilapia: Insights from Brockmann Body Xenotransplantation Studies1. *American Zoologist* 40: 234-245, 2015.
209. **Zalusky SGSaR**. Ion Transport in Isolated Rabbit Ileum. *The Journal of General Physiology* 47: 567-584, 1964.
210. **Zar JH**. *Biostatistical Analysis*. Prentice Hall, 2010.
211. **Zelenina M, Bondar AA, Zelenin S, and Aperia A**. Nickel and Extracellular Acidification Inhibit the Water Permeability of Human Aquaporin-3 in Lung Epithelial Cells. *Journal of Biological Chemistry* 278: 30037-30043, 2003.
212. **Zhao FQ, and Keating AF**. Functional properties and genomics of glucose transporters. *Current Genomics* 8: 113-128, 2007.
213. **Zheng Y, Scow JS, Duenes JA, and Sarr MG**. Mechanisms of glucose uptake in intestinal cell lines: role of GLUT2. *Surgery* 151: 13-25, 2012.
214. **Zimmerman AM, Wheeler PA, Ristow SS, and Thorgaard GH**. Composite interval mapping reveals three QTL associated with pyloric caeca number in rainbow trout, Oncorhynchus mykiss. *Aquaculture* 247: 85-95, 2005.